Biogas Purification:
H_2S Removal using Biofiltration

by

Mary Elizabeth Fischer

A thesis
presented to the University of Waterloo
in fulfillment of the
thesis requirement for the degree of
Master of Applied Science
in
Chemical Engineering

Waterloo, Ontario, Canada, 2010

AUTHOR'S DECLARATION

I hereby declare that I am the sole author of this thesis. This is a true copy of the thesis, including any required final revisions, as accepted by my examiners.

I understand that my thesis may be made electronically available to the public.

Abstract

Biogas, composed principally of methane, has limited use in energy generation due to the presence of hydrogen sulphide (H_2S). Biogas cannot be burned directly in an engine as H_2S present causes corrosion in the reaction chamber. There currently exist various technologies for the removal of H_2S from a gas stream, but most are chemically based, expensive, and are limited in use.

The purpose of this study was to determine a biogas purification technique suitable for a small scale farm application; including using a technology inexpensive, efficient, robust and easy to operate. As such, biofiltration was investigated for H_2S removal from biogas. Factors considered in the design of the biofiltration system included the source and conditioning of inoculum, type of packing material, and general operating conditions including inlet gas flow rate and H_2S loading rate to the biofilter.

Activated sludge conditioned in *A. ferrooxidans* media was an effective inoculum source. This was tested for growth support compatibility with gravel packing material, to be used in the biofilter. The inoculated packing material was loaded into the biofilter initially during start-up and acclimatization.

In this study, synthetic biogas ($49.9\%_{vol} CH_4$, $49.9\%_{vol} CO_2$, $2000 ppm_v$ H_2S) mixed with air (totalling $4\%_{vol}$ O_2) was added at 5-10L/hr to a biofilter of 0.4L gravel packing inoculated with conditioned activated sludge. Baseline H_2S removal studies in a non-inoculated biofilter were performed with anticipated operating conditions, including an inlet gas stream at 7.5L/h (25^oC, 1atm), resulting in 31-56% H_2S removal. A factorial test performed found that air content in the inlet gas stream was the significant factor affecting the removal of H_2S in the non-inoculated biofilter.

Operation of the biofilter with biogas was done for 61 days, including 41 days for start-up and acclimatization and 20 days of H_2S loading tests. Start-up and acclimatization with biogas resulted in complete H_2S removal after 2 days, with an average overall H_2S removal of 98.1%±2.9 std deviation over 34 days. Loading tests performed on the system ranged 5-12.4L/h (25^oC, 1atm), with a loading rate of 27.8 to $69.5 g H_2S/m^3h$ of filter bed. Throughout this test the average H_2S removal rate was 98.9%±2.1 std deviation over 20 days. Although complete H_2S breakthrough studies were not performed, these results indicate that biofiltration is a promising technology for H_2S removal from biogas in a small scale application.

Acknowledgements

I wish to sincerely thank my supervisors Christine Moresoli and Bernard Marcos for all of their guidance and support of this project and process.

I would like to thank Nicolas Galanis, chair holder of NSERC Chair in Industrial Energy Efficiency, as well as Hydro-Quebec for funding, without which this project would not have been possible.

I would also like to sincerely thank Claude Laflamme, Raynald Labrecque and Annie Trépanier for their technical assistance and expertise both in the laboratory and throughout design and analysis. Also the team of researchers, technicians, and students at Hydro-Quebec Energy Technology Laboratory (LTE) in Shawinigan, Quebec for all their support and encouragement. Their friendly, warm and helpful attitude made my experience in Shawinigan one that I will carry a lifetime.

Finally, I would like to thank my family for all their love and support throughout this interesting experience. They are always there to put a smile on my face.

Table of Contents

List of Figures ix
List of Tables xi
List of Abbreviations xii
Chapter 1 Introduction 1
1.1 Objectives of Study 1
Chapter 2 Literature Review 3
2.1 Biogas Composition 3
2.2 Anaerobic Digestion 4
2.2.1 Anaerobic digestion process 4
2.2.2 Operating parameters and optimization of anaerobic digestion 5
2.3 Chemical Hydrogen Sulphide Removal Techniques 6
2.3.1 Adsorption H_2S removal techniques 6
2.3.2 Adsorption techniques efficiency and comparison 8
2.3.3 Absorption H_2S removal techniques 10
2.3.4 Absorption techniques efficiency and comparison 12
2.3.5 Chemical oxidation for H_2S removal 14
2.4 Biofiltration Design 15
2.4.1 Type of biofiltration unit 15
2.4.2 Packing material 18
2.5 Microbial Population For Hydrogen Sulphide Removal 20
2.5.1 Microbial colony 20
2.5.2 Inoculum source 23
2.5.3 Inoculum conditioning 23
2.5.4 Inoculation 25
2.6 Biofiltration Operation 26
2.6.1 Biofiltration operating parameters 26
2.6.2 Summary of biofilter sizing and removal rates 29
2.6.3 Nutrient addition 30
2.7 Biofiltration Operating Conditions 31
2.8 Biofiltration Mechanisms 33
2.8.1 Physico-chemical H_2S removal mechanisms 33

2.8.2 Biological H_2S removal mechanisms 35
2.8.3 H_2S removal mechanisms specific for *A. ferrooxidans* 38
Chapter 3 Materials and Methods 39
3.1 Experimental Setup 39
3.1.1 System components 39
3.1.2 Biofilter size and volume 43
3.1.3 Nutrient addition 44
3.1.4 Inoculum source and nutrient addition 45
3.1.5 General system and monitoring information 45
3.1.6 Operating conditions 46
3.1.7 Compatible materials 47
3.1.8 Safety considerations for working with H_2S 47
3.2 Analytical Methods 48
3.2.1 pH and temperature 48
3.2.2 Gas composition 48
3.2.3 Fe^{2+} and Fe^{3+} 49
3.3 Experimentation Methods 50
3.3.1 Packing material characteristics 50
3.3.2 Inoculum preparation using *A. ferrooxidans* nutrient media 51
3.3.3 Bacterial attachment to packing material 52
3.3.4 Analysis during biofiltration operation 53
Chapter 4 Results and Discussion: Submitted Manuscript 54
4.1 Overview 54
4.2 Introduction 54
4.3 Materials and Methods 55
4.3.1 Biofilter setup 55
4.3.2 Filter material 56
4.3.3 Inoculum 57
4.3.4 Analytical methods 57
4.3.5 Experimentation 58
4.3.6 Biofilter startup and acclimatization period 59
4.3.7 Loading testing 60

4.4 Results and Discussion 60
4.4.1 H_2S removal in non-inoculated biofilter 60
4.4.2 Startup and acclimatization 62
4.4.3 Loading tests 64
4.5 Conclusion 65
4.6 Acknowledgements 66
Chapter 5 Material Balance 67
5.1 Material balance 67
5.1.1 Calculation basis and assumptions 68
5.2 Experimental Material Balance 70
5.2.1 Stream 1: Inlet gas - Experimental 71
5.2.2 Stream 2: Outlet Gas - Experimental 72
5.2.3 Overall total difference between streams - Experimental 72
5.3 Theoretical Material Balance of H_2S Removal System 75
5.3.1 Stream 1: Inlet gas –Theoretical 75
5.3.2 Stream 2: Inlet Liquid - Theoretical 77
5.3.3 Inside the biofilter - theoretical 78
5.3.4 Stream 3: Outlet Gas - Theoretical 80
5.3.5 Stream 4: Outlet Liquid –Theoretical 81
5.3.6 Overall balance equations 81
5.4 Comparison of Theoretical and Experimental Material Balance 84
5.5 Theoretical Pressure Drop 86
Chapter 6 Results and Discussion - Supplementary 88
6.1 Inoculum Conditioning With *A. ferrooxidans* Media 88
6.2 Packing Test 89
6.2.1 Packing test: colour 90
6.2.2 Packing test: pH evolution 92
6.2.3 Packing test: Fe^{2+}/Fe^{3+} results 96
6.3 H_2S Removal in Non-Inoculated Biofilter: Supplementary 100
6.4 Start up and Acclimatization: Supplementary 101
6.4.1 Biofilter startup and acclimatization: Outlet pH 104
6.4.2 Biofilter start-up and acclimatization: Outlet Fe^{2+} and Fe^{3+} 105

6.5 Biofilter H_2S Loading Tests: Supplementary 107
6.5.1 Biofilter H_2S loading test: filter bed blockage 107
6.5.2 Biofilter H_2S loading test: Inlet and outlet O_2 content 108
6.5.3 Biofilter H_2S loading test: Outlet pH 110
6.5.4 Biofilter loading tests: Outlet Fe^{3+} 111
6.6 Biofilter operation: Qualitative results 112
6.6.1 Filter bed 112
6.6.2 Outlet nutrient solution during loading test 114
Chapter 7 Conclusions 115
Chapter 8 Recommendations 117
8.1 Experimental Setup 117
8.2 Further Analysis 117
8.3 Scale up Considerations 118
Appendix 120
Bibliography 122

List of Figures

Figure 2.1 Typical anaerobic digestion process (adapted from Schomaker et al. (2000)) 4

Figure 2.2 Typical biofilter design (Delhomenie and Heitz 2005) 16

Figure 2.3 Typical bioscrubber design (Delhomenie and Heitz 2005) 17

Figure 2.4 Adsorption, absorption and oxidation in biofilter, no microorganisms (Barona et al. 2005). 34

Figure 2.5 Sulphur cycling in sulfuretum (Syed et al. 2006) 35

Figure 3.1 Instrumentation diagram of biofiltration system setup 42

Figure 4.1 Biofiltration system laboratory scale setup 56

Figure 4.2 H_2S removal in non-inoculated biofilter: H_2S concentration with varying $[O_2]$ inlet (1psig, 25^oC) 61

Figure 4.3 Biofilter start up phase: Inlet and outlet $[H_2S]$, biogas inlet added day 5 (1pisg, 25^oC) 63

Figure 4.4 Biofilter startup phase: Inlet and outlet $[H_2S]$, (1pisg, 25^oC) 64

Figure 4.5 H_2S loading rate and removal efficiency (Inlet 1740ppm H_2S, 1psig, 25^oC) 65

Figure 5.1 Theoretical process streams of biofiltration system for material balance (7.5L/h dry inlet gas, 4%$_{vol}$ O_2, 1atm, 25^oC) 68

Figure 5.2 Theoretical pressure drop with varying porosity, over 20cm packed bed 86

Figure 6.1 pH evolution for activated sludge in *A. ferrooxidans* media, n=2 (150rpm, 25^oC) 89

Figure 6.2 FPB samples at media change, day 13 (150rpm, 25^oC) 91

Figure 6.3 Packing test solutions at media change - Agitated, day 20 (grown at 150rpm, 25^oC) 91

Figure 6.4 Packing test solutions at media change – Settled, day 20 (grown at 150rpm, 25^oC) 92

Figure 6.5 pH of packing tests, n=2, (150rpm, 25^oC) Error bar represents standard deviation 92

Figure 6.6 pH of packing tests: Contamination in F sample, n=2, (150rpm, 25^oC) Error bar represents standard deviation 93

Figure 6.7 pH of packing tests: Contamination in FP sample, n=2 (150rpm, 25^oC) Error bar represents standard deviation 94

Figure 6.8 pH of packing tests, excluding contaminated points, n=2, (150rpm, 25^oC) Error bar represents standard deviation 95

Figure 6.9 Packing test: total dissolved iron at each media change, n=2 (150rpm, 25°C) Error bar represents standard deviation 97
Figure 6.10 Packing test: Fe^{2+} concentration at each media change, n=2 (150rpm, 25°C) Error bar represents standard deviation 98
Figure 6.11 Packing test: Fe^{3+} concentration at each media change, n=2 (150rpm, 25°C) Error bar represents standard deviation 99
Figure 6.12 48 hour test on non-inoculated filter: Outlet [H_2S] (inlet 0.15%$_{vol}$ H_2S, 1psig, 25°C) 100
Figure 6.13 Biofilter start up phase: Inlet and outlet [H_2S], biogas inlet added day 5 (1pisg, 25°C) 102
Figure 6.14 Biofilter startup phase: Inlet and Outlet [CH_4]%$_{vol}$, (1atm, 25°C) 103
Figure 6.15 Biofilter startup phase: Inlet and Outlet [O_2]%$_{vol}$, (1atm, 25°C) 103
Figure 6.16 Biofilter startup phase: Inlet and Outlet [N_2]%$_{vol}$ (1atm, 25°C) 104
Figure 6.17 Biofilter start-up phase: pH of liquid outlet solution 105
Figure 6.18 Biofilter start-up phase: Fe^{2+} and Fe^{3+} of inlet and outlet liquid nutrient solutions 106
Figure 6.19 Loading test: H_2S loading and outlet [H_2S] %$_{vol}$ (Inlet 0.17%$_{vol}$ H_2S, 1psig, 25°C) 107
Figure 6.20 Loading test: Inlet and Outlet [CH_4] %$_{vol}$, (1atm, 25°C) 108
Figure 6.21 Loading test: Inlet and Outlet [O_2] %$_{vol}$, (1atm, 25°C) 109
Figure 6.22 Loading test: pH of outlet tank and line solutions 110
Figure 6.23 Loading test: Inlet and outlet pH with biogas flow (1atm, 25°C) 111
Figure 6.24 Loading test: biogas flow and [Fe^{3+}] of outlet liquid solution (Inlet 0ppm Fe^{3+}) 112
Figure 6.25 Biofilter packed bed: Startup and acclimatization, day 7 113
Figure 6.26 Biofilter packed bed: Startup and acclimatization, day 21 113
Figure 6.27 Loading test: Biofilter outlet solution, orange left: day 6-15, clear right: day 18-20 114

List of Tables

Table 2.1 Composition of biogas, depending on source (Rasi et al. 2007) 3

Table 2.2 Comparison of factors for H_2S adsorption removal techniques 9

Table 2.3 Elementary reaction scheme for absorption using metal sulphides (ter Maat et al. 2005) 11

Table 2.4 Comparison of factors for H_2S absorption removal techniques 13

Table 2.5 Growth conditions for *Acidithiobacillus* sp. and *Thiobacillus* sp. (([a]Robertson and Kuenen 2006; Syed et al. 2006)) 22

Table 2.6 Biofilter operation conditions for H_2S removal 30

Table 2.7 Factors in biofiltration design for H_2S removal, various studies 32

Table 3.1 Volume and loading rates for biofilter design size, inlet 5-10L/h, 2000ppm H_2S . 44

Table 3.2 Relative nutritive flow rate of previous studies, for 0.4L packed bed biofilter 45

Table 4.1 Summary of packing material characteristics (n=12) 56

Table 4.2 Experimental design for biofilter H_2S removal baseline testing, (1psig, 23^oC) 58

Table 4.3 Biofilter startup and acclimatization: Operation conditions 59

Table 4.4 Loading stages with respective molar and gas flow rates 60

Table 5.1 Theoretical and experimental stream properties (7.5L/h dry gas basis) 70

Table 5.2 Inlet gas stream mass flow rate, all biofilter experiments (T variable, 1psig) 71

Table 5.3 Outlet gas stream mass flow rate for biofilter experiments (T variable, 0psig) 72

Table 5.4 Relative experimental mass flow rate and percent removal of gas species in system under varying experimental conditions 74

Table 5.5 Theoretical inlet gas composition - Stream 1 (25^oC, 1atm) 77

Table 5.6 Theoretical inlet liquid composition – Stream 2 (40mL/h) 77

Table 5.7 Solubilisation rates of gas components in system, calculated with ChemCad 6.0 . 80

Table 5.8 Mass flow rate and accumulation of each process stream of biofilter (Inlet 7.5L/h dry gas, 25^oC, 1atm) 84

Table 5.9 Experimental mass flow rate of inlet and outlet biofilter gas process streams (7.5L/h dry gas inlet, T and P variable) 85

Table 5.10 Theoretical mass flow rate of inlet and outlet biofilter gas process streams (7.5L/h dry gas inlet, 25^oC, 1atm) 85

Table 5.11 Difference of theoretical and experimental inlet and outlet biofilter gas streams 85

Table 6.1 Biofilter startup and acclimatization: Operation conditions 101

List of Abbreviations

C_{in}	inlet pollutant concentration	g/m^3
C_{out}	outlet pollutant concentration	g/m^3
d	diameter	m
d_p	diameter of particle in the packed bed	cm
EC	elimination capacity	g/m^3h filter bed
EBRT	Empty bed residence time	seconds
G	superficial mass velocity	–, g/cm^2s
h	height	m
$[_{H2S}]$	H_2S concentration	ppm_v or $\%_{vol}$
$H_A(T)$	Henry`s law constant of species A at a temperature T	atm
L	pollutant loading	g/m^3h filter bed
$\dot{m}_{A_{In}}$	inlet mass flow of gas species A	g/h
$\dot{m}_{A_{Out}}$	outlet mass flow of gas species A	g/h
Δm_A	difference in relative mass flow rate of gas species A	--
$\dot{m}_A(k)$	mass flow rate of species A in stream *k*	g/h
$m_{A\ sol}$	mass rate of gas species A solubilised in biofilter	g/h
M_{dry}	mass of dry packing	g
$M_{residual}$	mass of water remaining in 'wetted' packing material	g
M_{wet}	mass of 'wetted' packing	g
$n_A(k)$	moles of species A in stream *k*	mols
$\dot{n}_A(k)$	molar flow rate of species A in stream *k*	mols/h
$\dot{n}_A(metab)$	molar flow rate of species A metabolized in biofilter	mols/h
$n_{air}(1)$	molar flow of components in dry air	mols/h
$n_{biogas}(1)$	molar flow of components in dry biogas	mols/h
$n_{humidair}(1)$	molar flow components in inlet humidified air stream	mols/h
n_T	total molar flow	mols/h
Δp	pressure drop	psi
p_A	partial pressure of species A	atm
$p^*_A(T)$	vapour pressure of species A, at temperature T	mmHg

P_T	Total pressure	atm
Q	gas flow rate	m^3/h
r	radius	m
R_A'	relative removal of gas species A	%
RE	removal efficiency	%
S_{cell}	Sulphur bound in the cell	--
SurfaceArea	surface area of packing material	cm^2
SurfaceRatio	surface ratio of packing material	cm^{-1}
SV	space velocity	$seconds^{-1}$
t_{sat}	time to reach saturation in biofilter for gas species	seconds
u	superficial velocity	cm/h
V	volume of biofilter bed	m^3
$V_{residual}$	volume of water in 'wetted' packing material	mL
V_{total}	total volume of packing material	mL
V_{void}	void volume of dry packing material	mL
$V_{voidwet}$	void volume in 'wetted' packing material	mL
Water%	water content of 'wetted' packing material	%v/v
x_A	mass fraction of species A	--
y_A	mole fraction of species A	--
ε	porosity	--
ρ	density	g/L
ρ_{bulk}	bulk density of packing material	g/mL
$\rho_{particle}$	particle density of packing material	g/mL
τ	residence time	seconds
μ_G	gas viscosity	g/cm s

Chapter 1
Introduction

Biogas is the result of the anaerobic digestion process, and has a promising use in energy generation with 40-70% methane present in the gas. Using biogas in energy production is useful not only as a renewable energy source, but also because it captures and uses green house gases normally emitted into the atmosphere. Biogas is presently used in heating and in turbines for electricity production.

Anaerobic digestion is the process in which organic materials are degraded by anaerobic bacteria completing methanogenesis, and creating methane. This process is present in landfills, sewage sludge, and biomass digesters. The resulting biogas contains 55-70%$_{vol}$ methane (CH_4), 30-45% $_{vol}$ carbon dioxide (CO_2), and 0-1.5%$_{vol}$ hydrogen sulphide (H_2S); the exact composition depending on the feedstock and the anaerobic digestion conditions.

Biogas has limited use in energy generation due to the presence of H_2S. The H_2S present converts to sulphuric acid when combusted, and creates corrosion in the combustion chamber, especially with levels in excess of 100ppm H_2S in the biogas. By removing the H_2S present, the use of biogas can expand from heating and generators, to applications such as diesel engines.

1.1 Objectives of Study

This project focuses on a hydrogen sulphide removal technique of biogas created in a small scale farm installation. The technology chosen was required to be effective, inexpensive, reliable and robust for long-term use under variable conditions. Many of the current H_2S removal techniques are chemically based with high material costs and secondary pollution concerns. Although effective, generally these techniques are better suited for high budget, large scale installations treating large quantities of H_2S laden gas, which is not the case for a farm scale biogas purification unit.

Biofiltration was investigated for this application. Biofiltration uses microorganisms living in a support matrix to degrade the pollutant present into a secondary form. This emerging technology has uses in both gas and water purification, and is an inexpensive and robust alternative to chemical purification techniques.

This thesis focus on the development and assessment of a lab scale biofiltration system to remove H_2S from a biogas stream, with a specific focus on the use in small scale farm applications. This includes the design considerations such as type of biofilter, packing material, inoculum source and

conditioning of inoculum for use in the biofilter. The capacity of the designed biofilter was then tested using synthesized biogas under increasing rates of H_2S loading.

Chapter 2
Literature Review

2.1 Biogas Composition

Biogas is a mixture of gases including methane (CH_4), carbon dioxide (CO_2), and hydrogen sulphide (H_2S), and is the end product of the anaerobic digestion process, which is discussed in detail in 2.2. Biogas composition typically ranges from 55-70%$_{vol}$ CH_4, 30-45%$_{vol}$ CO_2, 0-1.5%$_{vol}$ H_2S, and is saturated with water (Schomaker et al. 2000). This can be an acceptable substitute of natural gas that is composed of 85%CH_4, with CO_2, N_2 and C_2H_6 making up the rest (Schomaker et al. 2000). Table 2.1 presents typical biogas composition, depending on the production source. The content of H_2S is highest from biogas produced from organic waste.

Table 2.1 Composition of biogas, depending on source (Rasi et al. 2007)

	units	Organic Waste	Sewage	Landfill
Methane	%$_{vol}$	60-70	55-65	45-55
Carbon Dioxide	%$_{vol}$	30-40	35-45	30-40
Nitrogen	%$_{vol}$	<1	<1	5-15
Hydrogen Sulphide	ppm$_v$	10-2000	10-40	50-300

More specifically, the H_2S content from landfill biogas is reported to be 1 to 1700ppm$_v$, with an average of 132ppm$_v$ (EIA, US department of Energy 1997). The biogas produced from organic waste on a farm can differ depending on the feed stream. Biogas from pig slurry contains 70-80%$_{vol}$ CH_4, 55-75% $_{vol}$ CH_4 for cow slurry, 60-80%$_{vol}$ CH_4 for chicken slurry, and 70-80% $_{vol}$ CH_4 for food slurry (Schomaker et al. 2000).

Biogas can also contain trace amounts of other compounds such as siloxanes and aromatic and halogenated compounds. Due to high vapour pressure and low solubility, volatile organic compounds (VOCs) are also present in biogas, and more prominent in biogas originating from landfills (Rasi et al. 2007). Water vapour is also present in the biogas stream after the anaerobic digestion process. Although water would need to be removed before use for most energy applications, this is not a focus in this study.

The H_2S present in biogas is both flammable and highly toxic. With exposure to 50ppm H_2S, headaches and dizziness result and exposure to levels above 300ppm can be fatal. As such, the presence of H_2S in biogas causes concerns for both safety and corrosion in energy applications.

2.2 Anaerobic Digestion

2.2.1 Anaerobic digestion process

Anaerobic digestion is a naturally occurring microbiological process present in an oxygen free environment. The bacteria species responsible for anaerobic digestion are specific to this oxygen free environment, and for some of the species present, oxygen can be fatal. Anaerobic digestion incorporates a number of microbial reactions breaking down an organic feed. A typical anaerobic digestion process is illustrated in Figure 2.1 for an organic feed that consists of carbohydrates, proteins, lipids and salts. The microbial population in anaerobic digestion is determined in part by the feedstock composition, and can be affected by sudden changes in its composition (Hobson and Wheatley 1993).

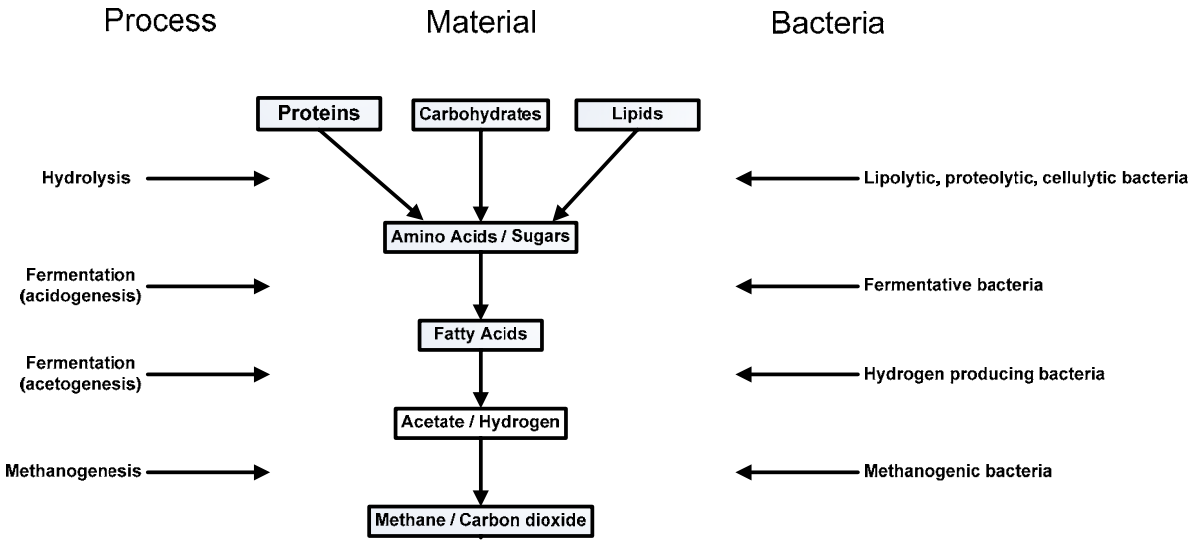

Figure 2.1 Typical anaerobic digestion process (adapted from Schomaker et al. (2000))

Anaerobic digestion happens in three steps according to Figure 2.1: hydrolysis, fermentation (both acidogenesis and acetogenesis) and finally, methane fermentation (Yadvika et al. 2004). Hydrolysis involves the enzyme mediated transformations of larger compounds and insoluble organic material (ie. lipids, proteins etc.) into soluble organic materials for an energy source and cell carbon. (ie. amino acids, monosaccharides etc.) This is carried out by anaerobic microorganisms such as *Bactericides*, *Clostridia* and *Streptococci*. In acidogenesis and acetogenisis, another group of microorganisms ferment the products into acetic acid, H_2, CO_2, and lower weight simple organic acids. In the final step of methane fermentation, the compounds are converted to a mixture of methane and carbon dioxide with the help of methanogenic bacteria. These bacteria include *Methanothrix*, *Methanococcus*, and *Methanobacterium* (Yadvika et al. 2004). H_2S is produced in the anaerobic digestion process through the breakdown of sulphur salts in the feed. The amount of H_2S in the outlet is dependent on the feed composition (Hobson and Wheatley 1993).

2.2.2 Operating parameters and optimization of anaerobic digestion

Optimization of anaerobic digestion to enhance biogas production is highly dependant on the operating parameters including temperature, pressure, retention time, loading rate, volume, with consideration of the microbial population. There are also a number of possible enhancement techniques for biogas production from an anaerobic digester including the use of additives, stream recycling, and variation of operating parameters (Yadvika et al. 2004). Microbial activity in anaerobic digestion can be aided by the addition of biological or chemical additives.

The temperature ranges for anaerobic fermentation include psychrophilic (<30^{o}C), mesophilic (30-40^{o}C), and thermophilic (50-60^{o}C). Anaerobic bacteria are more active in the mesophilic and thermophilic range, and extent of fermentation is dependant on the system temperature (Yadvika et al. 2004). Operation in the mesophilic or thermophilic range is desired with the optimum of mesophilic generally at 35^{o}C, and thermophilic at 55-60^{o}C (Hobson and Wheatley 1993). The pH is generally kept in the range of 6.8-7.2, but pH will change based on the amount of CO_2 and volatile fatty acids produced during the process. The feedstock can be pre-treated with an alkali or acid, or buffering solution can be added to the digester (Yadvika et al. 2004).

Particle size has an effect on anaerobic digestion, with smaller particles providing a larger surface area of substrate, resulting in an increase in microbial activity (Yadvika et al. 2004). Agitation is

important to ensure contact between the microorganisms and substrate. Hydraulic retention time and loading rate can be optimized based on the size of the digestion process and the digestion ingredients. Retention time depends heavily on temperature, as discussed above.

Bacterial and fungal strains have been found to enhance gas production by stimulating certain enzymes. Other biological additives can be used including plants, weeds, and crop residues. The suitability of the additive depends on the substrate type present (Yadvika et al. 2004). Inorganic additives can also be used including metal cations, iron salts, and chelating agents (Yadvika et al. 2004). Recycling of the digester slurry can mean that the microbial population is not discarded, and this can enhance production. This provides additional microbial population, while also conserving water (Yadvika et al. 2004). A study performed by Lastella et al. (2002) showed that in the anaerobic digestion of fruit and vegetable waste with and without recycling, recycling of digested sludge improved the biogas production as well as increased the methane content in the resulting biogas.

2.3 Chemical Hydrogen Sulphide Removal Techniques

2.3.1 Adsorption H_2S removal techniques

Adsorption is the process of a liquid or gas binding to a solid adsorbent. There are various adsorption media for the removal of H_2S including activated carbon, iron oxide, silica gel and others. A summary and comparison of adsorption techniques investigated is found in Section 2.3.2.

Activated carbon is commonly used for its high surface area, and catalytic properties. Functional groups and free valences present take part in the oxidation of sulphur containing gases to elemental sulphur and sulphuric acid (Yuan and Bandosz 2007). Only a relatively small quantity of H_2S can be retained on virgin, unmodified activated carbon. Even with surface treatments and impregnation, the cost of activated carbon often outweighs its effectiveness. Other drawbacks include blocking of the small pore sites and the formation of sulphuric acid (Yuan and Bandosz 2007).

The use of iron oxide pellets is a traditional H_2S removal technique. Ferric oxide (Fe_2O_3) results in the formation of ferric sulphide (Fe_2S_3) with the addition of a H_2S laden gas stream, as follows in Equation (2.1) below (Kohl and Riesenfeld 1979)

$$2Fe_2O_3 + 6H_2S \rightarrow 2Fe_2S_3 + 6H_2O \quad (2.1)$$

With exposure to oxygen, the Fe_2S_3 is oxidized to elemental sulphur and ferric oxide

$$2\ Fe_2S_3 + 3O_2 \rightarrow 2\ Fe_2O_3 + 6S \quad (2.2)$$

Forming the overall reaction

$$6H_2S + 3O_2 \rightarrow 6\ H_2O + 6S \quad (2.3)$$

As the sulphur stays on the surface of the oxide, this process can be repeated only until the interstices between oxide particles are full, at which time the sulphur must be removed. The efficiency of this removal technique depends on the temperature, moisture content, and pH of the material used in purification. The ferric oxide process is advantageous due to the low cost, and the ease of operation and maintenance. Disadvantages include the large amount of heat released during regeneration. Also, this method of treatment is adversely affected with high water content in the inlet gas, and the toxicity of the dust from the packing (Kohl and Riesenfeld 1979).

Adsorbents derived from sludge for the removal of H_2S from a gas stream were studied by Yuan and Bandosz (2007). Two types of sludge were used in differing amounts for an adsorbent material. These included dewatered sewage sludge from a municipality and sludge from a metal galvanizing plant. The sewage sludge contained various transition metals, while the metal sludge samples had increased amounts of iron, zinc and sulphur. Main components were silica, iron and calcium compounds. Ferric oxide and lime are added as part of wastewater treatment, and were present in the sludge. Sewage and metal sludge were mixed in ratios of 50:50, 70:30, and 90:10 (mass ratio), and pyrolysis was then performed at different temperatures (650, 800, 950^oC) to create adsorbent materials. The adsorbents were ground (0.6-1mm diameter) and packed into a column (packed volume 23cm^3) receiving simulated biogas (60%vol CH_4, 40%vol CO_2, 0.1%vol H_2S, 25^oC). All tests were stopped when the breakthrough concentrations reached 100ppm of H_2S. The removal capacity was approximately 1200 gH_2S/m^3packing, and the efficiency depended on the type of adsorbent used and the level of humidification in the inlet gas stream. It was found that the metal adsorbent capacity decreased with increasing pyrolysis temperature, but the opposite was true for the sewage adsorbent. Some synergetic effects for adsorbents were found at high temperatures. It was also found that water enhances the performance by providing a film of small pores where hydrogen sulphide can dissociate and be oxidized to elemental sulphur. Overall, although there is less surface area in the sludge derived adsorbent samples than activated carbon, the surface chemistry enabled the sludge to have a higher H_2S removal capacity.

A commercially available adsorbent (Sulfatreat 400-HP®) was studied for the removal of H_2S from biogas created in landfill or anaerobic digestion by Truong and Abatzoglou (2005). The active ingredients in the adsorbent were a combination of iron oxides (Fe_2O_3, Fe_3O_4) and an activator oxide consisting of one or more catalytic metals such as platinum, gold, silver, copper, cadmium, and nickel. The activator oxide was thought to catalytically enhance the reactive adsorption phenomenon. The active ingredients were supported onto a calcinated montmorillonite; a non-porous silica matrix (SiO_2) with small amounts of alumina (Al_2O_3). This matrix is an aluminosilicate coming from montmorillonite (montmorillonite being a very soft phyllosilicate mineral). The silica particle diameter varied from 4.0 to 6.5 mm. Also, the active material had a relatively high internal porosity of 0.75. The process of H_2S adsorption was concluded to be irreversible; with three principle steps including external and internal diffusion, and adsorption on the active site. If was found that the rates of internal and external diffusion and surface reaction steps are relatively close. Truong and Abatzoglou (2005) were also able to predict that the rate of the process is near first order for H_2S concentration and zero order with respect to the adsorbent. A study of the efficiency was performed based on the properties of adsorbent, biogas flow rate, contact time, velocity of flow, concentration of contaminant and humidity of biogas. It was found that the presence of water enhances the reaction between H_2S and the media, with a breakthrough capacity of 0.11g H_2S for every 1g of adsorbent.

Silica gel particles were used in the removal of H_2S in experimentation done by Chou et al. (1986). The silica gel particles of dry mesh 6 to 8 were packed into a column with total packed volume of 3.3L. Biogas was fed into the column from a digester, therefore with slight variations in the biogas composition. The H_2S was selectively removed, while the CO_2 was only slightly absorbed onto the silica gel (<0.2%). The absorption of H_2S decreased rapidly after the silica gel became saturated (after 120 minutes), and the efficiency of H_2S removal dropped from 100% to 26% after 3 hours. It was found that water present in the gas stream significantly reduces the adsorption capacity for H_2S, as the binding sites are then used by the water.

2.3.2 Adsorption techniques efficiency and comparison

Influential factors in adsorption techniques for H_2S removal are summarized in Table 2.2. Adsorption techniques are usually initially effective, but can be limited for long term H_2S removal. There are a limited number of active adsorption sites for each material, and over time they become full. In some cases the adsorbent can be partly regenerated, increasing the longer term usability. Regeneration, however, could require the removal of the adsorbent packing from the system, as is the case for the

silica gel adsorbent, also requiring high temperatures for regeneration. Delays in regeneration could be avoided if there were more than one adsorption column, one being regenerated with the other being online. Depending on the design size and adsorbent amount, the length of time before breakthrough could be extended from the amounts seen in these studies.

Table 2.2 Comparison of factors for H_2S adsorption removal techniques

	Silica Gel Adsorbent	**Reactive Adsorbent**	**Sludge Derived Adsorbent**
Literature Source	Chou et al. (1986)	Truong and Abatzoglou (2005)	Yuan and Bandosz (2007)
Reactor type	Fixed bed, 3.3L	Packed bed, 0.16-0.3L	Packed column, 0.023L
Regeneration	Oven (150-175^oC)	Not possible	Not Performed
Inlet Stream	From digester, 114L/h, 1600 ppm_v H_2S	Simulated biogas, 20L/h, 3000-10,000 ppm_v H_2S	Simulated biogas, 9L/h, 1000 ppm_v H_2S
Water content in gas stream	Dewatered or else H_2S competes for binding sites	Saturated and unsaturated tested. Water enhances adsorption	Dry gas or 70% humidity tested. Water enhances adsorption
Length of Trial	6 hours	Up to 120 hours	1-4 hours
Removal Efficiency	100% for 90 min, then dropped quickly	100% for < 24 hours	100% for 3 hours for best type

As the biogas to be treated would be saturated with water, the implications with water content in the gas must be considered. As can be seen in Table 2.2, in both the studies with reactive adsorbents, (Truong and Abatzoglou 2005) and sludge derived adsorbents, (Yuan and Bandosz 2007), water enhances the H_2S removal. The use of either silica gel (Chou et al. 1986) or ferric iron (Kohl and Riesenfeld 1979) however has decreased H_2S adsorption in the presence of water, as the H_2O competes for the reactive and binding sites. As such, vigorous dewatering has to be done before the gas stream enters treatment. If this technique was to be used in most biogas purification processes, an extra step would be required. Adsorption techniques could be considered for use in purification of biogas for farm scale anaerobic digestion except that cost, regeneration, and general length of adsorption life are important factors to consider.

2.3.3 Absorption H_2S removal techniques

Absorption techniques used in air pollution control involve a contaminant present in a gas stream being absorbed into a liquid. Techniques for H_2S removal from a gaseous stream are described this Section, and summarized and compared in Section 2.3.4.

Iron oxide suspensions are used in absorption treatments for the removal of H_2S (Kohl and Riesenfeld 1979). In this process, H_2S first reacts with an alkaline compound; sodium carbonate or ammonia:

$$H_2S + Na_2CO_3 \rightarrow NaHS + NaHCO_3 \quad (2.4)$$

This is then followed by the reaction of hydrosulfide with iron oxide:

$$Fe_2O_3\ 3H_2O + 3NaHS + 3NaHCO_3 \rightarrow Fe_2S_3\ 3H_2O + 3Na_2CO_3 + 3H_2O \quad (2.5)$$

Regeneration occurs when the iron sulphide is converted to elemental sulphur and iron oxide with the addition of O_2

$$2Fe_2S_3\ 3H_2O + 3O_2 \rightarrow 2Fe_2O_3\ 3H_2O + 6S \quad (2.6)$$

Overall, this process is similar to the adsorption of H_2S using dry iron oxide. Some undesired sulphur compounds (thiosulfate, for example) can be formed due to side reactions present, depending on the operating conditions and the composition of the gas being treated (Kohl and Riesenfeld 1979).

The use of different metal sulphates as absorbents in the removal of H_2S from a gas stream was studied by ter Maat et al. (2005). This was based on the knowledge that sulphides of most bivalent metal ions are highly insoluble, including metals as zinc, copper, silver, magnesium, nickel, and tin. The reaction between H_2S and the bivalent metal ion can be shown as

$$Me^{2+} + H_2S + 2H_2O \leftrightarrow MeS\downarrow + 2H_3O^+ \quad (2.7)$$

The elementary reactions which complete this process, as well as those which interfere, are shown in Table 2.3.

Table 2.3 Elementary reaction scheme for absorption using metal sulphides (ter Maat et al. 2005)

Reaction (stoichiometry)	Equilibrium expression
$H_2S_G \Leftrightarrow H_2S_L$	$m_{H_2S} = \frac{[H_2S_L]_i}{[H_2S_G]_i} = \left(\frac{[H_2S]_L}{[H_2S]_G}\right)_{Equilibrium}$
$H_2S_L + H_2O \Leftrightarrow HS^- + H_3O^+$	$K_{a1_{H_2S}} = \frac{[HS^-][H_3O^+]}{[H_2S_L]}$
$HS^- + H_2O \Leftrightarrow S^{2-} + H_3O^+$	$K_{a2_{H_2S}} = \frac{[S^{2-}][H_3O^+]}{[HS^-]}$
$S^{2-} + Me^{2+} \Leftrightarrow MeS\downarrow$	$K_{sp} = [S^{2-}][Me^{2+}]$
$CO_{2,G} \Leftrightarrow CO_{2,L}$	$m_{CO_2} = \frac{[CO_{2,L}]_i}{[CO_{2,G}]_i} = \left(\frac{[CO_{2,L}]}{[CO_{2,G}]}\right)_{Equilibrium}$
$CO_{2,L} + H_2O \Leftrightarrow HCO_3^- H_3O^+$	$K_{a1_{CO_2}} = \frac{[HCO_3^-][H_3O^+]}{[CO_{2,L}]}$
$HCO_3^- + H_2O \Leftrightarrow CO_3^{2-} H_3O^+$	$K_{a2_{CO_2}} = \frac{[CO_3^{2-}][H_3O^+]}{[HCO_3^-]}$
$CO_3^{2-} + Me^{2+} \Leftrightarrow MeCO_3\downarrow$	$K_{sp} = [CO_3^{2-}][Me^{2+}]$

Note that CO_3^{2-} also can bind to the metal ion and precipitate out, which can cause competition at certain pH, depending on the metal ion present. It was found that when 10ppmv H_2S, 20%$_{vol}$ CO_2 (25^oC, 1atm) was contacted with a solution of 1M metal sulphate solution, the pH needed for precipitation differed, depending on the metal. With $FeSO_4$, the metal sulphide, metal carbonate, and metal hydroxide precipitated at a pH of 3.15, 2.55 and 5.85 respectively. $CuSO_4$ however, precipitated a metal sulphide at <0 pH, metal carbonate at pH 5.2, and a metal hydroxide at pH 7.7. This showed that $CuSO_4$ had a much larger pH range where the metal sulphide will precipitate out while the metal carbonate will not. Because of this reason, a pilot scale study was conducted using $CuSO_4$ as the metal absorbent. As such, experimentation was performed using $CuSO_4$ as an absorbent solution for H_2S removal. A summary of the experimental setup and the results can be seen in Table 2.4.

Non aqueous Fe(II)/Fe(III) solutions for the removal of hydrogen sulphide from a gas stream was studied by Hua et al. (2006). This was in relation to another absorption technology using an Fe-NTA (nitrilotriacetic acid) system consisting of two separate processes involving an aqueous catalyst system which converts H_2S to S and then a non-aqueous phase that absorbs CO_2, H_2O and other organic contaminants. It was identified that a more efficient process was required to remove H_2S as well as CO_2 and H_2O in one step (Hua et al. 2006). Various organic solvents were screened based on the solubility and stability of $FeCl_3$ in the solvent. $FeCl_3$ dissolves in a solvent to give a stable homogeneous solution. N-Methylpyrrolidinone (NMP) was the only solvent found to possess all the desired characteristics, including the ability to produce crystalline sulphur with high removal

efficiency. The hydrogen removal efficiency study was performed in a 2 chamber reactor with a flow between chambers. One chamber induced an oxidizing environment with an air stream entering, and the other chamber is an absorbing chamber with the absorbent solution. In the mechanism present, H_2S first is dissolved in the solvent, and then solvated H_2S reacts with Fe(III) solvate to form elemental sulphur. In the oxidizer chamber mix, the oxygen mixes with the solvent, followed by the dissolved oxygen regenerating the active Fe(II) solvate. When the solvent becomes saturated with dissolved sulphur, crystallization of sulphur occurs. The elemental sulphur does not precipitate out immediately, but remains in the organic solvent until the solvent becomes saturated and then precipitates out gradually in both the absorber and oxidizer zones. Overall, the reaction mechanism can be written as:

$$H_2S(g) + 1/2O_2\ (g) \rightarrow S(s) + H_2O \qquad (2.8)$$

If this technique is operated at elevated temperatures (60-70^oC), the solubility of sulphur increases. The crystalline sulphur can be harvested by cooling the reaction mixture (Hua et al. 2006). Although this technique is a batch process, it could be adapted to function continuously.

2.3.4 Absorption techniques efficiency and comparison

Table 2.4 summarizes the different H_2S absorption removal techniques. Both a lab scale and pilot scale analysis of the use of aqueous metal sulphate for absorption are presented, as well as absorption by the non-aqueous solution. The removal efficiencies of the three removal scenarios are high, including the pilot scale, which was able to reach the efficiencies of the bench scale using the same technology.

Table 2.4 Comparison of factors for H_2S absorption removal techniques

	Aqueous Metal sulphate	Pilot scale metal sulphate with $CuSO_4$	Non-Aqueous Absorbent
Literature source	ter Maat et al. (2005)	ter Maat et al. (2005)	Hua et al. (2006)
Reactor	Bubble column, 0.43L	Co-current down flow packed bed, 14L	2 Chambers: absorber and oxidizer, 1L each
Inlet stream	Simulated biogas, 50.9L/h, 10,000-40,000 ppm_v H_2S	Industrial biogas, 1400-3000L/h, 500-2000ppm_v H_2S	Air and H_2S, 42L/h, 2800ppm_v H_2S
Water content	Not mentioned	Not mentioned	Dehydration achieved by hygroscopic solvent
Removal efficiency	All 99% (if in appropriate pH range)	85-99% depending H_2S loading and absorbent flow	98.7% converted to S_8
Trial length	1 hour	< 80 hours	300 hours
Products	MeS, $MeCO_3$	CuS	S_8, (SO_3^{2-} and SO_4^{2-} <0.1%)

Water content of the inlet gas stream was not mentioned for the aqueous metal sulphate absorbent, but most likely this does not affect the removal efficiency as this is water based absorbent. In the non-aqueous experiment, Hua et al. (2006) mentioned that dehydration of the gas stream could be achieved by the hygroscopic nature of the solvent, and would likely not pose a problem. The products of the aqueous metal sulphate studies are only metal sulphides if kept in the correct pH range for the metal sulphate used. Although $CuSO_4$ appears to be an efficient absorbent removal technique, excessive foaming was an issue when this sulphate was used (ter Maat et al. 2005). Because of this and the requirement for specific pH ranges, aqueous metal sulphates appear to be more complicated than is desired for a farm based H_2S removal application. The non-aqueous technique described by Hua et al. (2006) appears to be effective, but using organic solvents for the removal of H_2S would be costly as well as have disposal considerations, as is the case with most chemical technologies offered for H_2S removal from biogas. Using absorbent technologies for H_2S removal in a farm scale application have the same drawbacks as adsorbent techniques, the cost and disposal considerations of chemicals as well as the added step of regeneration, if possible. Absorption techniques may also require large amounts of water (Schomaker et al. 2000).

2.3.5 Chemical oxidation for H_2S removal

Hydrogen sulphide oxidation happens both biologically and chemically. In wastewater treatment, biological sulphide oxidation is typically associated with colourless sulphur bacteria. The bacteria utilize energy derived from the following reactions: (van der Zee et al. 2007)

$$2HS^- + O_2 \rightarrow 2S^0 + 2OH^- \quad \Delta G^o = -169.4 kJ/mol \tag{2.9}$$

$$2HS^- + 4O_2 \rightarrow 2SO_4^{2-} + 2H^+ \quad \Delta G^o = -732.6 kJ/mol \tag{2.10}$$

Sulphide oxidation, both biological and chemical, is believed to start with the formation of polysulphides that can be protonated to form elemental sulphur. Oxidation continues to produce other species such as thiosulfate, sulphite and sulphate. Sulphide oxidation is faster than the re-reduction of oxidized species, as well as effective in competition for oxygen with other oxidative processes like aerobic oxidation of organic COD (van der Zee et al. 2007).

The possibility of removing H_2S with slight oxygenation of an anaerobic environment was studied by van der Zee et al. (2007). This was performed by introducing a limited amount of oxygen into an anaerobic digester to lower the level of H_2S in the biogas. Batch experiments were performed in order to determine the fate of the sulphur and oxygen compounds during micro-aerobic conditions. A low airflow of 0.7-0.9m^3/m^3day-reactor was introduced into the reactor, corresponding to an O_2/S molar ratio of 8-10. This was enough to reduce the outlet H_2S level to an undetectable value. The sulphide was oxidized to elemental sulphur, thiosulfate and polysulfide. After three weeks, the bioreactor was much faster in oxidizing sulphur than the bioreactor sludge with fully anaerobic conditions.

This method of H_2S removal may be less effective in a system with a variable inlet for anaerobic digestion, as the level of H_2S in the gas stream could change, creating an imbalance in the anaerobic environment due to the addition of O_2. This imbalance would affect both the microorganisms present in the anaerobic digestion process, as well as their efficiency. With process control however, this could be an effective technique in biogas purification as it reduces the H_2S removal step to inside the anaerobic digester.

2.4 Biofiltration Design

Biofiltration is an emerging technology used in pollution control. It can be used for both water and air purification, with a wide range of contaminants. Biofiltration uses biological means for the degradation of pollutants in either an air or water stream. This technology is chosen as a pollutant removal technique due to its low investment and operating cost, high removal efficiency, reliable operating stability and low amount of secondary pollution (Chung et al. 1996). The effectiveness of biofiltration relies on the microbial population, type of packing material and type of enrichment done in the inoculation process. The microbial population present in the biofilter determines the efficiency and overall outcome of the removal. The packing material used in the biofilter is also important as it houses the microbial colony and maintains an environment in which the microorganisms can grow and prosper. Once the biofilter is running, the efficiency is dependent on temperature, moisture content, pH, flow rate, contaminant loading rate and structure (Kim et al. 2008). A summary of design parameters for previous studies involving H_2S removal using biofiltration is found in Section 2.7, Table 2.7.

2.4.1 Type of biofiltration unit

There are three major types of biofiltration units; biofilter, biotrickling filter and bioscrubber. They differ mainly by the setup, not necessarily by the contaminants treated.

Biofilter

The biofilter is a fixed bed bioreactor where the microorganisms used in the degradation process are immobilized in a packing media. The contaminated gases pass through the porous media. The contaminants pass into the biofilm surrounding the packing material and microbial colony, where degradation occurs. Two types of biofiltration include open designed biofilters and enclosed design biofilters. The open design generally requires a large area, and is usually installed outside with only ascending gas flow. The closed biofilter has a more restricted volume and can have either ascending or descending inlet gas flow (Delhomenie and Heitz 2005). The nutrient solution and irrigation are added non-continuously, as seen in Figure 2.2.

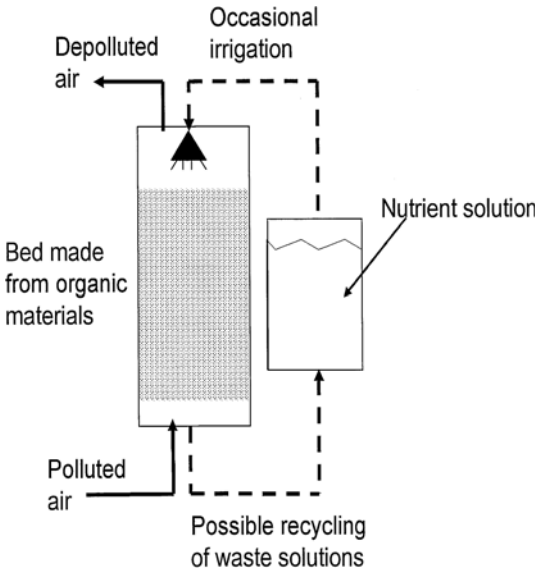

Figure 2.2 Typical biofilter design (Delhomenie and Heitz 2005)

Positive aspects of biofilters include low operating and capital costs and their self containment. Drawbacks include deterioration of packing material over time as well as being less suited for high concentration contaminants. Also, the moisture and pH are difficult to control and clogging and pressure drops may occur over time (Devinny et al. 1999).

Biotrickling filter

A biotrickling filter is similar to a biofilter except that the nutrient solution and irrigation is continuous. The polluted gas flows through a fixed bed, while the bed is continuously irrigated with an aqueous solution complete with nutrients needed for the microbial system. Some studies have shown that using a co-current versus counter-current flow system makes no difference to degradation performance (Delhomenie and Heitz 2005).

Biotrickling filters are more able to treat acid-producing contaminants as the acid gets washed to the bottom of the column with the nutrient solution. Also, a buffer could be added to the nutrient solution so that the packed bed is being continuously buffered. A biotrickling filter also ensures that the microenvironment is controlled as there is a continuous distribution of nutrient solution.

Some drawbacks of biotrickling filters include increased pressure drops, possible channelling and the creation of anaerobic zones (Delhomenie and Heitz 2005). This can also happen with biofilters, but will happen less as liquid is not continuously added.

Filtering materials for both a biofilter and a biotrickling filter must facilitate both gas and liquid flows through the bed while providing gas to biofilm transfers. This is in addition to a substance that resists crushing and compacting, as there would be a continuous water flow through it (Delhomenie and Heitz 2005). Because of this, generally the packing material chosen is inorganic as this ensures the longevity of the packing material (Delhomenie and Heitz 2005).

Bioscrubber

In general the bioscrubber is composed of an absorption tower and a bioreactor. The gas and liquid flow are counter-current to one another within the column. The absorption column can include packing, but it is not required. Packing can assist in increasing the transfer surface between the contaminant and the aqueous phase (Delhomenie and Heitz 2005). The microorganisms are suspended in the bioreactor in an aqueous growth medium.

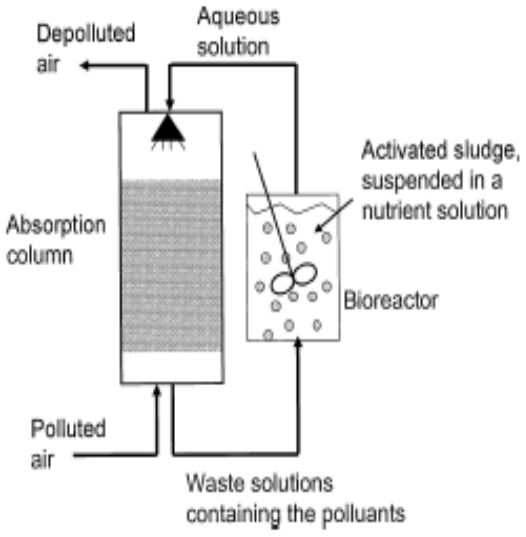

Figure 2.3 Typical bioscrubber design (Delhomenie and Heitz 2005)

Since the bioscrubber separates the absorption and the biological processes, both processes can be stabilized and optimized separately (Delhomenie and Heitz 2005). There are also no high pressure drops across the bed and installation space may be minimized. This design is adapted to convert highly soluble pollutants. One disadvantage is the production of sediment sludge at the base of bioreactor as well as waste water (Delhomenie and Heitz 2005). Also, there is added complication in such a system design as there are multiple steps.

2.4.2 Packing material

The choice of packing material is important to the design of a biofiltration unit. The packing material must have high surface area, as well as a surface that promotes microbial establishment and growth, while promoting gas exchange through the biofilm (Delhomenie and Heitz 2005). High porosity is also important to facilitate gas convection and homogeneous gas distribution throughout the bed. Water retention capacity is important for the enhancement of biofilm growth but also to ensure that the bed doesn't dry out and have permanent damage. The presence and availability of nutrients is also important, but this can be accomplished through the addition of extra nutrients. The presence of indigenous micro flora could be helpful, but can be accomplished by the addition of an enriched microbial colony (Delhomenie and Heitz 2005).

The filter bed material needs to have a consistent bed structure with limited compaction, decomposition and condensation. The packing material at the bottom of the column must be able to bear the weight of the material above it. Inert additives can help to minimize pressure drop issues by preventing compaction (Devinny et al. 1999).

The packing material can also have buffering capacities for systems with changing pH (as with H_2S biofiltration). The use of buffering materials such as limestone or crushed shells was studied, as well as the used of nutrient granules for the slow release of nutrients required in the system for nutrients or pH adjustment (Devinny et al. 1999). In most cases a homogeneous filter bed with high porosity or void volume of 40-80% will ensure gas plug flow and low pressure drop (Devinny et al. 1999).

Organic materials have both the presence of nutrients and water holding capacity, more so than inorganic packing materials. Most biofilter media include various proportions of biological residues including peat and compost with inert bulking agents such as activated carbon, wood chips, or beads. Organic materials can also be useful if the biofilter has a non-continuous inlet gas flow, to act as a secondary energy source. Peat is high in organic matter and surface area and has good water retention

capacity. Peat, however, does not contain high nutrient levels or an indigenous microorganism population. It is also naturally acidic and hydrophobic (Devinny et al. 1999). Composts are used frequently as they offer dense and more varied microbial population as well as good water holding capacity and nutrients. As compost breaks down however, it compacts and adds the complication of increased pressure drop. It has also been shown that common nutrients present in composts and other organic materials will be depleted over time in a biofilter (Delhomenie and Heitz 2005). Soils also can be limited in their effectiveness because they are prone to short circuiting and clogging. This can become a limiting factor in the biofilter performance over time.

Bacterial laden mixed agricultural residue was used for the packing material. The agricultural residue included rice husk, sawdust, and coconut coir (Rao et al. 2006). These materials offer advantages including low cost, a rich variety of indigenous microbial species, and an excellent biological medium for nutrient supply and growth and activity. Activated carbon is good, but very expensive (Chung et al. 1996). Pellets composed of sawdust and pig manure were used in a biofiltration study (Elias et al. 2002). The removal efficiencies were between 90 and 100% depending on the gas inlet velocity and the main by product of the biodegradation process was elemental sulphur, which accounted to more than 82% of the sulphur accumulated in the packing material. Sulphur deposition did not appear to clog the bed and flushing water through the inlet could easily clean the biofilter.

Inorganic packing material can be an effective support matrix for microbial growth. A study was done involving the comparison of four different inorganic packing materials including porous ceramics, cristobalite, obsidian, and granulated and calcinated soil. Various parameters were tested including water retention, porosity, mean pore diameter and removal rates with inoculated and non inoculated media. It was found that ceramics and obsidian were most effective (Hirai et al. 2001). A mixture of autotrophic sulphur oxidizing bacteria was immobilized in cell beads by Kim et al. (2008) and Chung et al. (1996). Porous biocompatible ceramics were used in a packed column for a bacterial support matrix (Lee et al. 2006). Other inorganic materials that have been used include gravel, plastics and glass.

2.5 Microbial Population For Hydrogen Sulphide Removal

2.5.1 Microbial colony

Microbial colonies are used in a biofilter to aid in degradation of pollutants present and to convert the pollutants into a more desirable chemical form. The functionality of a biofilter is highly based on the microorganisms present, and the selection of microorganisms for a biofilter is based on the composition of the inlet polluted stream.

All microorganisms require a carbon, energy, and electron source. Those acquiring carbon mainly from CO_2 are considered autotrophic, while those acquiring it from reduced or preformed organic molecules are considered heterotrophic. Microorganisms acquiring energy from light are considered phototrophs, while those obtaining energy from the oxidation of organic or inorganic compounds are considered chemotrophs. More specifically, organotrophs acquire electrons from organic molecules, while lithotrophs acquire them from reduced inorganic molecules (Willey et al. 2008). Most bacteria used in H_2S removal are chemolithotrophs as they obtain energy from the oxidation of H_2S, an inorganic compound. Both heterotrophic and autotrophic types of bacteria exist in H_2S removal.

Both isolated bacterial species and mixed colonies have been used in previous studies of H_2S removal. A number of biofiltration studies include the use of *Thiobacillus* sp.; or *Thiobacillus* sp. and *Acidithiobacillus* sp. as they are now divided. *Acidithiobacillus* are obligate acidiphiles, and were known before as autotrophic, acidophilic *Thiobacilli* (Robertson and Kuenen 2006). For example, *Acidithiobacillus ferrooxidans* and *Acidithiobacillus thiooxidans* are the current names, but have synonyms *Thiobacillus ferrooxidans* and *Thiobacillus thiooxidans*, respectively (Robertson and Kuenen 2006). As such, throughout this document these bacteria will appear as their current names unless reporting from a literature source that uses the synonym (or old) name.

Isolated species

A variety of isolated bacterial species have been studied for the elimination of hydrogen sulphide, including *Pseudomonas putida* (Chung et al. 1996), *Methanobacterium thermoautotrophicum* (Strevett et al. 1995), *Acidithiobacillus thiooxidans* (Lee et al. 2006) and *T. thioparus* CH11 isolated from pig manure (Chung et al. 2000). *Acidithiobacillus* sp. and *Thiobacillus* sp. are the most commonly used in biological H_2S removal strategies.

Pseudomonas putida belongs to the class of gammaproteobacteria. Many of these bacteria are chemoorganotrophic and facultatively anaerobic. They have respiratory metabolism with oxygen or nitrate as an acceptor, and some use H_2 or CO as the energy source (Willey et al. 2008). *Pseudomonas putida* is also known to be good at toluene degradation. *Methanobacterium thermoautotrophicum* is a strictly anaerobic methanogen obtaining energy from the conversion of CO_2, H_2, formate, methanol, acetate, and other compounds to either methane, or methane and CO_2. They are autotrophic when growing on H_2 and CO_2 (Willey et al. 2008). These bacteria were used in H_2S removal from biogas, while also degrading the CO_2 present, changing the CH_4 content of the biogas from 60 to 96%$_{vol}$ (Strevett et al. 1995).

Thiobacillus sp. are chemolithotrophic and highly diverse, and the most prominent of colourless sulphur bacteria. Many are unicellular rod-shaped or spiral sulphur-oxidizing bacteria, non motile, or motile by flagella (Willey et al. 2008). The members of the *Thiobacillus* sp. generally grow in soils and aquatic habitats (fresh water and marine). They can be appropriate for H_2S removal needs due to low nutritional requirements (Aroca et al. 2007). *Thiobacillus* sp. usually grow aerobically. They oxidize a variety of sulphur compounds including elemental sulphur, H_2S and thiosulfate to sulphate (Syed et al. 2006). In general, these species use S^0 and H_2S as an electron donor, O_2 or NO_3^- as an electron acceptor (depending if aerobic or not) and CO_2 as a carbon source (Syed et al. 2006). They are able to oxidize H_2S to elemental sulphur and store it in the cell. The elemental sulphur will be further oxidized to sulphite (SO_4^{2-}) when the concentration of H_2S is low (Chung et al. 1996). In general, all acquire energy from the oxidation of reduced sulphur compounds if they are provided with a terminal electron acceptor. The conditions that are required for this vary somewhat, for example pH (Robertson and Kuenen 2006).

Both *A. ferrooxidans* and *A. thiooxidans* grow in similar acidic environments from pH 2 to 4 for best growth (Robertson and Kuenen 2006), acidifying environments by sulphuric acid production. *T. ferrooxidans* having optimal growth from pH 1.3 to 4.5, and *T. thiooxidans* a pH growth range from 0.5 to 6, as seen in Table 2.5. The energy source and oxygen requirements of four *Thiobacillus* sp. are also summarized in Table 2.5.

Table 2.5 Growth conditions for *Acidithiobacillus* sp. and *Thiobacillus* sp. ((a)Robertson and Kuenen 2006; Syed et al. 2006))

Condition	Species			
	A. ferrooxidans	*A. thiooxidans*	*T. thioparus*	*T. novellus*
Synonym	*T. ferrooxidans*	*T. thiooxidans*	--	--
pH Growth	1.3 – 4.5	0.5 – 6.0	5 – 9	5.7 – 9.0
pH Optimal Growth	2 – 4[a]	2.0 – 3.5	6-8[a]	7.0
Temperature growth (^{o}C)	10 – 37	10 – 37	--	10 – 37
Temperature optimal (^{o}C)	30 – 35	28 – 30	28	30
Trophy	Obligate chemoautotroph	Obligate chemoautotroph	Obligate chemoautotroph	Mixotroph (facultative chemoautotroph)
Energy source	Ferrous ion, reduced sulphur compounds	H_2S, elemental sulphur, polithionates	Thiosulfate, sulphide	H_2S, dimethyl sulphide, methyl mercaptan
Oxygen Requirement	Facultative anaerobe	Strictly aerobe	Strictly aerobe	Strictly aerobe

It can be seen that *T. ferrooxidans* and *T. thiooxidans* differ from *T. thioparus* and *T. novellus* in pH range, as the final two species live at a more neutral pH. In general, colourless sulphur bacteria (including *Thiobacillus* sp. and *Acidithiobacillus* sp.) oxidize sulphur compounds by the following reactions (Robertson, 2006):

$$H_2S + 2O_2 \rightarrow H_2SO_4 \quad (2.11)$$

$$2H_2S + O_2 \rightarrow 2S^0 + 2H_2O \quad (2.12)$$

$$2S^0 + 3O_2 + 2H_2O \rightarrow 2H_2SO_4 \quad (2.13)$$

Common to all obligate and facultative autotrophic sulphur oxidizing bacteria is the ability to completely oxidize reduced sulphur compounds to sulphate (Robertson and Kuenen 2006).

More specifically, *T. ferrooxidans* uses ferrous iron as an electron donor and produces ferric iron as well as sulphuric acid. It is able to derive its energy from the oxidation of ferrous iron as well as reduced sulphur compounds. This is a known problem in acid mine drainage (Willey et al. 2008). The

following are reaction mechanisms for the oxidation of ferrous iron by *T. ferrooxidans* (Syed et al. 2006)

$$2FeSO_4 + H_2SO_4 + ½\ O_2 \rightarrow Fe_2(SO_4)_3 + H_2O \quad (2.14)$$

$$2FeS_2 + 7.5O_2 + H_2O \rightarrow Fe_2(SO_4)_3 + H_2SO_4 \quad (2.15)$$

Mixed Colonies

Using mixed colonies of bacteria for the removal of H_2S can be very effective and more stable over time than using isolated species. *Thiobacillus* sp. or a mix of other sulphur oxidizing bacteria are most commonly used. Studies have been done with such a population (Chung et al. 2000; Kim et al. 2008; Lee et al. 2006; Rao et al. 2006).

2.5.2 Inoculum source

Both pure cultures from culture banks and mixed or purified cultures have been used in sulphur oxidizing biofilters. Sludges or actived sludges are a common source for the conditioning of mixed sulphur oxidizing cultures, or in the purification of a single species. For H_2S removal purposes, activated sludge was taken from a wastewater plant of a resin producing industry (Jin et al. 2005b)), and another from sludge from a municipal wastewater treatment plant (Kim et al. 2008); both for the cultivation of a mixture of sulphur oxidizing bacteria. Pig feces and wastewater containing H_2S was used to isolate Pseudomonas putida CH11 (Chung et al. 1996). Enriched soil and activated sludge was used in the enrichment of 3 strains of *Acidithiobacillus thiooxidans* (Lee et al. 2006).

2.5.3 Inoculum conditioning

In general, bacterial enrichment using reduced sulphur compounds usually produces a mixture of acidophilic thiobacilli. Enrichment with Fe^{2+} rich solution is specific to *A. ferrooxidans*, as this characteristic to oxidize Fe^{2+} is unlike the other *Acidithiobacillus* sp. (Robertson and Kuenen 2006). *A. thiooxidans* is enriched in an acid media containing elemental sulphur as a substrate. This is not a media which is specific only to this species, and other acidophiles can grow. *T. thiooxidans* however can grow at a pH much lower than the other acidophiles, to pH 0.5 (Robertson and Kuenen 2006).

Several types of bacteria (including *T. ferrooxidans* and *T. thiooxidans*) can be cultivated using the same acidic mineral medium, but changing only the energy source. This basal mineral salt solution contains (%w/v): 0.2 $(NH_4)_2SO_4$, 0.01KCl, 0.025 K_2HPO_4, 0.025 $MgSO_4 \cdot 7H_2O$, and 0.001 $Ca(NO_3)_2$.

The pH is adjusted using 1N H_2SO_4 to 2-4. Both *T. ferrooxidans* and *T. thiooxidans* can be cultivated using this media by adding 1%(w/v) powdered sulphur. The sulphur was sterilized by heating at 105^oC for 0.5 hours on two consecutive days. As the pH is low for this nutrient solution, this amount of sterilization is enough. *T. ferrooxidans* can also be cultivated in the basal media described above containing 1- 4% (w/v) $FeSO_4 \cdot 7H_2O$ (Harrison 1984).

As stated by Vishniac and Santer (1957), *T. thioparus* can be cultivated using a media of 10g $Na_2S_2O_3 \cdot 5H_2O$, 4g KH_2PO_4, 4g K_2HPO_4, 0.8g $MgSO_4 \cdot 7H_2O$, 0.4 NH_4Cl, as well as 10mL of a trace metal solution, into 1L H_2O. *T. thiooxidans* can be isolated using the same media when adjusted to a pH of 3.5-4, showing a decrease to pH 2 after 2-3 days. *T. ferrooxidans* can also be grown using this media when adjusted to pH 2.5 (Vishniac and Santer 1957).

Inoculum in the study done by Rao et al. (2006) was prepared by combining a mixed aerobic bacterial culture from an activated sludge process reactor with *Thiobacillus* sp. media described by Vishniac and Santer (1957). This mixture was kept in an aerobic batch reactor for 15 days, replacing the media on alternating days. This enriched *Thiobacillus* sp. culture was then mixed with the agricultural residue and placed into the packed column.

Sludge taken from a soil treatment plant was used to inoculate various types of packing materials for H_2S removal experiments by Hirai et al. (2001). For analysis of types of microorganisms present and also enumeration, samples were streaked onto five different solid media; for heterotrophic bacteria a nutrient agar containing yeast, a Czapex-Dox agar for fungi, dimethyl sulfoxide agar for *Hypomicrobium* sp., thiosulfate agar for less acidophilic sulphur-oxidizing bacteria, and a modified Waksman gellan gum for acidophilic sulphur oxidizing bacteria. The last two medias are composed of (in g/L) 2 KH_2PO_4, 2 K_2HPO_4, 0.4 NH_4Cl, 0.2 $MgCl_2 \cdot 6H_2O$, 0.01 $FeSO_4 \cdot 7H_2O$, 8 $Na_2S_2O_3 \cdot 5H_2O$, 15 agar at pH 7 for the thiosulfate agar; and 8 KH_2PO_4, 0.1 NH_4Cl, 0.5 $CaCl_2 \cdot 2H_2O$, 0.3 $FeSO_4 \cdot 7H_2O$, 0.01 $Na_2S_2O_3 \cdot 5H_2O$, and 5 gellan gum at pH 4 for the modified Waksman media (Hirai et al. 2001).

Activated sludge from a wastewater treatment plant specifically for a resin producing industry was enriched for use in a biofilter treating H_2S. This enrichment was done in a solution with the same composition of the thiosulfate solution above, but in a water solution instead of agar (Jin et al. 2005b).

Before capsule immobilization for use in H_2S removal, Kim et al. (2008) conditioned municipal wastewater treatment plant sludge. The bacteria were placed in a rotary shaker in a mineral salt media

composed of (in g/L) 0.02g/L NH_4Cl, 0.01 $MgCl_2 \cdot 6H_2O$, 0.06 NaH_2PO_4, 0.06 Na_2HPO_4, 0.4 $Na_2S_2O_3 \cdot 5H_2O$, 0.01 $FeSO_4 \cdot 7H_2O$. These solutions with bacteria were left shaking at 150rpm at 30^oC for 30 days.

2.5.4 Inoculation

A lab scale biofilter incorporating microbial cells immobilized within a capsule was studied by Kim et al. (2008). This technique is able to provide high cell concentration and protection against sheer damage. The immobilization of the bacteria was done under aerobic conditions. A mixed microbial population was taken from municipal sewage and enriched in batch reactors as sulphur oxidizers in a well defined mineral salt media. The cells were harvested by centrifugation after cultivation of the autotrophic sulphur oxidizers at pH of 7 and 30±2^oC. The cells were mixed with sterilized sodium alginate solution and then with 7.5L of polyvinyl alcohol solution (PVA). The solution was freeze gelled into cubes and a cell concentration of 825mg/L obtained. Gel cubes or immobilized beads were then packed into pall rings so microorganisms could handle stresses better. The biofilter was constructed in an acrylic cylinder and randomly packed with the pall rings. A total packed bed volume of 6.5L was obtained (Kim et al. 2008).

Immobilized beads were also investigated by Chung et al. (1996). Heterotrophic *Pseudomonas putida* CH11 was isolated from pig feces and wastewater containing hydrogen sulphide. The bacteria cells were grown, washed and then immersed in 4% Na-alginate solution. The Na-alginate solution was then put into 4% $CaCl_2$ solution, which formed immobilized beads immediately, with a diameter of 3mm. The cells were immobilized to reduce the working height of the column, but also enhance the efficiency.

Sludge used as an inoculum source in a study done by Hirai et al. (2001) was seeded into the biofilter by soaking the inorganic packing material in the activated sludge used, and then adding it to the biofilter column. Another study, also involving a mixed culture taken from an activated sludge system, inoculated the packing material (a mixture of agricultural residue) by adding 1g of sludge for every 10g of filter material. This was then packed into the filter bed in layers with coconut coir so as to limit the compaction of the bed (Rao et al. 2006). In another study, a biofilter composed of plastic pall rings was inoculated by recirculating previously conditioned activated sludge through the packed bed of the reactor (Jin et al. 2005b).

2.6 Biofiltration Operation

2.6.1 Biofiltration operating parameters

Retention time

Two physico-chemical mechanisms that may limit the degradation taking place in the biofilter include pollutant diffusion transfer from gaseous state to biofilm, and the biodegradation reaction (Delhomenie and Heitz 2005). Depending on the flow rate and the concentration of pollutant entering the system, this can be controlled. The retention time must be long enough that proper diffusion can take place, and also that biodegradation can occur. If the input velocity is too high, then there is also the problem of stripping the water from the system (Delhomenie and Heitz 2005).

The residence time reported in literature refers to the empty bed residence time or residence time based on bulk volume, not based on void volume, summarized in Table 2.6. A study done by Rao et al. (2006) had a residence time that varied from 15 seconds to 150 seconds with an inlet pollutant concentration ranging from 275-2833 ppm. The efficiencies were >95% even at high concentrations, showing that the retention time chosen was effective, as well as the size of the unit in this application. Jin et al. (2005b) varied retention time from 11-85 seconds to verify the relationship between retention time and the removal efficiency, finding that with a retention time above 30 seconds, the removal efficiency of H_2S was 100%. An effective retention time of 30 seconds was also seen in another study (Hirai et al. 2001).

Oxygen content

Many of the H_2S removal studies using biofiltration involve the removal of H_2S from an air stream (Hirai et al. 2001; Jin et al. 2005a; Kim et al. 2008; Rao et al. 2006). As the oxygen present is unlimited, the amount of oxygen required for the biological H_2S removal from a biogas stream as well as the oxygen requirements of the sulphur oxidizing bacteria present has not been thoroughly investigated.

The addition of 4-6%$_{vol}$ air (0.8-1.2%$_{vol}O_2$) to biogas before biofiltration is to ensure proper sulphide conversion (Wellinger and Lindberg 2001). Soreanu et al. (2005) found that in a reactor with less than 3% $_{vol}$ O_2, >90% H_2S biological conversion was achieved. A 5%$_{vol}$ O_2 was also suggested by Schomaker et al. (2000) as being a low enough concentration of O_2 in the inlet gas to convert

biologically the H_2S present to elemental sulphur instead of SO_4^{2-}, which requires a higher amount of O_2. This difference in sulphide oxidation species is also reported by Duan et al. (2005) where 0.1mg/L was considered oxygen limiting conditions in which elemental sulphur would be the prominent end product from sulphide oxidation. This equates to $0.43\%_{vol}O_2$ in gaseous phase, calculated using Henrys Law, with $H_{O2}(25^oC)$ = 43,000atm. Sulphate would be the major product when sulphide was limiting.

Pressure drop

Pressure drop can be caused by a number of factors including packing materials, gas velocity, biomass growth and biofilter dimensions. Pressure drop is an indicator for physical dysfunctions in the biofilter including clogging, channelling, creation of anaerobic zones and can affect the overall performance (Devinny et al. 1999). Packing materials can be the cause of a pressure drop in the system due to low permeability. This happens due to small particles which offer high specific surface area, but can cause decreased gas flow. Over time this is further increased by the growth of biomass in the porous matrix. Larger particles offer a more constant gas flow, but lower surface area and therefore fewer sites for oxidation to occur (Delhomenie and Heitz 2005). Thus, it is a balance to find the best removal efficiency possible. Different designs of a biofiltration unit would help with this. Gas flow rate is also important for the pressure drop. The higher the superficial gas velocity, the more significant the pressure drop (Delhomenie and Heitz 2005). Overall, pressure drop can be remedied using mechanical, chemical or biological means (Delhomenie and Heitz 2005).

Temperature

The temperature of the process must be consistent with microbial requirements. *Thiobacillus* sp. grow in the temperature range of 10-39^{o}C with an optimum range around 28-32^{o}C (Syed et al. 2006). The inlet gas temperature and ambient temperature changes must be considered if biofiltration is to be thoroughly investigated as a biogas purification technique for small scale energy production.

Moisture content

Moisture content is an important parameter in biofiltration. A filter bed that is too dry can lead to bed desiccation and gas flow channelling, affecting the microorganisms. Also, after long periods of dryness a filter media that was originally hydrophilic could become hydrophobic (Delhomenie and Heitz 2005). On the contrary, a filter medium too wet can lead to decreased efficiency as the specific surface area for gas and biofilm exchange is decreased. It also causes bed compaction causing further complications (Delhomenie and Heitz 2005). The moisture content is influenced by the inlet gas moisture content and inlet gas flow, the holding capacity of the packing material, and reaction exothermicity leading to desiccation of the bed (Delhomenie and Heitz 2005). To avoid stripping the moisture from the column, the inlet air can be humidified. Moisture content of the biogas was found to be relevant in the study done by Rao et al. (2006). Minimum filter bed moisture levels of 55-65% were needed in order to maintain high removal efficiency. Biogas is generally fully saturated, making the moisture requirements in the biofilter less of a consideration.

pH level

Acid production and pH decrease can occur in the biofiltration of H_2S as the oxidation of H_2S by most bacteria can cause an acidic environment. In cases where the efficiency of H_2S removal is compromised due to a decrease in pH, buffers solutions can be added. This includes buffer material added to the packing material at the start to last the lifetime of the medium, or the addition of a buffer solution with the irrigation water or nutrient stream. The acidic regions will tend to be more concentrated where more biological activity is occurring (Devinny et al. 1999).

The optimal pH differs depending on the type of bacteria present, with either *Acidithiobacillus* sp. or *Thiobacillus* sp. showing the greatest differences. As is summarized in Table 2.5, the optimal pH of *Acidithiobacillus sp*. is much lower (pH 2-4) than that of *Thiobacillus* sp. (pH 6.5-7.5) (Syed et al. 2006). In a study done by Degorce-Dumas et al. (1997), calcium carbonate was added (10%w/w) and mixed with packing material to a pH of 7.5-7.8. It was found that this environment enabled a longer period of complete efficiency as well as the growth of heterotrophic bacteria, but was then disadvantageous to the acidifying thiobacilli population. Stabilization of pH around neutral can prolong the life of the biofilter, as was reported in a study by Degorce-Dumas et al. (1997) involving a biofilter inoculated with dry wastewater sludge. It was found that the initial population of bacteria

diminished with acidification of the packing, which was followed by an increase in the acidifying autotrophs present.

In a study done by Jin et al. (2005b), a biofilter containing sludge conditioned with a thiosulfate medium showed an initial drop in the pH of the outlet solution from 7 to 2 within 12 hours. When tested with changing pH in the trickling nutrient addition, it was found that the elimination capacity began to diminish with pH values less than 3-4. It was also found that with high sulphate content (1900mg/L) in the recycled nutrient stream, the H_2S removal efficiency decreased rapidly after 30 hours of operations at a pH of 2. Most likely this would not be the case with a non-recycled nutrient stream added. Soreanu et al. (2005) reported that a drop in the pH to 2-3 did not affect the performance of the biofiltration system in the removal of H_2S. Thus, the need for neutralization and addition of buffers is dependent on the population of bacteria present in the biofilter, since both sulphur oxidizing bacteria living at neutral or more acidic pH can exist.

2.6.2 Summary of biofilter sizing and removal rates

Table 2.6 displays loading ranges for different H_2S removal studies using biofiltration. The loading rates are based on the sulphur or H_2S removed per unit volume of packing per hour, and thus is not based on the actual volume representing where the degradation occurs (void volume). The loading rates vary depending on the experiment, with $155 g H_2S/m^3 h$ of packing being the highest (Hirai et al. 2001). As the biofilter in the study by Soreanu et al. (2005) had a large volume, the loading rate was lower than those seen in other studies. The residence time varies between studies also, from 15 to 155 seconds (Rao et al. 2006). Overall, the studies summarized give a range of parameters values in effective biofilter size estimation.

Table 2.6 Biofilter operation conditions for H_2S removal

Literature Source	Hirai et al. (2001)	Rao et al. (2006)	Soreanu et al. (2005)
Inlet concentration (ppm_v)	0-2100	275-2833	1000-4000
Inlet flow (L/hr)	42	128-927	10-70
Residence time (sec)	30	15-155	612-4320
Loading rate (gH_2S/m^3h packing)	155	91	11.25-14.58
Packing volume (L)	0.35	3.87	12
Packing type	Various inorganic	Agricultural residue	Plastic fibres

2.6.3 Nutrient addition

The biofilter containing mixed agricultural residue designed by Rao et al. (2006) required minimal nutrient addition due to the organic packing. To minimize a decrease in pH, $CaCO_3$ was added to the packing material at 500mg $CaCO_3$/10mg material to act as a buffer.

In a study done by Degorce-Dumas et al. (1997) with a 2.27L biofilter composed of wastewater sludge and peat packing material treating an H_2S laden (250-3260mg/m^3) air flow at 16m/h, a nutrient solution was added to the unit at a rate of 60mL/day. This solution was composed of (g/L) 75 glucose, 0.85 K_2HPO_4, 0.67 NaH_2PO_4, 2 NH_4Cl, and was not recycled.

Nutrient addition to the 2.83L biofilter composed of plastic pall rings (Jin et al. 2005b) was added at a flow rate of 0.75-12.13L/h, with a composition of (g/L) 2 KH_2PO_4, 2 K_2HPO_4, 0.4 NH_4Cl, 0.2 $MgCl_2 \cdot 6H_2O$, 0.01 $FeSO_4 \cdot 7H_2O$. This solution was the same as the inoculum conditioning solution, with the exception of the 8g/L $Na_2S_2O_3 \cdot 5H_2O$ that was omitted. This solution was recycled.

In the study using immobilized conditioned bacteria (Kim et al. 2008), a nutrient solution was added with the composition (g/L) 0.2 $MgCl_2 \cdot 6H_2O$, 0.78 NaH_2PO_4, 0.89 Na_2HPO_4, 0.00075 $CaCl_2$, 0.01 $FeSO_4 \cdot 7H_2O$, $8x10^{-5}$ $CuSO_4$, 1 $NaHCO_3$. This solution was added to the 6.5L packed bed at a rate of 500mL/min for 1 minute every 30 minutes. This nutrient solution was recycled, and was replaced with a fresh solution every 48 hours.

2.7 Biofiltration Operating Conditions

Comparison of important factors in biofiltration study and design are summarized in Table 2.7. Those studies discussed in this review, including those in Table 2.7, utilize an inlet gas stream of air and H_2S to simulate the removal of H_2S from a biogas stream. This gives an indication of H_2S removal efficiencies using biofiltration, but cannot be used to assume that the behaviour would be the same if biogas was present in the inlet stream.

It can be seen that biofilters for hydrogen sulphide removal use either organic or inorganic packing material, as well as cell laden beads. The inoculum sources are generally conditioned from bacteria rich sources, such as sludges. In all studies except that done by Hirai et al. (2001), an inoculum conditioning stage was performed in which the sludge was conditioned outside of the biofilter, enabling a faster biofilter startup period as the desired bacteria were already selected.

Table 2.7 Factors in biofiltration design for H_2S removal, various studies

	Hirai et al. (2001)	Jin et al. (2005b)	Kim et al. (2008)	Rao et al.(2006)
Biofilter type	biofilter	biotrickling filter	Biofilter	Biofilter
Feed Components	H_2S and air	H_2S and air	H_2S and air	H_2S and air
Inlet H_2S concentration (ppm)	0 to 2100	0 to 190	10-130	275 - 2833
Inlet flow	42 L/h	300 to 420 L/h	loading rate: 0.1-13 gH_2S/m^3h	128 to 927L/h
Packed bed Volume (L)	0.98	2.83	6.5	3.87
Residence time (sec)	30	11 to 85	51 and 32	15 to 155
Operating Temp (^oC)	22	Not discussed	30	30+/- 5
pH	held above 2, $NaHCO_3$ added	2 to 7	not measured	8.9 initial, 4.1 final
Type of packing	4 inorganic types compared	plastic pall rings	immobilized beads packed in pall rings	rice husk, sawdust, bagasse, coconut coir (equal amt)
Liquid addition	40 mL/day, bed at 70-80% moisture	2.77 to 12.13L/h	500mL/min, once ever 30 min	Inlet humidified
Inoculum Source	sludge from soil treatment plant	activated sludge from resin-producing industry wastewater	sludge from municipal wastewater plant	act sludge from reactor treating distillery wash
Inoculum conditioning	None	sodium thiosulfate mineral medium	batch reactors in mineral salt media for sulphur oxidizers	mixed with *Thiobacillus sp.* media, in aerobic batch reactor
Inoculation	soaked packing in sludge	sludge recirculated through filter	made gel cubes of cells in sodium alginate solution. Then packed them into pall rings	filter material mixed with inoculum (1g/10g filter material)
Acclimatisation	800ppm and space velocity 10/h for 12 days	Not discussed	12ppm for 5 days	275ppm for 20 days
% Removal	99% if $[H_2S]$ < 1200ppm (packing dependant)	99% with EBRT 28-84sec	82 - 99%: 99% if loading < $6gH_2S/m^3h$	over 99% if $[H_2S]$< 2020ppm
Removal capacity ($g\ H_2S/m^3h$)	154	22.5	6 to 8	91
Length of trial (days)	50-60	Not discussed	66	150

The removal capacity is seen as the highest loading rate attempted in the biofilter study which resulted in a sufficient H_2S removal rate (>95%), represented in weight of sulphur (or H_2S) per volume per hour of packing bed. Overall, the removal efficiencies remain highly efficient, even with the variation in loading rates present (seen as removal capacity). As displayed in Table 2.7, removal efficiencies with biofiltration can be very high if proper considerations are taken.

The production of biogas is a dynamic process, and as such there can be inconsistencies in the biogas produced. This is true for all components of biogas, including the H_2S content. Therefore, having an H_2S removal technology with high removal efficiencies with variable inlet H_2S content is crucial. The ability of a biofilter to adjust efficiently to changes in the inlet H_2S feed loading confirms this technology as an ideal candidate for use in biogas purification. Similarly, the ease of design and operation as well as the low initial and operating cost makes biofiltration a viable candidate for biogas purification in a small scale application such as farm use.

2.8 Biofiltration Mechanisms

2.8.1 Physico-chemical H_2S removal mechanisms

Biofiltration incorporates adsorption, absorption and oxidation. The biofiltration mechanism for hydrogen sulphide happens in two steps: first, the hydrogen sulphide absorbs into the liquid film and is adsorbed on to the solid medium. The hydrogen sulphide is then metabolized by the cells present on the biofilter solid support matrix (Chung et al. 1996). Continuous absorption of the contaminant into the biofilm surrounding the biofilter material is required for biodegradation. Also, high adsorption capacity is desired in the filter bed. This makes the system able to handle upsets in contaminant loading since there is a place for excess contaminant to adsorb onto the support material and await the metabolism step (Barona et al. 2005). Figure 2.4 illustrates adsorption, absorption and oxidation of H_2S occurring in a biofilter in the absence of microorganisms.

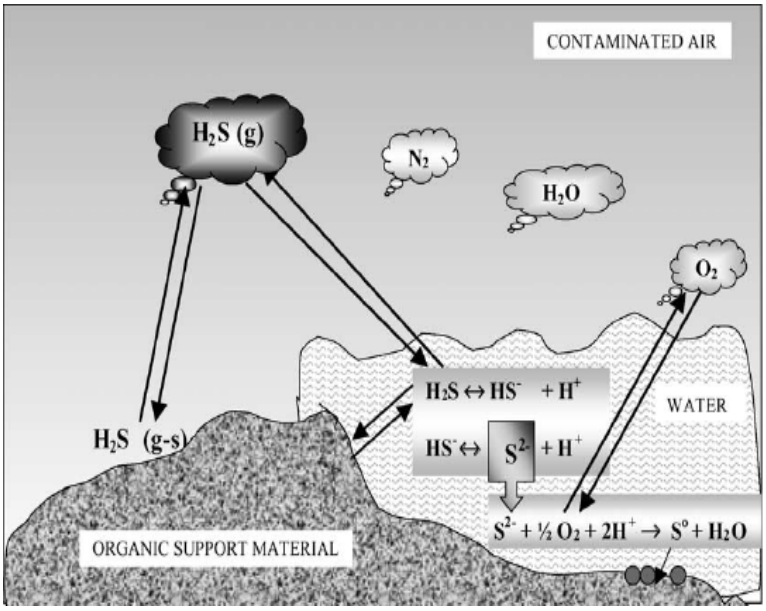

Figure 2.4 Adsorption, absorption and oxidation in biofilter, no microorganisms (Barona et al. 2005).

The distribution of gas in the liquid phase is governed by Henry's Law, correlating vapour pressure with its solubility in water. Hydrogen sulphide is highly soluble in water (pH dependant) with a very low Henry's Law constant, of 545 atm at 25°C (*Perry's Chemical Engineers' Handbook,* 1984).

$$y_{H2S}\, P_T = x_{H2S}\, H_{H2S}(T) \tag{2.16}$$

where y_{H2S} is the mole fraction of H_2S in gaseous phase, P_T is the total pressure, and x_{H2S} is the mole fraction of molecular H_2S in the liquid phase, and H_{H2S} is the Henry's law constant of H_2S in a specific solvent, in this case water. The solubility of H_2S in water is related to pH, as the increase in H^+ in solution will shift the dissociation of H_2S, displayed in the following reaction;

$$H_2S_{(aq)} \leftrightarrow HS^-_{(aq)} + H^+_{(aq)} \tag{2.17}$$

Then the dissociation of the bisulfide ion to sulphide ion

$$HS^-_{(aq)} \leftrightarrow S^{2-}_{(aq)} + H^+_{(aq)} \tag{2.18}$$

And finally ionization of water

$$H_2O \leftrightarrow H^+_{(aq)} + OH^-_{(aq)} \tag{2.19}$$

The reversible adsorption of a pollutant on the particle surface can be described by an equilibrium isotherm including linear, Langmuir or Freundlich, for example (Barona et al. 2005).

Methane and other short chain alkanes are generally more recalcitrant when treating volatile organic compounds in a biofilter (Delhomenie and Heitz 2005). As such, methane would remain undegraded in biogas purification. The mass transport in the biofilm resembles molecular diffusion in an aqueous phase, which can be represented by Fick's Law (Delhomenie and Heitz 2005). The removal rate of H_2S in the biofilter can be estimated using the Michaelis-Menten equation (Chung et al. 2000; Hirai et al. 2001).

2.8.2 Biological H_2S removal mechanisms

Sulphur cycling in an environment with microorganisms present was discussed (Syed et al. 2006). Figure 2.5 displays the sulphur cycle in a sulfuretum, indicating how different microorganisms degrade sulphides, depending on the environment. Where oxygen is available and there is a low sulphide concentration, as on the surface of water containing sulphur, chemoautotrophs metabolize the H_2S to produce SO_4^{2-}. Further down in the water, the environment is anaerobic but light still penetrates. Here, photoautotrophs convert H_2S into S^0. Where it is still anaerobic but with a high sulphide concentration, two reactions may take place, where SO_4^{2-} and organic sulphur are converted back into H_2S.

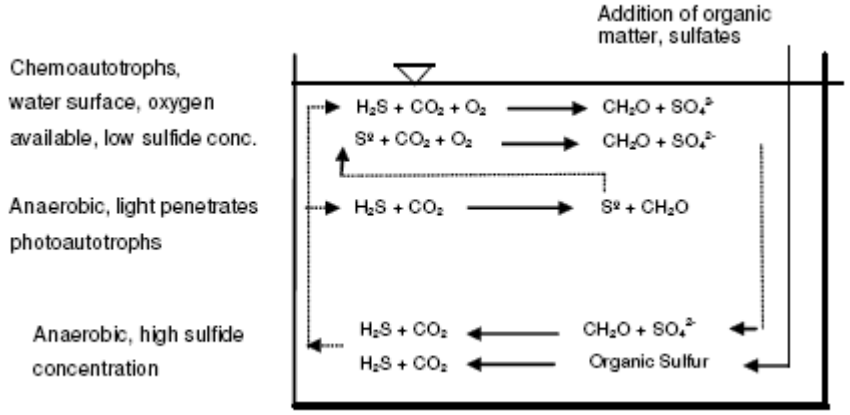

Figure 2.5 Sulphur cycling in sulfuretum (Syed et al. 2006)

Although this is different from a biofiltration system treating H_2S, some of the reaction mechanisms would be similar, as some of the zones resemble those found in a biofilter. In general, the removal of

H_2S in a biofilter can be represented by the following equation (Syed et al. 2006); thus displaying characteristics of the chemoautotrophic region at the waters surface as displayed in Figure 2.5 where oxygen is available, or in the middle of the sulfuretum where oxygen is limited.

$$H_2S + CO_2 + nutrients + O_2 \xrightarrow{chemotrophs} cells + S^0 and / or SO_4^{2-} + H_2O \quad (2.20)$$

When H_2S has incomplete oxidation, it is usually reflected by high values of SO_3^{2-} and S^{2-} (Syed et al. 2006). From this there could be a number of different H_2S metabolism pathways present in the biofiltration unit. The pathway of sulphide biological oxidation is (Duan et al. 2005)

$$H_2S \rightarrow S^0 \rightarrow S_2O_3^{2-} \rightarrow S_4O_5^{2-} \rightarrow S_3O_6^{2-} \rightarrow SO_3^{2-} \rightarrow SO_4^{2-} \quad (2.21)$$

The exact H_2S biological degradation mechanism depends heavily on the type of bacteria present. Chemotrophic bacteria are able to oxidize H_2S using O_2 as an electron acceptor. The electron donors could be S^0, H_2S, or $S_2O_3^{2-}$ (Kim et al. 2008). Devinny et al. (1999) and Soreanu et al. (2005) discussed simplified reactions present in both the absence and presence of oxygen. For aerobic environments:

$$H_2S + 1/2\ O_2 \rightarrow S + H_2O \quad (2.22)$$

$$H_2S + 2O_2 \rightarrow SO_4^{2-} + 2H^+ \quad (2.23)$$

And for anaerobic environments:

$$3H_2S + NO_3 \rightarrow 3S + 1/2\ N_2 + 3H_2O \quad (2.24)$$

$$3H_2S + 4NO_3 \rightarrow 3SO_4^{2-} + 2N_2 + 6H^+ \quad (2.25)$$

Those bacteria used in the anaerobic removal of H_2S are not discussed in detail here. Both aerobic and anaerobic conditions can produce a mix of S and SO_4^{2-}, and under aerobic but oxygen limiting conditions, sulphur is the major end product. When sulphide is limited instead of oxygen, sulphate is formed (Syed et al. 2006).

The oxidation of H_2S occurs in stages, where H_2S starts as the electron donor. The first oxidation mechanism results in elemental sulphur produced (Duan et al. 2005), (ΔG for Equations (2.26) and (2.28) calculated with HSC Chemistry 6, 0^oC)

$$2\ H_2S + O_2 \rightarrow 2S + 2H_2O \quad \Delta G = -209.03\ kJ/mol \quad (2.26)$$

$$2HS^- + O_2 \rightarrow 2S^0 + 2OH^- \quad \Delta G = -169.35 kJ/mol \tag{2.27}$$

If the supply of H_2S is diminished or depleted, energy can be obtained from the further oxidation of elemental sulphur to sulphate,

$$S^0 + H_2O + 1\ ½\ O_2 \rightarrow SO_4^{2-} + 2H^+ \quad \Delta G = -516.5\ kJ/mol \tag{2.28}$$

where ΔG is the Gibbs energy under standard temperature and pressure conditions (P=1atm, T=0^oC). These equations show the two step process involved in the oxidation of sulphide, including the initial oxidation of sulphur followed by the additional oxidation to sulphate. It can be seen from the Gibbs energy values that the initial oxidation requires less energy than additional oxidation to sulphate, via Equation (2.28). Oxygen limiting conditions ($[O_2] < 0.1mg/L$) results in elemental sulphur being the major end product, following Equations (2.26) and (2.27) (Duan et al. 2005).

In other cases, where sulphide is limited in place of oxygen, the final product in the oxidation process is sulphate (SO_4^{2-}) based on Equations (2.28), (2.29), (2.30) (Duan et al. 2005)

$$2HS^- + 4O_2 \rightarrow 2SO_4^{2-} + 2H^+ \quad \Delta G = -732.58 kJ/mol \tag{2.29}$$

$$S_2O_3^{2-} + H_2O + 2O_2 \rightarrow 2SO_4^{2-} + 2H^+ \quad \Delta G = -409.4\ kJ/mol \tag{2.30}$$

Thus, the intermediate products could be any of sulphur (S^0), thiosulfate ($S_2O_3^{2-}$), tetrathionate ($S_4O_6^{2-}$), trithionate ($S_3O_6^{2-}$), or sulfite (SO_3^{2-}) (Duan et al. 2005).

The oxidation of sulphide by dissolved oxygen in a sterile peat filled column was reported by McNevin et al. (1999). It was found that in the presence of an excess of dissolved oxygen and an absence of sulphur oxidizing bacteria, the sulphide undergoes a chemical oxidation:

$$S_2^- + ½\ O_2 + 2H^+ \rightarrow S^0 + H_2O \tag{2.31}$$

Thus, in the presence of sulphur oxidizing bacteria, it is thought that the elemental sulphur produced will be further oxidized to sulphate at a much lower rate. First the sulphur is bound in the cell (McNevin et al. 1999)

$$S^0 \rightarrow S_{cell} \tag{2.32}$$

Followed by the oxidation inside the cell

$$S_{cell} + 3/2\ O_2 + H_2O \rightarrow H_2SO_4 \tag{2.33}$$

The above reactions show that biotransformation is a very effective way of removing hydrogen sulphide from an air stream.

2.8.3 H_2S removal mechanisms specific for *A. ferrooxidans*

A. ferrooxidans oxidize ferrous iron by the following (Syed et al. 2006; Jensen and Webb 1995))

$$2FeSO_4 + H_2SO_4 + \frac{1}{2}O_2 \xrightarrow{A.\ ferooxidans} Fe_2(SO_4)_3 + H_2O \quad (2.34)$$

This is useful in the removal of H_2S from gas using ferric iron, as discussed in Section 2.3.3. The H_2S is removed from the gas in contact with ferric sulphate. The ferric sulphate solution absorbs and oxidizes the H_2S to elemental sulphur (Jensen and Webb 1995)

$$H_2S + Fe(SO_4)_3 \rightarrow S\downarrow + 2FeSO_4 + H_2SO_4 \quad (2.35)$$

The elemental sulphur is recovered from solution while the ferrous sulphate is reoxidized by *A. ferrooxidans* according to Equation (2.34) (Jensen and Webb 1995).

This suggests that in an environment where both ferric iron and H_2S are present with *A. ferrooxidans*, there could be oxidation of H_2S both chemically by the ferric iron present and biologically by *A. ferrooxidans*. Also, the reoxidation of the ferrous iron to ferric could be done by *A. ferrooxidans* present, creating a regenerating removal technique.

Chapter 3
Materials and Methods

3.1 Experimental Setup

The entire biofiltration system was composed of three major sections; gas inlet, biofiltration, and gas outlet. The various aspects of the biofiltration setup are discussed in the next sections in order from air inlet mixing with the biogas, to the biofilter, and finally the exiting gas to the atmosphere. Figure 3.1 displays the entire setup, including key pieces of instrumentation, discussed in the following sections. In addition, a list of pieces and reference numbers can be found in Appendix A, referencing the pieces found in Figure 3.1.

3.1.1 System components

Gas inlet incorporated the inlet of both the air needed for the microorganisms present in the system as well as the biogas to be treated. Air entered the system from a compressed air cylinder and was sent directly through a humidification column. This was done to ensure that the biofilter bed would not dry out as it would with a dry inlet gas stream. The humidification column was composed of a plexi-glass cylinder with internal diameter of 5cm and height 25cm. The top and bottom were secured by a plastic ring on either end that tightened against the main body via nuts and bolts. The cylinder was filled with water and gravel (3-6mm diameter). The packing was added to increase the contact surface area and thus the air to water contact. The air entered the humidification column at the bottom and then diffused through a membrane type gas diffuser (Coleparmer# 06614-25) to disperse the air.

After the humidification column, the humidified air stream entered a flow meter with controlling valve (Coleparmer #03219-03). At this point the air entered the gas mixing chamber where it mixed with the incoming biogas. The biogas was added after humidification so that the H_2S present will not change by dissolution in water. The synthetic biogas was supplied by Linde with composition 50%$_{vol}$ CH_4, 49.8 %$_{vol}$ CO_2 and 2000ppm$_v$ H_2S. Initially the 0.7m^3 bottles (#24084261) used were small enough to be placed in the ventilation hut. Larger bottles (3.7m^3) of the same composition (Linde #24088126) were later used, and were placed in the laboratory under a ventilation hood surrounded with plastic curtains.

To monitor pressures for equality of both the air and biogas lines, two manometers of range 0-15psi were installed on both the air and biogas inlet streams (Matheson #63-5615M). The flow of both gas streams were controlled with flow meters equipped with valves (Coleparmer #03219-11).

The gas mixing chamber was used to ensure the air and gas streams were well mixed before entering the biofilter. Each entering stream was equipped with a low pressure backflow valve (0.3psi) placed before the gas mixer. This further ensured that the proportions of biogas and air would be as desired by preventing back-flow of gases at varying pressures. The gas mixer was composed of a stainless steel tube of 1" diameter. There was a piece of stainless steel turned in a screw design inside. After this step, the mixed gas entered the biofilter after passing a gas sample port (Swagelok# SS-1VS4-X), and temperature (Precision Measurements, Type K) and pressure transmitter (Coleparmer #68075-14), described in more detail in Section 3.1.5.

The biofilter was composed of a plexi-glass column similar to the humidification column. The diameter was 5cm ID, with a height of 50cm. Designed the same as the humidification column, it had matching hard plastic rings on either end that tightened against the main body with a nut bolt system The mixed gas entered through a port in the bottom of the column where it passed through a gas diffuser (Coleparmer# 06614-25) to aid in more uniform gas distribution across the biofilter.

Nutrient solution was added via a 5L airtight enclosed reservoir (Fisher Scientific #02-923-11(bottle), #02-923-24 (lid)) and fed to the top of the biofilter with a peristaltic pump and L/S 16 Masterflex tygon tubing (Coleparmer #06409-16). A timer was used to control the nutrient addition interval by cutting power to the pump. A spray nozzle (Coleparmer #EW-832151-00) was placed inside the biofilter to aid in nutrient dispersion across the packed bed. The excess nutrient and waste solution from the biofilter exited from the bottom of the biofilter with 1/4" tygon tubing to an identical 5L reservoir as the inlet. There was no recycling of liquid between the inlet and outlet nutrient tanks, and the only communication between them was an air bridge to equalize the pressure.

The packing material used in both the humidification column and the biofilter was small untreated and uncoated gravel 3-6mm in diameter, like that found in an aquarium. An inorganic packing material was chosen to limit pressure drop across the biofilter while ensuring longevity of the packing material. Inorganic packing was also chosen to limit the unknown variables present in the system, including changes in nutrient content of the packing material over time, as would exist when using organic material. Small aquarium gravel was chosen based on availability and low cost, as well as suspected high surface area.

The exiting biofilter gas stream was positioned at the top of the biofilter, and was equipped with pressure (Coleparmer# 68075-14) and temperature transmitters (Precision Measurements, Type K), as well as a 3 way sample valve (Swagelok# SS-1VS4-X), described in detail in Section 3.1.5. A flow meter (Coleparmer#03219-11) was also installed here to verify exiting gas flow levels. After this step the gas entered a coalescing filter, followed by an H_2S scrubber to remove any remaining H_2S, described in Section 3.1.8.

All aspects of the system were located inside a sealed and ventilated area. Tubing was composed of 1/4" stainless steel, unless otherwise specified. All aspects of the system were gas tight, and were leak tested with at least 5psi. Twelve valves (Swagelok #SS4P4T) located throughout the setup acted to segment the setup, and were used during pressurized leak testing of the system. During operation, these valves were also used in aspects of inlet gas and nutrient outlet control.

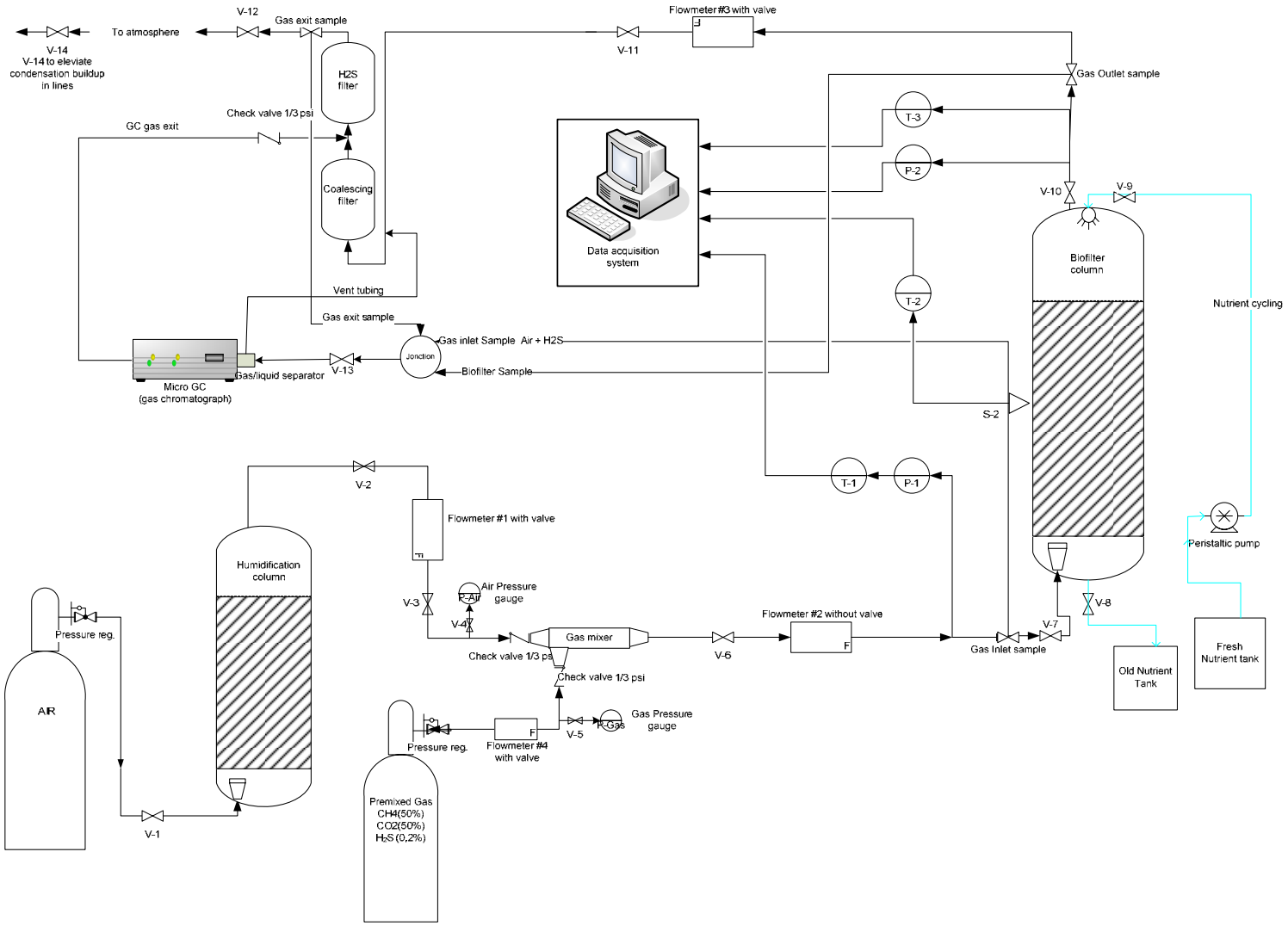

Figure 3.1 Instrumentation diagram of biofiltration system setup

3.1.2 Biofilter size and volume

The loading rate of H_2S on the biofilter varies significantly (11.25-155g H_2S/m^3h packing material) depending on the inlet H_2S concentration and gas flow, as seen Table 2.6 (Hirai et al. 2001; Rao et al. 2006). Loading rate and elimination capacity are based on packing volume or weight, not on the void volume. Based on this, a loading rate in the range of 20-100 gH_2S/m^3hr packing material gives an approximate starting range.

A diameter of 5cm for the biofilter was used as a starting basis for the development of the set-up. This diameter was used as it was wide enough for bulky packing material, but still thin enough to ensure a volume that would allow sufficient residence time and gas solid contact along the length of the filter bed. It was known that the inlet H_2S concentration would range from 1600 to 2000ppm, and the outlet [H_2S] was desired to be less than 100ppm. All calculations were based on ideal gas law at 25°C, and 1atm.

Volume of biofilter (based on internal diameter of 5.0cm),

$$V = \pi r^2 h \tag{3.1}$$

Residence Time (τ),

$$\tau = \frac{V}{Q} \tag{3.2}$$

where Q is gas flow rate in (m^3/h), and V is the volume of the packed bed, in m^3.

Space velocity (SV) is calculated by

$$SV = \frac{1}{\tau} \tag{3.3}$$

Pollutant Loading (L) is calculated as

$$L = \frac{C_{in}}{V} \times Q \tag{3.4}$$

(in g/m^3h filter bed) while elimination capacity (EC) is defined as

$$EC = \frac{C_{in} - C_{out}}{V} \times Q \tag{3.5}$$

(also in g/m^{3}h filter bed). C_{in} and C_{out} are the inlet and outlet pollutant concentrations respectively, in g/m^3. The removal efficiency, RE, is defined as

$$RE = \frac{C_{in} - C_{out}}{C_{in}} \times 100\% \tag{3.6}$$

With an inlet H_2S concentration of 2000ppm and a desired outlet H_2S concentration of 100ppm, the removal efficiency would be

$$RE = \frac{2000\,ppm - 100\,ppm}{2000\,ppm} \times 100\% = 95\% \tag{3.7}$$

Table 3.1 shows the calculated packing volume, loading rate and residence time based on different packing heights of the biofilter. These were calculated with the basis of a column of 5cmID, an inlet biogas flow rate of 5-10L/h and an inlet H_2S concentration of 2000ppm using Equations (3.1), (3.2), and (3.4).

Table 3.1 Volume and loading rates for biofilter design size, inlet 5-10L/h, 2000ppm H_2S

Packing Height	Packing volume	Loading rate range	Residence time
cm	*L*	*g H_2S/m^3 hr*	*sec*
10	0.19	69.89 – 139.78	141 to 71
15	0.29	46.59 – 93.19	212 to 106
20	0.39	34.95 – 69.89	283 to 141
25	0.49	27.96 – 55.91	353 to 177
30	0.59	23.30 – 46.59	424 to 212

By comparing the range of values for loading rates and residence times of Table 2.6 (previous studies) to the proposed biofilter dimensions and theoretical loading rates in Table 3.1, it can be seen that a packing height of 20cm is a conservative estimate and good starting point. A packing height of 20cm corresponds to a volume of 0.39L and a loading range of 34.95 – 69.89gH_2S/m^{3}h of packing material. The residence time range for this loading is 283-141 seconds.

3.1.3 Nutrient addition

Table 3.2 displays nutrient addition for previous experiments involving biofilters for H_2S removal. As the nutrient flows and biofilter volumes are different for each study, a relative nutrient flow was calculated based on the proposed biofilter, with a packing volume of 0.39L.

Table 3.2 Relative nutritive flow rate of previous studies, for 0.4L packed bed biofilter

Source	Nutrient flow	Biofilter Volume (L)	Biofilter Type	Relative nutrient flow, based on 0.4L biofilter
Kim et al. (2008)	500mL for 1min every 30 min	8.5	Immobilized cell beads in pall rings	22.9mL/min for 1 min every 30 min
Chung et al. (2000)	25mL/min	0.7	Ca-alginate cell beads	13.9 mL/min continuously
Jin et al. (2005b)	0.75-12L/hr	2.83	Plastic pall rings	1.72-27.6 mL/min continuously
Hirai et al. (2001)	40 mL/day added manually	0.35	Various inorganic	44.6mL/day added once daily

In order to change the liquid present in the biofilter (40mL) once every hour, the nutrient solution was added at 40mL/hr, or rather at 80mL/min for 30 seconds every hour. This higher flow rate over a shorter period of time enabled a wider coverage for the liquid sprayed into the biofilter. The nutrient solution was added intermittently in place of continuously, and it was decided that a change of the liquid solution in the biofilter every hour was sufficient.

3.1.4 Inoculum source and nutrient addition

Activated sludge was used as the inoculum source for the biofilter and was acquired from the Ville de Sherbrooke from the non-aerated clarifier. A 4L sample of clarifier sludge was taken on May 26th 2009. The activated sludge was stored at 4^{o}C until ready to use.

Nutrient addition is required when using inorganic packing material to ensure the microbial population had the required nutrients for growth. The biofilter system was designed such that the nutrient solution was fed into the top of the biofilter and then permeated down the packed column, exiting out the bottom. The liquid flow was counter-current to the gas inlet. The nutrient solution used in both the inoculum conditioning step and the biofilter operation was composed of 2g/L $(NH_4)_2SO_4$, 0.1g/L KCl, 0.25g/L K_2HPO_4, 0.25g/L $MgSO_4 \cdot 7H_2O$, 0.01g/L $Ca(NO_3)_2$ and either 25g/L or 8g/L $FeSO_4 \cdot 7H_2O$, as well as H_2SO_4 to create a pH of 3 solution.

3.1.5 General system and monitoring information

Four flow meters were located throughout the system; entering air flow, entering biogas flow, mixed gas flow, and exiting mixed gas flow. Both the entering gas flow meters were equipped with regulating valves, where the system gas flow was adjusted. Biogas and mixed gas flow meters were

150mm correlated flow meters with 316 SS float for liquids and gases, flow 0-264mL/min air (Coleparmer #03219-11). The air flow meter was the same design as the others except with flow range of 0-60mL/min air (Coleparmer #03219-03).

Pressure and transmitters were located in the entering biofilter stream as well as the exiting. A third temperature transmitter was placed into the center of the biofilter via a port at the top of the biofilter to see any internal temperature changes. This enabled the tracking of any pressure changes across the biofilter, as well as temperature changes. The pressure transmitters (Coleparmer # 68075-14) were of range 0-25psi and 0-20mA, accurate within ±0.25% of the full scale. The temperature transmitters used were Type K, ranging from 0 to 1250^{o}C, accurate to within ±0.75%. These were linked to an Agilent 34970A Data Acquisition/Switch Unit which was linked to the computer. The data was compiled on the computer using Agilent BenchLink Data Logger, with data exportable to Microsoft Excel. Scans were set to once every 5 seconds initially, and changed to once every 5 minutes from the biofilter start-up and acclimatization period, onward.

There were three gas sampling ports, located on the inlet and exit gas streams of the biofilter, and one after the H_2S scrubber. Gas samples were transported directly from sampling valves in the system to the entrance of the gas chromatograph via 1/8" PTFE sampling tubes. The sampling tubes were connected to a T junction equipped with valves to permit the choice of which sample was sent to the GC. The GC used for analysis was an Agilent 3000 Micro Gas Chromatograph (see Section 3.2.2). Both the GC inlet overflow line and the exiting gas sample lines of the GC were sent through ¼" SS tubing to the exiting gas stream to ensure no H_2S present in the ambient air. Refer to Figure 3.1, and Appendix A for summary of system design and additional information on pieces used in system.

3.1.6 Operating conditions

Except for specific testing with increased inlet gas flows, the overall gas flow rate into the system ranged between 5-10 L/hr, including both air and biogas. In general, the ratio of air to biogas was maintained for 4% O_2 in the biofilter gas inlet, as discussed in Section 2.6.1. The temperature of the system was not controlled, and thus was room temperature, ranging from 20-25^{o}C. The pressure of the system was kept as close to atmospheric pressure as possible while still ensuring a pressure gradient across the system to ensure constant flow. Generally the inlet biogas pressure was between 0.5-1psig, and air was 0-0.5psig. The nutrient addition was constant throughout all biofilter operation at 80mL/min for 30 seconds every hour.

3.1.7 Compatible materials

All materials used in the setup were verified to be compatible with H_2S. Overall, the materials selected for this included stainless steel (preferably 316), PTFE, Kalrez, and neoprene. These materials were also compatible with all other components in the system. In some cases, o-rings, seals and packing of flow meters and valves composed of Viton or Fluorocarbon FKM were replaced with neoprene or Kalrez to ensure no loss of function over time due to H_2S contact. Refer to Appendix A for changes made to specific pieces.

3.1.8 Safety considerations for working with H_2S

As H_2S is extremely toxic, a number of safety aspects were implemented including laboratory and personal detectors, system design, and system shut down. As mentioned above, all aspects of the setup were located inside an enclosed ventilation hood. The ventilation was controlled by a fan of 0.5HP, with an air flow of 200 CFM. The gas exiting the biofiltration system was sent through an H_2S scrubber system to remove any remaining H_2S. This was composed of a coalescing filter to remove any water followed by an H_2S scrubber. The coalescing filter (Advanced Instruments, #30TR) was composed of aluminum polycarbonate. The scrubber (Advanced Instruments #A-2839) was composed of a 2"x 24" plexi-glass column filled with beads coated in aluminum oxide and potassium permanganate. It was equipped with a life indicator in which it changes from purple to brown then to white when completely consumed. Finally, the entire exiting gas stream was routed separately outside where it was sent through a burner to remove any CH_4 present.

A detector for both methane and H_2S were located inside the enclosed setup area. These had detection limits of 10 and 15ppm for H_2S, and 20 and 40%$_{vol}$ for methane (Armstrong). There were also two identical H_2S detectors located in the laboratory, outside the biofiltration system hut. These both were set to 10 and 15ppm limit of detection (Armstrong). The first located outside at the bottom of the ventilation hood, and the other across the lab beside another laboratory ventilation hood. These detectors were placed 1-1.5m off the ground, as H_2S is heavier than air. Upon detection, an alarm would sound in the main building, alerting the onsite fire and safety squad.

A system shut-off option was in place which would close power to both a normally closed valve located on the inlet biogas stream as well as power to the peristaltic pump supplying nutrients to the biofilter. The system shut-off option would activate either upon detection of H_2S or CH_4 from any of

the mentioned detectors, or manually by an emergency stop button. The only components which remained on upon shut-off were the air and the ventilation fan.

Personal H_2S detectors were also worn by anyone in the laboratory. These detectors had a minimum detection of 10ppm H_2S and a maximum detection of 15ppm H_2S (Honeywell #GA24XT-H). Detection was signified by a series of audible beeps and vibrations. Full face respiration masks equipped with cartridges specific for H_2S gas were used during system manipulation. Both the face mask and cartridges were supplied by North Safety. The cartridges are able to block H_2S (#RT21P100). When operating and manipulating the system, both the H_2S detectors and the full face masks were worn.

3.2 Analytical Methods

3.2.1 pH and temperature

The pH and temperature of solutions were measured using a Fisher Scientific accumet® pH meter 25 installed with a Thermo Sure-flow combination pH probe (Orion 9172BNWP), Accumet temperature and probe (1362016New). Calibration was done with three points, including pH of 1, 4, and 7. The range of accuracy of this instrument was ± 0.05%.

3.2.2 Gas composition

The gas composition of all gas streams was analysed using an Agilent 3000 Micro Gas Chromatograph. As the GC was equipped with an internal pump to pull in the sample, sample lines were linked directly from the experimental setup to the gas chromatograph, eliminating the need to take gas samples manually. The Agilent 3000 was linked to a computer using Agilent EZChrom Elite software for chromatograph integration and data compilation.

The micro gas chromatograph was equipped with a Thermal conductivity detector (TCD) and two separate columns (or Channels) using Helium as a carrier gas at 80 psi inlet pressure. The carrier gas was filtered for fine particles and water before entering the gas chromatograph with a gas purification oxygen and water filter (Agilent Technologies #G3440-60003). The sample was filtered before analysis first with an external membrane separator filter to remove moisture (Genie Model 170-505), and then by an internal 10μm filter disk to remove particulates (Agilent Technologies #5183-4652).

Channel A was used to detect O_2 and N_2 concentrations, while Channel B measured CH_4, CO_2 and H_2S.

Channel A was a 1.0uL Backflush injector with MolSieve 5A 10mx0.32mm column with PLOT U 3m x 0.32mm pre-column. The method created for Channel A had the following conditions: Injection options: injection time 10msec, post run time 10 sec, timed sample pump at 10 sec, backflush 12sec. Temperature options: sample inlet 100^{o}C, injector 100^{o}C, column 110^{o}C. Pressure options: pressure control on, column pressure 30.0psi, post run 30.0psi, pressure equilibrium time 10sec. TCD filament on, sampling frequency 50Hz, runtime 2.5 minutes, high sensitivity.

Channel B was a PLOT U 8m x 0.32mm column, with the created method containing the following conditions: Injection options: injection time 15msec, post run time 60 sec. Temperature options: injector 70^{o}C, column 70^{o}C. Pressure options: pressure control on, column pressure 15.0psi, post run 25.0psi, pressure equilibrium time 60sec. TCD filament on, sampling frequency 50Hz, runtime 2.5 minutes, high sensitivity.

Each channel was calibrated separately using a 3 point calibration curve for each gas, each point replicated 3 times. The gases used for calibration of Channel A and B were supplied by Linde with the following compositions (all $\%_{vol}$): Channel A level 1: 0.1% O_2, 0.5% N_2, 99.4% He; Level 2: 10% O_2, 40% N_2, 50% He; Level 3: 20% O_2, 80% N_2. Channel B level 1: 0.1% H_2S, 12.5% CO_2, 12.5% CH_4, 74.9% He; Level 2: 0.2% H_2S, 25% CO_2, 25% CH_4, 49.8% He, Level 3: 0.3% H_2S, 49.7% CO_2, 50% CH_4, 0% He. Gas samples were analysed in a sequence of 10 runs. The last 3 run results of each 10 run set were taken and averaged. For any outlying values, the run previous to the 3 runs was used instead. The range of accuracy for this instrument when integrating the chromatograms using the peak area is ± 0.24%.

3.2.3 $Fe^{2+}$and Fe^{3+}

Both dissolved [Fe^{2+}] and [Fe^{3+}] were analysed by spectrophotometry analysis; Fe^{2+} at 505nm, and Fe^{3+} at 480nm (Pharmacia Biotech, Ultrospec 1000E). Fe^{2+} stock solutions for analysis were prepared by adding 10mL of pH 4.6 buffer solution (Fisher Scientific #SB100-1), 2mL of phenanthroline solution, and either Fe^{2+} standard solution (Absolute Stds #54141) or the sample, diluted to 50mL with deionized water. The phenanthroline solution was prepared by diluting 0.2g phenanthroline (Acros #157530250) to 100mL with buffer pH 4.6 buffer solution, and dissolved using and ultrasonic bath. Fe^{3+} stock solutions for analysis were prepared by adding 10mL pH 4.6 buffer solution and 5mL

of 0.1M HCl solution and either Fe^{3+} standard solution (Spex Certiprep #PLFE1-2X) or the sample, diluted to 50mL with deionized water. Further details of the chemicals used are found in Appendix A.

Standard solutions for both Fe^{2+} and Fe^{3+} were prepared by diluting 1mL standard 1000ppm Fe^{2+} or Fe^{3+} solution into 100mL deionized H_2O, making a solution of 10ppm. A standard curve was created using this standard solution by adding 0, 5, 10, and 25mL to create calibration points for 0, 1, 2, and 5ppm Fe^{2+} or Fe^{3+}. For sample addition, 0.1mL was added and then increased until a shade was seen similar to those of the middle of the calibration curve. Samples were left for precipitate to settle as suspended solids affect the spectrophotometer reading. The range of accuracy for Fe^{2+} and Fe^{3+} measurements were ±0.2%and ±2.1%, respectively.

3.3 Experimentation Methods

3.3.1 Packing material characteristics

Packing material used in both the biofilter and humidification columns consisted of untreated and uncoated gravel (3-6mm diameter), normally used in aquariums. Physical properties of this packing material were tested after rinsing the packing and placing in an oven 110^{o}C for 4 hours. Four different volumes (V_{total}) were tested, (n=3): 10mL samples in a 25mL graduated cylinder, 30 mL samples in a 100mL graduated cylinder, and 50mL and 100 mL samples in a 500mL graduated cylinder. The specified volume of dry packing material was measured into a graduated cylinder, and mass of dry packing was noted, M_{dry}. Water was then added to the dried packing material until it just covered the top packing (V_{void}). The packing material was then drained by placing a towel over the end of the graduated cylinder and inverting it. The mass of the remaining 'wetted' gravel being M_{wet}. The mass of water remaining in the 'wetted' filter bed ($M_{residual}$) is

$$M_{\text{residual}} = M_{\text{wet}} - M_{\text{dry}} \tag{3.8}$$

Assuming that the density of water is 1g/cm^3, the volume of water remaining in the packing when 'wetted' ($V_{residual}$) is obtained from $M_{residual}$. The void volume in the 'wetted' bed ($V_{voidwet}$) is calculated as

$$V_{\text{voidwet}} = V_{\text{void}} - V_{\text{residual}} \tag{3.9}$$

The porosity (ε) is defined as

$$\varepsilon = \frac{V_{\text{void}}}{V_{\text{total}}} \tag{3.10}$$

Porosity of 'wetted' packing represents the initial actual available volume in the biofilter, and is calculated substituting $V_{voidwet}$ for V_{void} into Equation (3.10). The bulk density (ρ_{bulk}) of the packing material in a given volume is

$$\rho_{\text{bulk}} = \frac{M_{\text{dry}}}{V_{\text{total}}} \tag{3.11}$$

The particle density ($\rho_{particle}$) is the actual density of the packing material used, calculated as

$$\rho_{\text{particle}} = \frac{M_{\text{dry}}}{(V_{\text{total}} - V_{\text{void}})} \tag{3.12}$$

Water content of 'wetted' packing (%v/v) is defined as

$$Water\% = \frac{V_{\text{residual}}}{V_{\text{total}}} \times 100\% \tag{3.13}$$

The diameter (d) and surface area of the packing was measured from 36 randomly selected pieces of packing material, assumed to be spherical. The surface area was calculated as

$$SurfaceArea = \pi d^2 \tag{3.14}$$

$$SurfaceRatio = \frac{SurfaceArea}{Volume} \tag{3.15}$$

The characteristics of the packing material used are summarized in Section 4.3.2, Table 4.1.

3.3.2 Inoculum preparation using *A. ferrooxidans* nutrient media

Conditioning of activated sludge for the enrichment of sulphur oxidizing bacteria was done by using a nutrient media specific for the growth of *A. ferrooxidans*. This nutrient media is similar to that of Harrison (1984), with suggested changes of Arsenault (2009). In the presence of *A. ferrooxidans*, the nutrient media changed colour and decreased in pH (Arsenault 2009; Harrison 1984).

To prepare 100mL of nutrient media; 0.2g $(NH_4)_2SO_4$ (Sigma# A5132), 0.01g KCl (Sigma#P5405), 0.025gK_2HPO_4 (Sigma#PX1570), 0.025g $MgSO_4 \cdot 7H_2O$ (Sigma#M1880) and 0.001g $Ca(NO_3)_2$

(Sigma#C1396) were added to 50mL of distilled water. This solution was adjusted to pH 3 using 1N H_2SO_4. In parallel, a solution of 2.5g of $FeSO_4 \cdot 7H_2O$ (VWR#CA99501-856) was made in 50mL of distilled water. Once mixed separately, the solutions were combined. For uses requiring a sterile media, this solution can then be filtered using a 0.22um filter setup (Coleparmer#29530-24) (not performed).

The activated sludge used in this stage of conditioning was a clarifier sludge sample taken May 26, 2009 from the Ville de Sherbrooke. Cultivation was done in 500mL Erlenmeyer flasks containing 200mL of *A. ferrooxidans* nutrient solution and 40mL of the activated sludge sample (1:5 ratio). Three reactors were placed onto a shaking table at 150rpm, and at room temperature, and grown for 20 days monitoring any visual or pH changes. Media changes were done every 7 days by taking 40mL of agitated old inoculated nutrient solution and adding it to 200mL of fresh nutrient solution. Both mixed samples and the liquid portion of a settled sample were used in media transfers, having no noticeable difference. As each reactor was expected to have a mixture of bacteria species present, cross contamination due to pH measurements was not considered a factor.

3.3.3 Bacterial attachment to packing material

Testing with packing material was done to assess the ability of microorganisms to use packing material as a growth support. Assessment of this included monitoring pH, as well as visually observing the media colour and any growth and attachment to packing material. The progress of inoculum growing in the presence of packing material was assessed by comparing it to 3 other media combinations; without inoculum or packing, with packing only, and with inoculum only.

Four different reactors were monitored (in duplicate); nutrient media (F), nutrient media and packing (FP), nutrient media and conditioned activated sludge (FB), and nutrient media, packing and conditioned activated sludge (FPB). Each reactor comprised of 500mL Erlenmeyer flasks, 150mL of nutrient media, 50mL of packing material (if present), and 30mL of cultivated activated sludge (if present). The inoculum source for this experiment was the resulting bacteria rich nutrient solutions from inoculum conditioning using activated sludge, as mentioned previously in Section 3.3.1. After conditioning, the inoculum was then stored in the refrigerator for 3 weeks until ready for use in the packing compatibility testing.

The growth media used was similar to that in initial inoculum conditioning using *A.ferrooxidans* media, as mentioned in 3.3.1, except with a change in the manner of preparation. Instead of preparing

the nutrient and $FeSO_4$ solution separately, the components were mixed together initially, and then the pH of the entire solution was changed to 3 with 1N H_2SO_4. This nutrient solution was always prepared in this manner hereafter.

Media transfers were done every 5-7 days. This involved the liquid transferred to sample storage containers for possible future use, while the packing material remained in the flask and was rinsed lightly to remove excess precipitate formed. Flasks without packing material were rinsed also. A new *A. ferrooxidans* nutrient solution was made, and 150mL was put into each flask. 30mL of well agitated old solution was then placed in each of their respective reactors. At this time the pH was measured. For the 3rd media change and those afterwards, the old solutions were left to settle, and then 30ml of the liquid portion was taken and added to the fresh media.

3.3.4 Analysis during biofiltration operation

Throughout all biofiltration operation experiments the sampling and analysis procedures were the same. Biofilter outlet gas composition was measured 4 times daily, and the inlet gas composition was analysed at least once daily, both with the gas chromatograph. These samples were taken using the inline sample ports located before and after the biofilter and connected directly to the gas chromatograph. A sample of the outlet nutrient solution was taken from the outlet nutrient tank, unless otherwise stated. This was analysed for pH and also for Fe^{3+} daily. Since the approximate total dissolved iron was known, only one of Fe^{3+} or Fe^{2+} needed to be followed daily for changes. Fe^{3+} analysis was done as it is easier to perform. Fe^{2+} samples were performed intermittently for verification, but Fe^{3+} was the main factor followed. Also, 1-2 times weekly the inlet nutrient solution was analysed for Fe^{3+}/Fe^{2+} values. Samples were measured the same day for pH and Fe as it was found that the Fe^{3+}/Fe^{2+} changed daily even if stored in the refrigerator between analyses. Secondary observations such as the colour of the outlet solution and packed bed were also noted throughout experimentation. These biofiltration operation analysis techniques pertain to startup and acclimatisation and loading testing.

Chapter 4
Results and Discussion: Submitted Manuscript

4.1 Overview

A laboratory scale biofiltration system was tested for its ability to remove H_2S from biogas. The biofilter was composed of small gravel (3-6mm diameter) inoculated with activated sludge conditioned in an *A. ferrooxidans* media. Packing material physical characteristics were tested, and porosity of the initial dried packing was found to be 0.43. The 0.4L packed bed biofilter volume received 5-12L/hr of inlet gas flow; synthesized biogas mixed with humidified air, [H_2S] ranging from 1015 – 1645ppm$_v$. H_2S removal in the non-inoculated biofilter was 56% with air being the significant factor. Biofilter experimentation involved startup and acclimatization followed by loading tests, ranging from 27.8 to 69.5 gH_2S/m^{3}h of filter bed. Startup of the biofilter showed a 98% H_2S removal after 2 days. The H_2S removal efficiency averaged 99% during the loading tests.

Keywords: Biofiltration, H_2S, biogas, sulphur oxidizing bacteria, *A. ferrooxidans*

4.2 Introduction

Biogas is the product of anaerobic digestion of organic matter, with composition varying depending on the feedstock. Biogas composition typically ranges from 45-80%$_{vol}$ CH_4, 30-45%$_{vol}$ CO_2, 0-1.5%$_{vol}$ H_2S, and is saturated with water (Schomaker et al. 2000). Biogas presently has limited use in energy generation applications due to its corrosive properties when burned. This is caused by the presence of hydrogen sulphide (H_2S), and biogas produced from small scale facilities such as farms requires treatment before using in an engine. Current biogas purification techniques are largely chemically based, with high cost and disposal considerations.

Biofiltration uses biological degradation to remove pollutants from a gaseous stream. It has low initial and operating costs, and minimal secondary pollution, and can be effective in the removal of H_2S due to the high solubility of H_2S (Barona et al. 2005). The objective of this study was to assess the

performance of a biofilter for use in a farm scale application constructed with readily available inoculum and packing material for the removal of H_2S from a synthetic biogas stream.

4.3 Materials and Methods

4.3.1 Biofilter setup

The laboratory scale biofiltration system is shown in Figure 4.1. The biofilter column was made of 5cmID PVC, with a packed bed height of 20cm and a total height of 50cm. Two ports were installed on either end; with gas entering the bottom, and liquid nutrient entering the top of the column. The humidification column resembled the biofilter, except with liquid stationary in the column, and a total column height of 25cm. Packing was added to the humidification column with water, in order to increase the contact surface area. Transmitters for temperature (Precision Measurements, Type K) and pressure (Coleparmer 68075-14) were located in the inlet and outlet gas streams around the biofilter. Another temperature transmitter was also located in the center of the packed bed. Synthetic biogas with $50\%_{vol}CH_4$, $50\%_{vol}$ CO_2 and $2000ppm_v$ H_2S (Linde#24088126) mixed with humidified air entered the bottom of the biofiltration column, while a liquid nutrient flow entered the top of the biofilter via a peristaltic pump. A nutrient solution was added once every hour. The flow of gas was maintained using flow meters (Coleparmer#03219-11).

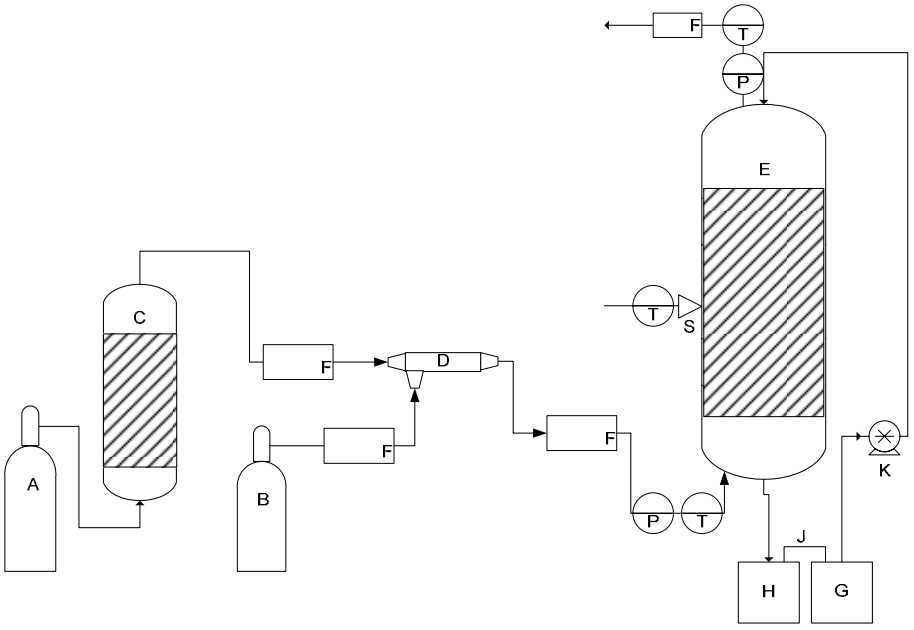

A- air cylinder, B – Synthetic biogas cylinder, C – humidification column, D – gas mixer, E – Biofilter, F – flowmeter, G – inlet nutrient tank, H – outlet liquid tank, J – pressure bridge, K – peristaltic pump, P – pressure transmitter, T – temperature transmitter, S – sample port

Figure 4.1 Biofiltration system laboratory scale setup

4.3.2 Filter material

Packing material used in both the biofilter and humidification columns consisted of untreated and uncoated gravel (3-6mm diameter), normally used in aquariums. Physical properties of the packing material are summarized in Table 4.1.

Table 4.1 Summary of packing material characteristics (n=12)

Characteristic	Units	Value
Particle diameter	cm	0.36±0.11
Bulk density	g/ml	1.42±0.07
Particle density	g/ml	2.51±0.19
Porosity	--	0.43±0.02
Porosity 'wetted'	--	0.34±0.03
Water content of 'wetted' packing	%	9.40± 1.47
Surface area (particle)	cm^2	4.4 ±2.86
Surface Ratio	/cm	3.42

A porosity of 0.4-0.8 is suggested to ensure gas plug flow and low pressure drop (Devinny et al. 1999). Porosity of 0.43 for this study is within the suggested range, while the 'wetted' packing porosity is lower. A study comparing different inorganic materials as filter material in H_2S biofiltration showed porosity ranging 0.43-0.89, and bulk density 0.12-0.92g/cm^3, both calculated from dry packing material (Hirai et al. 2001). A similar surface ratio of 3.5/cm was reported by Jin et al. (2005b) with a biofilter composed of polypropylene Pall rings.

4.3.3 Inoculum

Activated sludge from the Ville de Sherbrooke, QC, Canada was used as an inoculum source, and was conditioned for sulphur oxidizing bacteria using a nutrient media specific for *A. ferrooxidans* (Harrison 1984) composed of 2g/L $(NH_4)_2SO_4$, 0.1g/L KCl, 0.25g/L K_2HPO_4, 0.25g/L $MgSO_4$ $7H_2O$, 0.01g/L $Ca(NO_3)_2$ and 25g/L $FeSO_4$ $7H_2O$ and adjusted to a pH of 3 with H_2SO_4. Conditioning of the activated sludge was done in 500mL Erlenmeyer flasks with 200mL nutrient media and 40mL of activated sludge to start (n=4), grown on a rotary shaker at 150rpm, 25^{o}C. Media changes were done every 5-7 days by taking 40mL of old solution and adding it to 200mL of fresh nutrient media. The activated sludge was conditioned like this for 20 days, at which time 50mL of packing material was added to inoculate the packing material (n=8). Growth on the packing material was done on the rotary shaker at 150rpm, 25^{o}C, for 41 days.

4.3.4 Analytical methods

Inlet and outlet gas composition was analysed using a Micro gas chromatograph (Agilent Technologies, 3000A) equipped with a thermal conductivity detector (TCD) and two channels. Channel A, 1.0uL Backflush injector with MolSieve 5A 10mx0.32mm column with PLOT U 3m x 0.32mm pre-column, was used to detect O_2 and N_2 concentrations. Channel B was a PLOT U 8m x 0.32mm column and detected CH_4, CO_2 and H_2S. Samples were taken directly from the system setup via sample lines. Each sample was analysed in a series of 10 runs, and the results of the final 3 runs were averaged for use in analysis. Analysis of pH was done using a Fisher Scientific accumet® pH meter 25 installed with a Thermo Sure-flow combination pH probe (Orion 9172BNWP) and Accumet temperature probe (#1362016New).

4.3.5 Experimentation

Non-biological H_2S removal

Baseline testing involved 3 factors for significance in the removal of H_2S in the filtration system in the absence of known bacteria, using a full factorial 2^3 design. Factors included packing material type, $FeSO_4$ content in liquid stream, and air. Except for factors changed for experimentation, experimental conditions were the following: biogas flow of 100mL/min, inlet pressure approximately 1psig, and room temperature (23°C). There was no nutrient flow during each run, and the packing material was only moistened before each run with the respective liquid solution. This was done by flooding the column with liquid until the packing material was fully submerged, and then draining the liquid off. The pH was variable depending on which solution was added; 6-7 for pure water, and 3 for $FeSO_4$ rich nutrient solution, but was not measured during experimentation.

The packing material was either 0.3mm diameter gravel or 0.5cm glass raschig rings. The air flow rate and $FeSO_4$ content in the liquid solution added were varied between 0 or 25mL/min and 0 or 25g/L respectively. The experimental conditions for each run can be seen summarized in Table 4.2.

Table 4.2 Experimental design for biofilter H_2S removal baseline testing, (1psig, 23°C)

Run	Packing	$FeSO_4$ (g/L)	Air Flow (mL/min)
1	Glass	25	25
2	Glass	25	0
3	Glass	0	25
4	Glass	0	0
5	Gravel	25	25
6	Gravel	25	0
7	Gravel	0	25
8	Gravel	0	0

Gas composition was analysed three times throughout each run; 'initial outlet' gas sample taken at the start of the run, 'inlet' gas sample taken 1 hour after the start, and 'final outlet' sample taken 2.5 hours after the start of the run. Between each run, the filter was purged with air, and the filter bed was rinsed with deionised water or $FeSO_4$ rich nutrient solution. Packing material and column were cleaned between runs by rinsing the packing with deionised water, as well as rinsing the column with HCl (Fisher Scientific #SB100-1) to remove any remaining iron. Packing material was then placed in the oven at 105°C for at least 24 hours. The system was cleaned with diluted bleach, and although the

overall system was not sterile, there was assumed to be little biological effect, and that any effect would be seen throughout the sampling runs. Runs were done in random batches, based on the packing material used. Those with $FeSO_4$ content were performed after those with only water. Complete run replication was performed.

The effect of the level of O_2 present in the inlet gas was tested using run #7 in Table 4.2 as a model. In a bed composed of gravel packing, and with an initial liquid addition of deionised water only, the air flow was decreased by 50% (12.5mL/min, 1psig, 23°C) while keeping the biogas flow constant at 100mL/min. The extended baseline testing was performed for 48 hours under the conditions of run 7; having gravel packing, no $FeSO_4$ content in the liquid solution, and an air flow of 25mL/min (1psig, 23°C) with biogas at 100mL/min (1psig, 23°C). The packed bed was wetted only once at the beginning of the 48 hour period, with deionised water.

4.3.6 Biofilter startup and acclimatization period

Inoculated and preconditioned packing material (0.4L) was added to the biofilter at the start of the acclimatization period. The biofilter start up and acclimatization period lasted 41 days in total, changing experimental factors to transition the bacteria from living with full air to with 19%$_{vol}$ air, as is summarized in Table 4.3. $FeSO_4$ content in the nutrient solution was decreased at the end of this acclimatization period from 25g/L to 8g/L based on a similar growth media used for *A.ferrooxidans* in the dissolution of pyrite (Konishi et al. 1990). Nutrient addition was constant throughout all biofiltration experiments at 80mL/min once every hour for 30 seconds.

Table 4.3 Biofilter startup and acclimatization: Operation conditions

Factor	***Unit***				
Day	*day*	0 - 5	5 – 19	19 – 22	22 - 41
Total Gas flow	*L/h*	7.5	7.5	5	5
Air flow	*L/h*	7.5	3.75	0.95	0.95
Biogas flow	*L/h*	--	3.75	4.05	4.05
Air (O_2)	$\%_{vol}$	100 (21)	50 (10.5)	19 (4)	19 (4)
$FeSO_4$ content in nutrient	*g/L*	25	25	25	8
H_2S loading rate	$gH_2S/m^3h\ bed$	0	28	30	30
$[H_2S]$	ppm_v	--	1015	1645	1645

4.3.7 Loading testing

Loading capacity of previous H_2S removal biofiltration studies ranges from 23 to 145 gH_2S/m^3h filter bed, based on the total packed bed volume, not the void volume (Harrison 1984; Hirai et al. 2001; Jin et al. 2005b; Rao et al. 2006). Tests to evaluate the H_2S loading capacity of the biofilter involved increasing the biogas and air inlet flows until a breakthrough of H_2S was seen at the outlet of the biofilter. Air was added to have $4\%_{vol}$ O_2 present as a low level of O_2 encourages sulphide conversion to elemental sulphur in place of sulphates (Schomaker et al. 2000, Duan et al. 2005). Tests were performed over 20 days, but unfortunately, due to technical problems with the gas chromatograph, this experiment was not fully completed. A summary of the first 4 loading stages is presented in Table 4.4, where EBRT represents the empty bed residence time. Each loading stage had an inlet [H_2S] of $1600ppm_v$ and was performed for 2 days after the H_2S removal was considered constant. The nutrient flow was constant at 80mL/min for 30 seconds every hour and contained 8g/L $FeSO_4$.

Table 4.4 Loading stages with respective molar and gas flow rates

Loading	Biogas	Air	Total flow	H2S loading	EBRT	RT (wetted void vol)
Stage	*L/h*	*L/hr*	*L/h*	gH_2S/m^3h	*sec*	*sec*
Initial	4	0.96	5.0	27.81	290.3	96.2
1	6.1	1.46	7.6	42.41	190.4	63.1
2	8	1.92	9.9	55.61	145.2	48.1
3	9	2.16	11.2	62.57	129.0	42.8
4	10	2.4	12.4	69.52	116.1	38.5

4.4 Results and Discussion

4.4.1 H_2S removal in non-inoculated biofilter

In order to eliminate the effect of air being present or absent, the [H_2S] was normalized using the biogas components by

$$H2S\%(excl.air) = \frac{H2S\%_{vol}}{CH4\%_{vol} + CO2\%_{vol} + H2S\%_{vol}} \quad (4.1)$$

The observed average entering [H_2S] for all runs was 0.202%±0.012. Variability was seen in the concentrations of the gases in the initial outlet samples, and ANOVA analysis showed that air had a

significant effect in initial outlet H_2S concentration with an F value of 6.13 compared to $Fcrit_{5,18}$ of 5.32. Packing and $FeSO_4$ content were not significant. More emphasis was placed on the final biofilter outlet [H_2S] results, allowing for equilibrium to be reached. Upon ANOVA analysis, air was found to be the only significant factor in the final outlet H_2S concentration, with an F value of 60.4 compared to $Fcrit_{5,18}$ of 5.32. Therefore, it was concluded that the addition of air to the inlet biogas stream had the largest affect on the removal of H_2S in a non-inoculated biofilter.

The effect of the amount of air in the inlet stream on H_2S removal was further investigated by changing the inlet air flow while keeping the inlet biogas flow constant, thus changing the concentration of air in the inlet gas stream. Four runs were performed at different air flow rates (0, 12.5, 15, 25mL/min at 25^{o}C, 1atm), with constant parameters of gravel packing, biogas flow 100mL/min (25^{o}C, 1atm), and without $FeSO_4$ in the solution added to moisten the filter bed. It was found that in decreasing the amount of air added, an increase of the outlet H_2S concentration was reported, as in Figure 4.2.

Figure 4.2 H_2S removal in non-inoculated biofilter: H_2S concentration with varying [O_2] inlet (1psig, 25^{o}C)

Considering conditions for actual biofilter operation for H_2S removal, gravel packing, 25g/L $FeSO_4$ in nutrient and air flow totalling 4% $_{vol}O_2$ of inlet gas stream, the average H_2S removal after 2 hours (outlet final) was 56.1%±14.0 (n=2). Further experimentation with a long-term test (48 hours)

displayed an overall H_2S removal of 30.7%±6.3 std deviation over 45 hours in the non-inoculated biofilter. An aqueous phase is present in the moistened non-inoculated biofilter, and in the presence of excess oxygen in the aqueous phase, the sulphide undergoes a chemical oxidation (McNevin et al. 1999)

$$S^{2-} + ½\ O_2 + 2H^+ \rightarrow S^0 + H_2O \qquad (4.2)$$

This confirms that the presence of oxygen in the aqueous phase shows an increase in H_2S removal when compared to little or no oxygen present. Thus, there is H_2S removal in the non-inoculated biofilter, accounting for 30.7 to 56% H_2S removal in the system, with an inlet $[O_2]$ of $4\%_{vol}$. This rate of H_2S removal would likely decrease over time as the liquid phase becomes saturated or the water in the column is evaporated, resulting in less aqueous sulphide for the oxygen to react with.

4.4.2 Startup and acclimatization

Initial biofilter startup with biogas was started on day 5, after the startup stage with air only (day 0-4). As can be seen in Figure 4.3, the addition of biogas showed an initial outlet $[H_2S]$ similar to the inlet $[H_2S]$, with H_2S removal during day 5-7 of 25.1%±10.9 std deviation over 3 days. This removal is thought to be due to adsorption, absorption and oxidation with oxygen in the filter bed, as a similar H_2S removal was seen previously with the non-inoculated biofilter. As seen in Figure 4.3, on day 7 the outlet $[H_2S]$ fell below the detectable range of the micro gas chromatograph used ($50ppm_v$), showing that the inoculum was degrading more than 95% of the H_2S present. This shows that the bacteria present required a 2 day adjustment period to start degrading the H_2S present. After day 7 the H_2S removal was constant at 98.1%±2.9 std deviation over the extent of the 34 day startup period with biogas (See Figure 4.4).

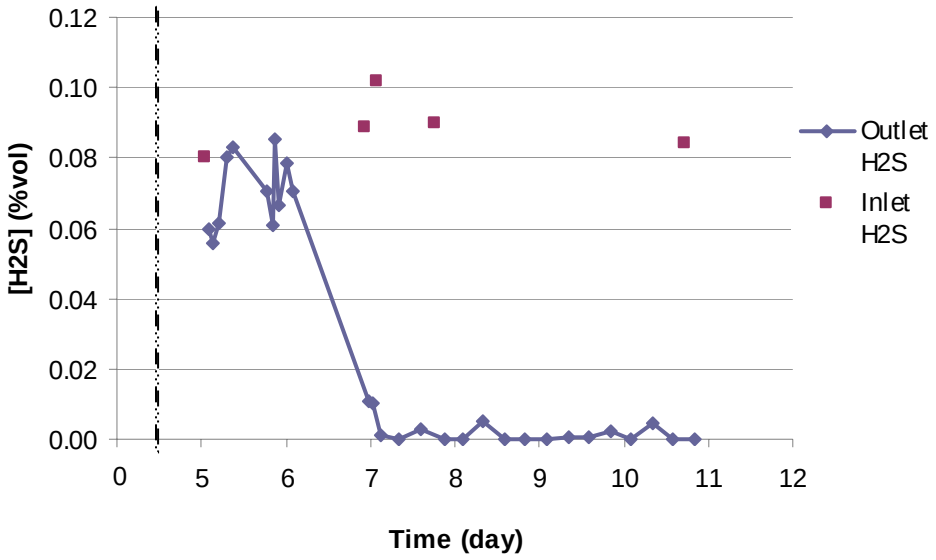

Figure 4.3 Biofilter start up phase: Inlet and outlet [H_2S], biogas inlet added day 5 (1pisg, 25^oC)

Figure 4.4 displays the inlet and outlet H_2S concentration over the entire startup period. The inlet [H_2S] was increased at day 19 from 1015ppm$_v$ to 1645ppm$_v$, resulting in the H_2S loading rate changing slightly from 28 to 30gH_2S/m^{3}hr filter bed, as summarized in Table 4.3. As can be seen from Figure 4.4, the increase in inlet [H_2S] did not change the removal efficiency significantly.

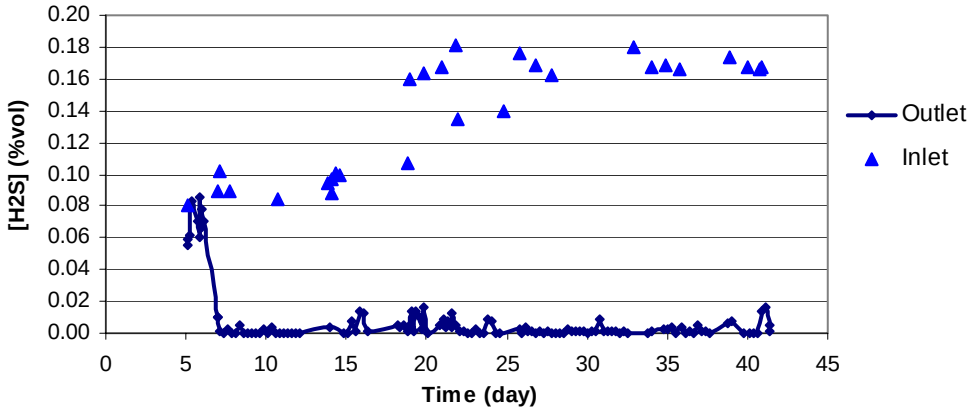

Figure 4.4 Biofilter startup phase: Inlet and outlet [H_2S], (1pisg, 25°C)

4.4.3 Loading tests

The increase in loading is displayed in Figure 4.5 with the H_2S removal efficiency over the loading test period of 20 days. The loading stages are summarized in Table 4.4. As the inlet air and biogas flow were changed in relation to a constant $4\%_{vol}O_2$ present, the inlet H_2S concentration remained constant at 0.174%±0.012.

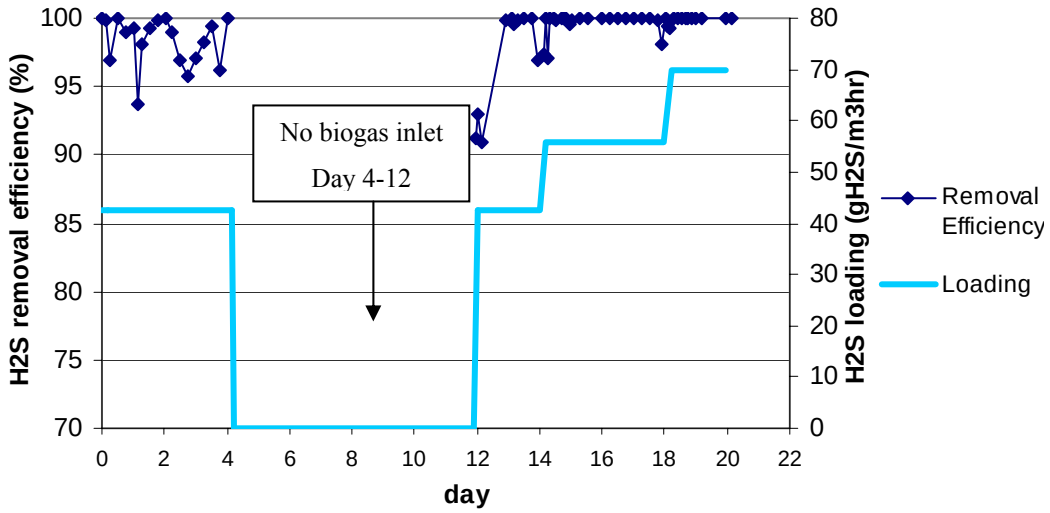

Figure 4.5 H_2S loading rate and removal efficiency (Inlet 1740ppm H_2S, 1psig, 25°C)

As is seen in Figure 4.5, Stage 1 showed a small variability in the H_2S removal efficiency. On day 12, after 8 days of the biofilter having only air (no biogas) and nutrient solution, the H_2S removal efficiency on day 12 dropped to 91.7% (outlet [H_2S] 0.016%$_{vol}$) initially before increasing to 100% removal within 24 hours. The H_2S removal efficiency on day 14 dropped to 97.1%. These periods of slightly decreased removal efficiency showed that biological reacclimatization occurred after a period of no inlet biogas flow for the biofilter, as well as increases in biogas load. The desired [H_2S] outlet was 80ppmv or less, and these decreases in removal efficiency were therefore considered insignificant (<50ppm$_v$) for the purposes of this study. The H_2S removal efficiency averaged 98.9% ± 2.1 std deviation over the 20 days of the H_2S loading test study.

4.5 Conclusion

A biofiltration system was designed for the removal of H_2S from a synthesized biogas stream. Initial baseline testing with the non-inoculated biofilter showed H_2S removal of 30.7%±6.3 std deviation over a 48 hour test, with air being the only significant factor causing the non-biological H_2S removal. Inoculation of the biofilter was done with preconditioned activated sludge. The biofilter was operated

for a total of 61 days, including a period of startup and acclimatization of 41 days, followed by H_2S loading tests for 20 days. The initial startup and acclimatization stage with biogas showed complete H_2S removal after 2 days, with overall H_2S removal of 98.1%±2.9 std deviation over 34 days. Biofilter H_2S loading tests were performed with inlet H_2S concentrations of 1600ppm_v and loading rate from 27.8-69.5 gH_2S/m^3h filter bed. An average H_2S removal of 98.9%±2.1 std deviation over 20 days was observed. This study showed that activated sludge and gravel packing could be used as effective inoculated filter medium in a biofilter treating H_2S in biogas; effectively removing >95% H_2S from an inlet biogas flow up to 10L/hr, 1600ppm_v H_2S.

4.6 Acknowledgements

This project was in collaboration with the University of Waterloo, the Université de Sherbrooke, and Hydro-Quebec. Funding was provided by the NSERC Chair in Industrial Energy Efficiency (chairholder: N. Galanis) established in 2006 at Université de Sherbrooke with the support of Hydro-Quebec (Energy Technology Laboratory, LTE), Alcan International Ltd, and the CANMET Energy Technology Center (CETC-Varennes, Natural Resources Canada). Laboratory funding was provided by Hydro-Quebec (Energy Technology Laboratory, LTE).

Chapter 5
Material Balance

5.1 Material balance

A material balance was performed both experimentally and theoretically for the biofiltration system used. The experimental material balance was calculated for the inlet and outlet gas streams for each experimentation stage performed. This was then compared with a theoretical material balance of the same inlet mixed dry gas basis of 7.5L/h (25^{o}C, 1atm). A summary of the composition of the theoretical process streams is displayed in Figure 5.1. Conditions for calculations were at 25^{o}C and 1atm, unless otherwise specified. The results of both the experimental and theoretical material balances can be seen in Sections 5.2 and 5.3 respectively, followed by a comparison in Section 5.4. This paralleled analysis begins with an outline of the values and assumptions in Table 5.1 of which both the experimental and theoretical material balances were based.

It was assumed that the gas in the system runs under nearly steady state; with the exception of H_2S which is assumed to accumulate in the biofilter as elemental sulphur. Calculations and compositions of each stream are followed in mass flow rate. Equation (5.1) represents the overall material balance.

$$\text{Mass flow (1)} + \text{Mass flow (2)} = \text{Mass flow (3)} + \text{Mass flow (4)} + \text{Accumulation} \qquad (5.1)$$

The inlet and outlet gas mixtures are considered as ideal gas mixtures and both the system and each mixed stream are in equilibrium.

Figure 5.1 displays both the gas and liquid process streams for the biofiltration process. The values and assumptions presented in Figure 5.1 pertain to the theoretical material balance.

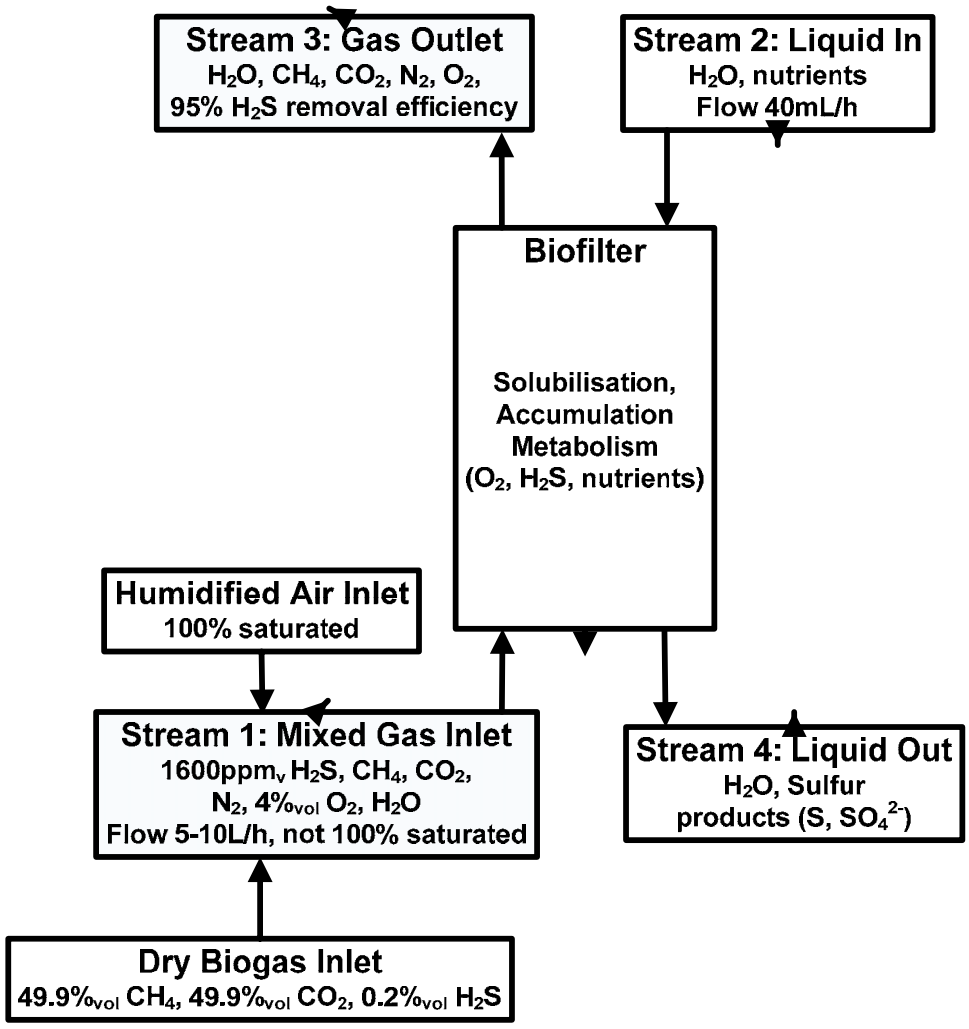

Figure 5.1 Theoretical process streams of biofiltration system for material balance (7.5L/h dry inlet gas, 4%$_{vol}$ O_2, 1atm, 25^{o}C)

5.1.1 Calculation basis and assumptions

Table 5.1 displays the value and any assumptions made for the physical properties of each stream, including the temperature, pressure, flowrate and composition. For the experimental inlet and outlet pressure values, an estimate was made due to inaccurate pressure transmitter values. For the purpose of calculating an experimental mass balance, the inlet pressure (P1) was estimated at 1 psig and the outlet pressure (P2) at atmospheric pressure, or 0 psig. The volumetric flow rates used in calculations

were target flow rates that the flow meters were set to, and do not necessarily represent exact flow rates in the system. The assumptions for the parameters for each process stream, including pressure and flow rate, are summarized in Table 5.1. As seen in Table 5.1, the experimental inlet and outlet gas flow rates were assumed to be equal, and this was confirmed with the presence of a flow meter on the exiting gas stream. Average temperatures for each experimental time period were calculated from temperature transmitter readings, and the values are presented in experimental calculations in Sections 5.2.1(inlet) and 5.2.2 (outlet).

Table 5.1 Theoretical and experimental stream properties (7.5L/h dry gas basis)

Stream	Theoretical		Experimental	
	Source	*Value*	*Source*	*Value*
Stream 1:Gas In				
Pressure	Stated	1atm	No experimental data: Assumed	1.07 atm (1psig)
Temperature	Stated, constant	25°C	Experimental: Temp transmitter	Variable
Volumetric flow rate	Stated: basis dry gas	7.5L/h	Set and maintained	7.5L/h
Composition	Stated	See below	Experimental: GC results	Variable
Stream 2:Liquid In				
Pressure	Stated	1atm	Not applicable	--
Temperature	Stated	25°C	Not applicable	--
Volumetric flow rate	Stated	40mL/h	Not applicable	--
Composition	Stated	See below	Not applicable	--
Stream 3:Gas Out				
Pressure	Stated	1atm	No experimental data: Assumed	1atm
Temperature	Stated, constant	25°C	Experimental: Temp transmitter	Variable
Volumetric flow rate	Calculated	See below	No experimental data: Assumed equal to inlet	7.5L/h
Composition	Calculated	See below	Experimental: GC results	Variable
Stream 4:Liquid Out				
Pressure	Stated	1atm	Not applicable	--
Temperature	Stated	25°C	Not applicable	--
Volumetric flow rate	Calculated	See below	Not applicable	--
Composition	Calculated	See below	Not applicable	--

5.2 Experimental Material Balance

The experimental material balance was calculated for gas components at each stage of biofilter operation, including the startup and acclimatization period as well as the loading test period. Average inlet and outlet gas stream compositions were compiled from gas chromatograph results and used in the calculations. Gas concentrations were taken as is, and not normalized. Although the gas streams were humidified, the humidification amount was not experimentally analysed, and therefore not

discussed in this experimental material balance. The summary of these stages is displayed in Table 5.2 and Table 5.3, which display the inlet and outlet mass stream flow rates respectively.

5.2.1 Stream 1: Inlet gas - Experimental

The inlet gas flow rate and composition changed depending on the experimental type and stage. For the most part (all tests from start up and acclimatization stage 4 onward) were air and biogas mixed to have a composition of $4\%_{vol}$ O_2 present, at varying total flow rates. In these cases it was seen that although the inlet gas flows were set to have $4\%_{vol}$ O_2 in the gas inlet, differences in the air and biogas inlet pressure and flow caused less air to be present than was calculated. This is displayed by the inlet gas stream containing between 2-3.5% $_{vol}$ O_2. Table 5.2 displays the estimated mass flow rates of each of the components of the inlet gas for each of the experimental stages, as well as total mass flow rates for each experimental stage.

Table 5.2 Inlet gas stream mass flow rate, all biofilter experiments (T variable, 1psig)

Experiment	Stage	start time	elapsed time	T	Air	Biogas	O2	CH_4	CO_2	H_2S	O_2	N_2	Total
Type	#	*Day*	*Days*	*°C*	*L/hr*	*L/hr*	*%vol*	*g/h*	*g/h*	*g/h*	*g/h*	*g/h*	*g/h*
Start&Acc	1	0.0	5.0	22.4	7.5	0.0	19.2	0.00	0.00	0.000	2.03	7.39	9.42
Start&Acc	2	5.1	13.7	22.5	3.8	3.8	9.5	1.26	3.42	0.011	1.00	3.54	9.23
Start&Acc	3	18.8	3.0	22.2	1.0	4.0	3.7	1.35	3.72	0.013	0.26	0.94	6.28
Start&Acc	3-low	22.0	2.8	22.2	1.0	2.1	6.5	0.65	1.80	0.006	0.29	1.10	3.84
Start&Acc	4	24.8	16.6	22.6	1.0	4.0	3.7	1.37	3.70	0.013	0.26	0.95	6.29
Loading	1	41.8	4.2	22.5	1.4	6.1	3.2	2.17	5.70	0.019	0.34	1.26	9.49
Loading OFF	None	46.0	7.8	22.5	1.4	0.0	NA	0.00	0.00	0.000	0.00	0.00	0.00
Loading	1	53.8	2.1	22.5	1.4	6.1	3.0	2.14	5.94	0.020	0.31	1.08	9.49
Loading	2	56.0	3.8	23.3	1.9	8.0	3.3	2.75	7.65	0.026	0.46	1.56	12.45
Loading	3	59.9	2.1	23.3	2.4	10.0	3.0	3.56	9.88	0.033	0.52	1.78	15.77
						Total		**15.25**	**41.81**	**0.140**	**5.46**	**19.60**	**82.26**

5.2.2 Stream 2: Outlet Gas - Experimental

The outlet gas stream mass flow rates were calculated under the assumption that the outlet gas had a volumetric flow rate identical to the inlet flow rate, except the outlet flow at atmospheric pressure (or 0 psig).

Table 5.3 Outlet gas stream mass flow rate for biofilter experiments (T variable, 0psig)

Experiment	Stage	T	Total gas	CH_4	CO_2	H_2S	O_2	N_2	Total
Type	#	^oC	*L/hr*	*g/h*	*g/h*	*g/h*	*g/h*	*g/h*	*g/h*
Start&Acc	1	22.9	7.5	0.00	0.00	0.000	1.87	6.79	8.66
Start&Acc	2	22.6	7.5	1.17	3.17	0.002	0.94	3.32	8.60
Start&Acc	3	22.3	5.0	1.24	3.43	0.000	0.22	0.88	5.77
Start&Acc	3-low	22.3	3.1	0.58	1.60	0.000	0.28	1.10	3.57
Start&Acc	4	22.7	5.0	1.27	3.42	0.000	0.23	0.87	5.78
Loading	1	22.5	7.5	1.96	5.19	0.000	0.33	1.24	8.72
Loading OFF	None	22.5	1.4	0.00	0.00	0.000	0.00	0.00	0.00
Loading	1	22.5	7.5	1.98	5.49	0.001	0.31	1.09	8.87
Loading	2	23.4	9.9	2.52	6.97	0.000	0.44	1.61	11.54
Loading	3	23.4	12.4	3.21	8.92	0.000	0.49	1.78	14.41
			Total	**13.93**	**38.18**	**0.00**	**5.11**	**18.68**	**75.91**

5.2.3 Overall total difference between streams - Experimental

The mass flow rate of each gas component was calculated in reference to N_2, since the N_2 content is assumed not to change from the inlet to the outlet stream. The difference in relative mass (Δm_A) for each gas component from inlet to outlet compared to N_2, was calculated by the following equation:

$$\Delta m_A = \left. \frac{\dot{m}_{A_{In}}}{\dot{m}_{N2_{In}}} \right|_i - \left. \frac{\dot{m}_{A_{Out}}}{\dot{m}_{N2_{Out}}} \right|_i \qquad (5.2)$$

Calculated for the i^{th} experiment/stage, where $\dot{m}_{N2_{In}}$, $\dot{m}_{N2_{Out}}$ $\dot{m}_{A_{In}}$ and $\dot{m}_{A_{Out}}$ represent the inlet and outlet mass flow of N_2 and the gas flow rate to be calculated, respectively. Since the mass flow rate of N_2 is assumed to be constant from the inlet to the outlet,

$$\dot{m}_{N2_{In}} = \dot{m}_{N2_{Out}} \tag{5.3}$$

Calculating the relative percent of removal ($\dot{R}_{Gas}$) of each gas species

$$\dot{R}_A = \frac{\Delta \dot{m}_A\big|_i}{\left.\frac{\dot{m}_{A_{In}}}{\dot{m}_{N2_{In}}}\right|_i} \tag{5.4}$$

gives a percentage removal relative to the amount of N_2 present. The values of both the relative mass flow rate and the relative percent of removal for each gas species present in the system are displayed in Table 5.4. Table 5.4 was calculated from Table 5.2 and Table 5.3. With the exception of H_2S, the gas species present in the system experience limited loss from the inlet to the outlet of the system, in relation to N_2 present. The H_2S present in the system had significant relative removal from the inlet to the outlet streams, with an average of 98.3% ±1.5std deviation over 55 days, after the second startup and acclimatization stage. The other gas component relative removal rates vary significantly, and it is presumed this variation is due to experimental error.

Table 5.4 Relative experimental mass flow rate and percent removal of gas species in system under varying experimental conditions

Experiment	*Stage*	$\Delta \dot{m}_{CH4}$	$\Delta \dot{m}_{CO2}$	$\Delta \dot{m}_{H2S}$	$\Delta \dot{m}_{O2}$	$\Delta \dot{m}_{N2}$	$\Delta \dot{m}_{Tot}$		$\dot{R}_{CH4}$	$\dot{R}_{CO2}$	$\dot{R}_{H2S}$	$\dot{R}_{O2}$
Type	#								*%*	*%*	*%*	*%*
Start&Acc	1	0.000	0.000	0.000	-0.002	0.000	-0.002					-0.72
Start&Acc	2	0.006	0.016	0.002	0.000	0.000	0.025		1.71	1.64	79.65	0.12
Start&Acc	3	0.019	0.039	0.013	0.024	0.000	0.095		1.31	1.00	95.97	8.54
Start&Acc	3-low	0.058	0.183	0.006	0.003	0.000	0.250		9.94	11.16	98.78	1.30
Start&Acc	4	-0.006	-0.033	0.013	0.013	0.000	-0.013		-0.44	-0.84	98.74	4.63
Loading	1	0.145	0.338	0.015	0.008	0.000	0.506		8.40	7.46	98.37	2.92
Loading OFF	NA	NA	NA	NA	NA	NA	0.000					
Loading	1	0.172	0.491	0.018	0.012	0.000	0.693		8.69	8.91	96.78	4.19
Loading	2	0.200	0.570	0.017	0.017	0.000	0.804		11.36	11.66	99.72	5.70
Loading	3	0.193	0.544	0.019	0.015	0.000	0.771		9.65	9.78	99.83	5.19
	Total	0.788	2.149	0.102	0.090	0.000	3.128	**Avg**	6.33	6.35	95.98	3.54
								stdev	*4.65*	*4.98*	*6.73*	*2.94*

The total loss of H_2S from the inlet to the outlet is assumed to either remain in the biofilter and accumulate as sulphur, or exit in the liquid outlet phase as sulphate. This is discussed further in the theoretical material balance, Section 5.3.3, and in Section 5.4 comparing a theoretical material balance with that of experimental loading stage 1.

The flow rate measurements are not entirely accurate, and a portion of the difference seen in Table 5.4 between the inlet and outlet gas mass flow rates are assumed to be due to these inconsistencies. One example of this is how nitrogen shows a slight gain from the inlet to the outlet in loading stage 2, even though it is assumed to be constant for these calculations. Overall, nitrogen should be the gas with the most constant values between the inlet and the outlet as it is inert in this system. As the air inlet was at a lower pressure than the biogas at mixing, the desired ratio between the two was difficult to regulate. When biogas flow was increased to the desired inlet flow, the concentration of air in the inlet stream was essentially reduced.

5.3 Theoretical Material Balance of H_2S Removal System

The theoretical material balance is based on process stream compositions and conditions, displayed in Figure 5.1 above. Theoretical calculations are based on a mixed gas inlet at 7.5L/h with 4%O_2 (1atm, 25^{o}C), corresponding to 0.3067mol/h inlet dry gas. Figure 5.1 also gives a basis for the experimental material balance for Loading Stage #1, which has the same flow conditions as the theoretical calculations. Summarized in this figure are the factors that affect the material balance, including the humidification of the air inlet stream, the gas mixing, and material transfer including solubilisation, metabolism and accumulation of the compounds present. The following sections outline the calculations of each inlet and outlet gas and liquid stream, including losses and reactions present.

5.3.1 Stream 1: Inlet gas –Theoretical

The composition of the synthetic biogas was 2000ppm$_v$ (0.2% $_{vol}$) H_2S, and 49.9%$_{vol}$ of both CH_4 and CO_2, mixed with air to have 4%$_{vol}$ O_2 in the inlet stream, as summarized in Figure 5.1. It was assumed that the air is composed of 21% $_{vol}$ O_2 and 79% $_{vol}$ N_2 for the purpose of these theoretical calculations. The air inlet stream contains dry air that enters a humidification column and the humidified air exiting the humidification column is assumed to be 100% saturated (25^{o}C, 1atm). The saturated air is then mixed with dry synthetic biogas before entering the biofilter.

A 4% $_{vol}$ O_2 level is desired for the gas stream entering the biofilter, corresponding to 0.0123 mol/h O_2 (25^{o}C, 1atm) as shown in Equation (5.5), where n_T is 0.3067mol/h as mentioned before.

$$n_{O2}(1) = y_{O2} n_T(1) = 0.04 \times 0.3067 \frac{mol}{h} = 0.0123 \frac{mol}{h} \tag{5.5}$$

From the correlation of N_2 content in air, it is found that the inlet gas stream contains 0.0462mol/h N_2 (25^{o}C, 1atm);

$$n_{N2}(1) = \frac{79 molN2 / molAir}{21 molO2 / molAir} \times n_{O2}(1) = 0.0462 \frac{mol}{h} \tag{5.6}$$

The amount of water present in the air stream exiting from the humidification column is calculated using Raoult`s Law;

$$y_A P = x_A p_A^*(T) \tag{5.7}$$

Since the liquid is pure (x_A=1), Raoult`s law reduces to

$$p_A = p_A^*(T) \tag{5.8}$$

From vapour pressure tables, p^*_{H2O} (25^{o}C) = 23.76mmHg

Therefore, the fraction of water in the gaseous phase after humidification is

$$y_{H2O} = \frac{23.76mmHg}{760mmHg} = 0.0313 \tag{5.9}$$

The humidified inlet air stream has P_T= 1atm and a volume of 1.4276L/h (25^{o}C, 1atm).

$$n_{H2O}(1)(1 - y_{H2O}) = y_{H2O}(n_{O2}(1) + n_{N2}(1)) \tag{5.10}$$

Therefore the molar content of water in Stream 1, $n_{H2O}(1)$, is calculated to be

$$n_{H2O}(1) = 0.0018\frac{mol}{h} \tag{5.11}$$

Therefore, the total moles of humidified air exiting the humidifier column and entering the mixing chamber to mix with the biogas:

$$n_{humidair}(1) = n_{O2}(1) + n_{N2}(1) + n_{H2O}(1) = 0.0603\frac{mol}{h} \tag{5.12}$$

And the moles of dry air in the mixed gas stream entering the biofilter is

$$n_{air}(1) = n_{O2}(1) + n_{N2}(1) = (0.0123 + 0.0462)\frac{mol}{h} = 0.0584\frac{mol}{h} \tag{5.13}$$

Thus, the number of moles of dry biogas entering the mixing chamber per hour is:

$$n_{biogas}(1) = n_T(1) - n_{air}(1) = (0.3067 - 0.0584)\frac{mol}{h} = 0.2483\frac{mol}{h} \tag{5.14}$$

The premixed synthetic biogas is made up of H_2S 0.2% $_{vol}$, CH_4 49.9% $_{vol}$, CO_2 49.9% $_{vol}$.

For this stream y_{H2S}=0.002, y_{CH4}=0.499, y_{CO2}=0.499

The molar flow of each component is as follows (at 25^{o}C, 1atm)

$$n_{CH4}(1) = y_{CH4} \times n_{biogas}(1) = 0.499 \times 0.2483 \frac{mol}{h} = 0.1239 \frac{mol}{h} \quad (5.15)$$

Table 5.5 Theoretical inlet gas composition - Stream 1 (25°C, 1atm)

	mol wt	Composition (dry basis)	Molar flow	Mass flow	Volume
	g/mol	*% vol*	*mol/h*	*g/h*	*L/h*
CH_4	16	40.40	0.1239	1.9823	3.0296
CO_2	44	40.40	0.1239	5.4513	3.0296
H_2S	34	0.16	0.0005	0.0169	0.0121
O_2	32	4	0.0123	0.3926	0.3000
N_2	28	15.05	0.0462	1.2922	1.1286
H_2O	18	--	0.0018	0.0329	0.0447
Total		100.00	0.3085	9.1681	7.5447

5.3.2 Stream 2: Inlet Liquid - Theoretical

The composition the inlet liquid nutrient inlet stream is summarized in Table 5.6. The nutrient solution has a pH 3, and an inlet flow rate of 0.04L/h (80mL/min for 30 seconds every hour)

Table 5.6 Theoretical inlet liquid composition – Stream 2 (40mL/h)

	mol wt	Concentration	Molar flow	Mass Flow
	g/mol	*g/L*	*mol/h*	*g/h*
Water	18	1000	2.22	40.00
$(NH_4)_2SO_4$	132	2	6.05E-04	8.00E-02
KCl	75	0.1	5.37E-05	4.00E-03
K_2HPO_4	174	0.25	5.74E-05	1.00E-02
$MgSO_4\ 7H_2O$	246	0.25	4.06E-05	1.00E-02
$Ca(NO_3)_2$	164	0.01	2.44E-06	4.00E-04
$FeSO_4\ 7H_2O$	278	25	3.60E-03	1.00
Total			2.22411	41.10

It is known that the liquid nutrient inlet solution is at a pH of 3. From this, the amount of H^+ ions and amount of H_2SO_4 added can be estimated.

$$pH = -\log\left[H^+\right] \tag{5.16}$$

With a pH of 3, (H^+) = 1x 10^{-3}M. Therefore, 0.5x 10^{-3}L of 1M H_2SO_4/L of solution must be added.

5.3.3 Inside the biofilter - theoretical

The solubility of gas in water can change depending on temperature, pressure and pH. The pH is important since the pH of the water inside the system is 3 or less. ChemCad Version 6.0 simulation software was used to determine the solubility of CO_2, H_2S, N_2, O_2, and CH_4 at a temperature of 25°C, pressure 1atm, and a pH of 2.7. In this simulation, an air stream (1.80g/h) was first humidified and then mixed with a biogas stream (8.17g/h). It then entered a packed column where it contacted a water stream, chosen at 3L/h, to simulate a wet filter bed. The resulting mass fraction for each gas in the exiting liquid stream was considered as the solubility under these conditions. This simulation was done with the changing solubility of CO_2 and H_2S in acidic conditions in mind. It is assumed that the other gas components (CH_4, O_2 and N_2) solubility remain constant over changing pH. Table 5.7 below displays the solubilisation rates for each gas present in the system.

Below is an example of an alternative calculation of methane solubility as well as a calculation for the amount of methane solubilised in the system. The solubility of CH_4 is calculated based on Henrys law relating to solubility in water with

$$p_A = x_A H_A = y_A P \tag{5.17}$$

where p_A is the partial pressure of component A, H_A is the Henrys constant and x is the mole fraction of the solute dissolved in water.

In this case, H_{CH4} = 39,000 atm at 25°C (*Perry's Chemical Engineers' Handbook,* 1984). Therefore,

$$x_{CH4} = \frac{y_{CH4}P}{H_{CH4}} = \frac{0.1230 mol_{CH4}}{0.3085 mol_{gas}} \times \frac{1atm}{39000} = 1.0223 \times 10^{-5} \frac{molCH4}{totalmol} \tag{5.18}$$

or a solubility of 0.0092g/kg H_20 at 25°C.

The effect of solubility is calculated using the volume of water present in a 'wetted' biofilter. This 'wetted' volume is the amount of water remaining in the biofilter when all standing water has been drained (see Section 3.3.1 and 4.3.2).

Water content of 'wetted' packing (%v/v):

$$Water\% = \frac{V_{residual}}{V_{total}} \times 100\% \tag{5.19}$$

The average water content (%v/v) was found to be 9.40% ±1.47 (See Section 4.3.2). Given that the total volume of the packed bed is 0.39L, the volume of water content in the biofilter when `wetted` is 0.036L. The inlet mass of CH_4 entering the biofilter in the mixed gas stream is 1.9874g/h. Given that the solubility of CH_4 is 9x 10^{-6} gCH_4/gH_2O, the time for the CH_4 to reach saturation in the water present in the biofilter (t_{sat}) is 0.59seconds:

$$t_{sat} = \frac{9 \times 10^{-6} \frac{gCH4}{gsoln} \times 36 gsoln}{1.9874 g/h} \times 3600 \frac{\sec}{h} = 0.59 \sec \tag{5.20}$$

The hourly rate of a gas solubilised in the biofilter is calculated with the rate of nutrient flow entering the biofilter. If the nutrient flow is replenishing the liquid volume of the wetted biofilter (36mL) every hour at 80mL/min for 30 seconds; then the liquid in the biofilter will fully refresh every 54 minutes. The amount of each gas that is lost for every hour of nutrient cycling was calculated, including the assumption that the density of the nutrient solution is that of pure water, $1g/cm^3$. The transfer of liquid present in the biofilter from the partially saturated inlet gas stream to the completely saturated outlet gas stream (0.15g/h H_2O transferred to outlet gas) was considered insignificant for the purpose of the solubilisation calculations.

$$m_{CH4sol} = 9 \times 10^{-6} \frac{gCH4}{g\text{soln}} \times 40 \frac{g\text{soln}}{cycle} = 3.6 \times 10^{-4} g/h \tag{5.21}$$

since each cycle is based on 1 hour.

Table 5.7 Solubilisation rates of gas components in system, calculated with ChemCad 6.0

Species	Mass Fraction	Solubility	Mass flow solubilised	Mole flow solubilised	Time to Saturation	Mass flow after solubilisation
	g solub/gH_2O	*g of gas/kg H_2O*	*g/h*	*mol/h*	*sec*	*g/h*
CH_4	9.00E-06	0.009	3.60E-04	2.25E-05	0.59	1.9819
CO_2	6.00E-04	0.60	2.40E-02	5.45E-04	14.26	5.4273
H_2S	5.00E-06	0.005	2.00E-04	5.88E-06	38.38	0.0167
O_2	1.00E-06	0.001	4.00E-05	1.25E-06	0.33	0.3925
N_2	2.00E-06	0.002	8.00E-05	2.86E-06	0.20	1.2921

With 0.0169gH_2S/h entering in the inlet gas stream and 0.0002gH_2S/h solubilised in the liquid present, this corresponds to a 1.2% loss of H_2S due to solubilisation. From Table 5.7 it is also seen that 0.024gCO_2/h is solubilised in the biofilter. As the inlet CO_2 flow is so high (5.45gCO_2/h in Table 5.5), the loss due to solubilisation is considered minimal with 0.44%CO_2 loss due to solubilisation.

It is assumed that the absorption onto the packing material is minimal in comparison to the solubilisation, and reaches an equilibrium quickly, having no effect on the outlet gas concentration. Other factors considered to affect the gas compounds include the oxidation of H_2S, as seen in the species material balances in Section 5.3.6.

5.3.4 Stream 3: Outlet Gas - Theoretical

As a basis for calculations of the outlet gas stream composition, the temperature and pressure of the outlet stream were considered to be the same as the inlet stream, or 25^oC and 1atm respectively. The following assumptions were made for determining the composition of the biofilter outlet gas stream, displayed in Figure 5.1. The outlet gas stream is 100% saturated with water, and biogas is assumed to have the same humidification capacity as air, or a moisture content of 0.02kg/kg dry air at 25^oC (see Section 5.3.6). A 95% H_2S removal efficiency was assumed from the biofilter, including that only a portion of the O_2 is consumed by the microorganisms during H_2S oxidation. Finally, it was assumed that CH_4 and N_2 were not consumed or reacted in the biofilter, apart from minor solubilisation, and that CO_2 was only consumed in solubilisation with the usage of CO_2 by bacterial activity considered minimal. The amount of humidification is based on mass and was found from a psychometric chart.

As such, it was necessary to estimate the mass flow of the gas components present in the outlet gas stream before calculating the amount of water exiting with the outlet gas. The mass flow rate of each component in the outlet gas stream is found in Table 5.8.

5.3.5 Stream 4: Outlet Liquid –Theoretical

It is assumed that some nutrients in the inlet liquid stream are consumed, but that the inlet nutrients are in excess for the purpose of calculations, and that these compounds exit in the outlet liquid stream without changing composition. Although the elemental sulphur produced in H_2S oxidation either accumulates in the biofilter or exits through the outlet liquid stream, it is assumed that accumulation or sulphur in the biofilter occurs, and thus the elemental sulphur is not present in the outlet liquid stream. The flow of the liquid outlet is the same as the liquid inlet, with the exception of water taken up by the nearly saturated inlet gas. Mass flow rates of the components in the outlet liquid stream are found in Table 5.8.

5.3.6 Overall balance equations

The overall molar balances for each compound are presented below. The mass flow rate of each compound present in the system is summarized in Table 5.8. Each stream for each compound is denoted by (1), (2), (3) and (4) respectively.

The nitrogen present in the mixed inlet gas stream will be minimally affected by solubilisation. The nitrogen molar balance is therefore

$$\dot{n}_{N2}(1) = \dot{n}_{N2}(3) + \dot{n}_{N2}(4) \tag{5.22}$$

where $\dot{n}_{N2}(4)$ is assumed to be zero.

Methane present in the mixed inlet gas stream would be susceptible to solubilisation only, and this portion would leave the system in the liquid exit stream. The methane molar balance is therefore

$$\dot{n}_{CH4}(1) = \dot{n}_{CH4}(3) + \dot{n}_{CH4}(4) \tag{5.23}$$

Hydrogen sulphide present in the inlet gas stream enters into the liquid format and is then oxidized by bacteria present through Equation (5.24) (Soreanu et al. 2005), forming elemental sulphur. A second

route of metabolism for H_2S is given by Equation (5.25), but it is assumed however that in the oxygen limiting conditions Equation (5.24) prevails.

$$H_2S_{(aq)} + ½\ O_{2(g)} \rightarrow S_{(s)} + H_2O \tag{5.24}$$

$$H_2S_{(aq)} + 2O_{2(g)} \rightarrow H_2SO_{4(l)} \tag{5.25}$$

As 95% H_2S removal is assumed, 5% of the H_2S entering will exit in the outlet gas stream. The rest is assumed to accumulate in the biofilter packing in the form of elemental sulphur.

$$\dot{m}_{H2S}(1) = \dot{m}_{H2S}(3) + \dot{m}_{H2S}(4) + \dot{m}_{H2S}(metab) \tag{5.26}$$

The oxygen in the inlet gas stream is both solubilised in the system as well as consumed by the bacteria present in the biofilter. From the reaction in Equation (5.24) above showing the biological degradation of H_2S, $2.36x10^{-4}$ mol/h (0.0075g/h) of O_2 will be consumed, and 0.0120mol/h (0.385g/h) of O_2 remain for the gas outlet stream.

$$\dot{m}_{O2}(1) = \dot{m}_{O2}(3) + \dot{m}_{O2}(4) + \dot{m}_{O2}(metab) \tag{5.27}$$

From this it can be presumed that the amount of O_2 present in the system is in fact in excess, as the degradation of 0.00047mols/hH_2S would require only $2.36x10^{-4}$ mol/h O_2 in the biological degradation process, according to Equation (5.24). This is equivalent to $0.076\%_{vol}$ O_2 in the inlet gas stream.

A portion of carbon dioxide in the inlet gas stream would solubilise in the water present in the biofilter. Also carbon dioxide would be consumed by the bacteria in the biofilter would occur via reaction Equation (5.28) (Duan et al. 2005)

$$CO_2+H_2O+E. \rightarrow [CH_2O] + O_2 \tag{5.28}$$

As the growth rate of the bacteria is not known, the amount of CO_2 consumed by the bacteria is assumed to be minimal. Thus it was neglected for the purpose of these calculations as CO_2 was of less interest than H_2S or CH_4 in this study.

$$\dot{m}_{CO2}(1) \cong \dot{m}_{CO2}(3) + \dot{m}_{CO2}(4) \tag{5.29}$$

The amount of water in the inlet to outlet gas stream changes since the outlet gas stream is fully humidified while the inlet gas stream is only partially humidified (the inlet air stream is 100% humidified before mixing with the biogas). As such, the outlet gas stream will take water from the nutrient solution to become humidified. Also, a small amount of water is produced when H_2S is degraded by the bacteria (see Equation (5.24) above). This water is produced at a rate of $5x10^{-5}$ g/h based on 95% H_2S removal by this mechanism in the biofilter.

$$\dot{m}_{H2O}(1) + \dot{m}_{H2O}(2) = \dot{m}_{H2O}(3) + \dot{m}_{H2O}(4) + \dot{m}_{H2O}(metab) \tag{5.30}$$

The amount of water present in the 100% saturated gas outlet stream was found using the psychometric chart. It was assumed that the mixed gas stream had the same saturation characteristics as air. According to the psychometric chart for air with a relative humidity of 100% and a dry bulb temperature of 25°C, the moisture content of this humidified air stream would be 0.02kg/kg dry air.

Therefore, based on a mass flow of 9.2689g/hr for the gas components in the outlet gas stream, the amount of H_2O in this stream would be 0.1817gH_2O/h (0.0101molsH_2O/h), by the following equation;

$$\dot{m}_{H2O}(3) = 0.02\frac{kg}{kg_{dryair}}\sum\left(\dot{m}_{CH4}(3) + \dot{m}_{CO2}(3) + \dot{m}_{H2S}(3) + \dot{m}_{O2}(3) + \dot{m}_{N2}(3)\right) \tag{5.31}$$

The nutrients added in the inlet liquid nutrient stream are consumed and degraded by the bacteria. For the purpose of these calculations, it was assumed that the nutrients were in excess and also that any nutrients degraded would not change composition. Thus, it was assumed that the nutrients in the system would leave in the outlet liquid stream in the same composition as they entered.

$$\dot{m}_{nutr}(2) = \dot{m}_{nutr}(4) + \dot{m}_{nutr}(metab) + \dot{m}_{nutr}(accum) \tag{5.32}$$

Table 5.8 displays the composition of each of the 4 process streams in mass flow bases. It is seen that a small amount of the gas components exit in the liquid stream. This amount incorporates the gas that is solubilised as well as that used in the H_2S oxidation process (ie O_2). Removal of H_2S in the system is represented by an accumulation which is considered to be an accumulation of elemental sulphur. Therefore, 0.00047 mol/h (0.015g/h) of elemental sulphur is accumulated in the biofilter with an inlet

biogas flow of 6L/h (25^{o}C, 1atm). As seen by the nutrient components, they are assumed not to be consumed during this process.

Table 5.8 Mass flow rate and accumulation of each process stream of biofilter (Inlet 7.5L/h dry gas, 25^{o}C, 1atm)

	Stream 1	Stream 2	Stream 3	Stream 4	Accumulation
Component	*g/h*	*g/h*	*g/h*	*g/h*	*g/h*
CH_4	1.98E+00	--	1.98E+00	3.60E-04	0.0
CO_2	5.45E+00	--	5.43E+00	2.40E-02	0.0
H_2S	1.69E-02	--	8.44E-04	2.00E-04	1.58E-02
O_2	3.93E-01	--	3.85E-01	7.59E-03	0.0
N_2	1.29E+00	--	1.29E+00	8.00E-05	0.0
H2O	3.29E-02	4.00E+01	1.82E-01	3.99E+01	0.0
$(NH_4)_2SO_4$	--	8.00E-02	--	8.00E-02	0.0
KCl	--	4.00E-03	--	4.00E-03	0.0
K_2HPO_4	--	1.00E-02	--	1.00E-02	0.0
$MgSO_4$ $7H_2O$	--	1.00E-02	--	1.00E-02	0.0
$Ca(NO_3)_2$	--	4.00E-04	--	4.00E-04	0.0
$FeSO_4$ $7H_2O$	--	1.00E+00	--	1.00E+00	0.0
H_2SO_4	--	9.81E-02	--	9.81E-02	0.0
Total	9.17	41.20	9.27	41.09	0.0158

5.4 Comparison of Theoretical and Experimental Material Balance

Results of the experimental and theoretical material balances were compared using loading experiment Stage #1 with 2 runs at total gas flow of 7.5L/h; 1.5L/h air and 6L/h biogas. The results of these two time periods were tabulated and then averaged, in Table 5.9. These results were then compared with the theoretical calculations at the same flow rate conditions, which are tabulated in Table 5.10.

Table 5.9 Experimental mass flow rate of inlet and outlet biofilter gas process streams (7.5L/h dry gas inlet, T and P variable)

	CH_4	CO_2	H_2S	O_2	N_2
	g/h	*g/h*	*g/h*	*g/h*	*g/h*
Stream 1 : Inlet gas average	2.16	5.82	0.0193	0.33	1.17
Stream 1 std deviation	*0.03*	*0.17*	*0.00*	*0.02*	*0.13*
Stream 3 : Outlet gas average	1.97	5.34	0.00	0.32	1.17
Stream 3 std deviation	*0.01*	*0.21*	*0.00*	*0.01*	*0.10*
Difference	0.19	0.48	0.02	0.01	0.00

Table 5.10 Theoretical mass flow rate of inlet and outlet biofilter gas process streams (7.5L/h dry gas inlet, 25^{o}C, 1atm)

	CH_4	CO_2	H_2S	O_2	N_2
	g/h	*g/h*	*g/h*	*g/h*	*g/h*
Stream 1: Inlet Gas	1.98	5.45	0.017	0.39	1.29
Stream 3: Outlet Gas	1.98	5.43	0.001	0.38	1.29
Difference	0.00	0.02	0.016	0.01	0.00

In Table 5.11 the experimental mass flow rates for each gas compound were compared with the theoretical mass flow rate under the same conditions.

Table 5.11 Difference of theoretical and experimental inlet and outlet biofilter gas streams

	CH_4	CO_2	H_2S	O_2	N_2
	%	*%*	*%*	*%*	*%*
% Difference, Inlet	8.7	6.8	14.6	16.7	9.6
% Difference, Outlet	0.6	1.6	43.6	18.1	9.8

The inlet and outlet theoretical and experimental mass flow rates of the inlet and outlet gas of the biofilter have similar values. The inlet biogas experimental flow rate is higher than expected, and in response, the air component experimental values are lower than the theoretical. This is most likely related to inaccurate flow rate measurements, as described above. Overall, the theoretical material balance is able to give an indication of the expected experimental values.

5.5 Theoretical Pressure Drop

The pressure drop across the packed bed was estimated using the Ergun equation,

$$\frac{\Delta p}{h} = \left(\frac{1-\varepsilon}{\varepsilon^3}\right)\frac{G^2}{d_p \rho_G}\left[\frac{150(1-\varepsilon)\mu_G}{d_p G} + 1.75\right] \tag{5.33}$$

where ε (porosity) was 0.43 for dry packing (see Section 4.3.2), d_p (diameter of particle in the packed bed) was 0.36cm; and h (height of packed bed) was 20cm. The superficial velocity, u, was calculated to be 382cm/h with gas at 7.5L/hr and a pipe diameter of 5cm. The viscosity of each gas was gathered from *CRC Handbook of Chemistry and Physics,* (1982) for 300K. The viscosity, μ_G, of the mixed gas stream was found to be 14.18μPas (or 14.18×10^{-4}g/cm s), calculated from the composition of the gas stream (40.4%$_{vol}$ CH_4, 40.4%$_{vol}$ CO_2, 0.16%$_{vol}$ H_2S, 4%$_{vol}$ O_2, and 15.05%$_{vol}$ N_2) and each species respective viscosity. The density of the gas, ρ, was calculated to be 1.218g/L. The superficial mass velocity, G, was calculated to be 1.29×10^{-3}g/cm^{2}s, where G = ρu, with a column surface area of 19.6cm^2. The pressure drop was calculated to be 1.04×10^{-4} psi/m or 0.21×10^{-4}psi for 20cm of the initial dry packed bed present. Figure 5.2 displays the theoretical pressure drop as a function of porosity. A porosity of 0.34 represents the 'wetted' packed bed, while decreasing porosity of 0.3 to 0.1 would represent an accumulation in the packed bed due to bacterial and biofilm growth on the packing material. Although it is not known exactly how the porosity would change with bacterial growth, this trend gives an idea of how the pressure drop would change.

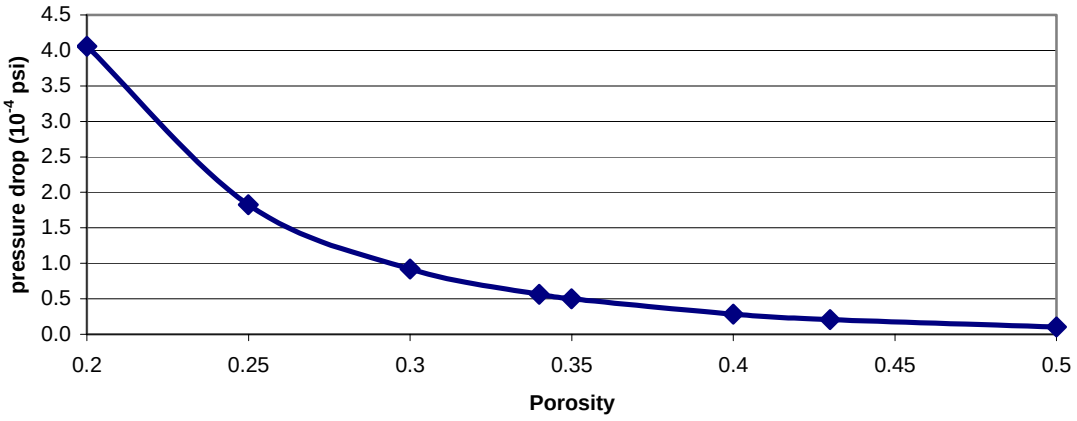

Figure 5.2 Theoretical pressure drop with varying porosity, over 20cm packed bed

From Figure 5.2 it can be seen that as the porosity drops below 0.25, the pressure increases substantially. As the porosity drops below 0.1, the pressure drop increases to 0.04psi over the 20cm column, not shown here.

Chapter 6
Results and Discussion - Supplementary

6.1 Inoculum Conditioning With *A. ferrooxidans* Media

Preliminary conditioning of sulphur oxidizing bacteria from activated sludge was done using *A. ferrooxidans* media for the use as a biofilter inoculum. Experimentation lasted 18 days with a media change every 5-7 days. The pH of the media solution containing activated sludge started at 3.8 and decreased to 3.1 within 5 days, as can be seen in Figure 6.1. The pH of the non inoculated reference media solution remained at 3.0, indicating that the decrease in pH of the inoculated solution was a result of the presence of the activated sludge. A change in colour was observed with the inoculated media solutions, as the solution became brown/orange and opaque. A second set of experiments of activated sludge and growth media was started 5 days later. The initial pH of the solution was higher at 4.5 most likely due to the change in the activated sludge while being stored in the refrigerator. The pH of this solution decreased more quickly than the first set but still reached a similar stable pH of 3.1 within 5 days also, as can be seen in Figure 6.1. In this preliminary experiment the pH of the blank nutrient solution was monitored for 5 days to verify the behaviour of the pH of this solution over time. In the packing test carried out under the same conditions, the pH of a similar reference solution was monitored for a longer period of time, verifying these results with consistent pH values.

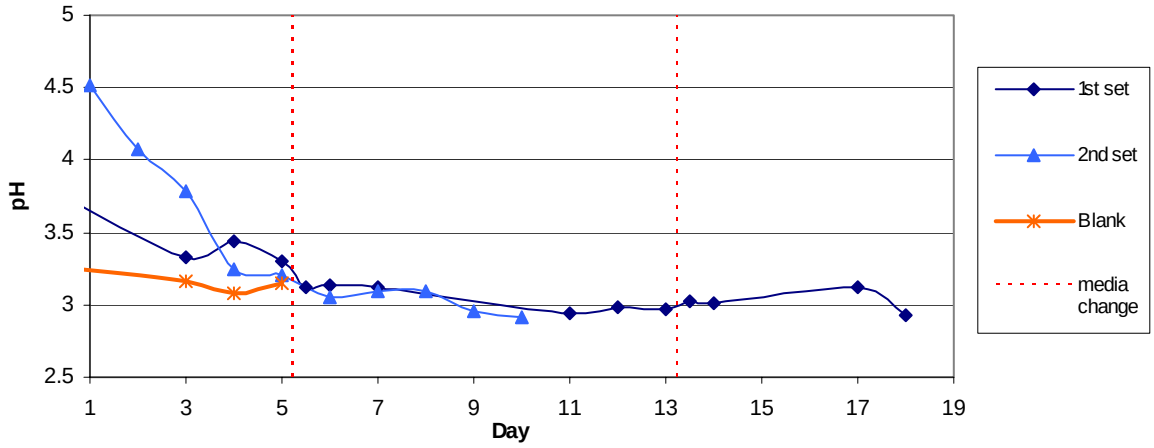

Figure 6.1 pH evolution for activated sludge in *A. ferrooxidans* media, n=2 (150rpm, 25°C)

When using the *A. ferrooxidans* media (Harrison 1984) in the growth of pure *A. ferrooxidans* species, a decrease of pH is seen (Harrison 1984) as well as a colour change in the solution to a rusty orange colour (Arsenault 2009). Both a slight a colour change to orange/brown a slight decrease in pH were seen, and as such it was concluded that there were bacteria present in the inoculum that were growing in the *A. ferrooxidans* media solution. As the exact species of bacteria present was not verified, it was assumed that *A. ferrooxidans* is not the only bacteria species present, but rather a consortium of bacteria which all live under these growth conditions.

6.2 Packing Test

The effect of the packing material selected for use as a bacterial growth support was tested. Four experimental conditions were selected; reference flasks with only the *A.ferrooxidans* media (F), the nutrient media and packing material (FP), the nutrient media and inoculum (FB), and finally the nutrient media, packing and inoculum (FPB). Colour, pH and Fe^{2+} /Fe^{3+} were investigated.

6.2.1 Packing test: colour

The reference flasks (F), containing only the *A. ferrooxidans* nutrient media remained light yellow throughout the experiment, with slight faint yellow precipitate forming in the bottom of the flask, as seen in Figure 6.4.

Those with media and packing material (FP) displayed an opaque orange rust colour initially on day 1. The orange colour present was mainly due to a precipitate, which settled out if left undisturbed. Each media change that followed resulted in less of this orange precipitate present, since less precipitate was being formed, and the packing material was rinsed during media changes. Figure 6.3 and Figure 6.4 are the solutions from the 3rd media change, and the difference in colour between the F and FP samples is seen. By the 4th media change, there was only slight orange/beige opaque colouring in the FP solutions.

The media and inoculum sample flasks (FB) remained light yellow initially until after 4 days when the colour changed to rusty orange. This colour deepened until media change. After the third media change there was less yellow colour initially, and mainly the deep orange/red colour, as can be seen in Figure 6.3. When the samples were left undisturbed, the orange colour settled out in precipitate, leaving a deep orange/red solution, as seen in Figure 6.4.

The flasks with media, packing and inoculum (FPB) displayed the greatest changes throughout the experiment. The first 5 days showed relatively no change, with a fairly clear solution. At this point the solution changed to an opaque orange/rust colour. After 8-16 days depending on the conditions, this orange colour changed to yellow, with yellow precipitate material suspected to be sulphur. Figure 6.2 displays the differences in FPB solutions on the second media change, on day 13 where the FPB1 solution was producing more yellow, while the other FPB2 and FPB3 samples were more orange. The colour of the FPB2 and FPB3 solutions changed to yellow 1 week later. The FPB solutions continuously produced the yellow precipitate, as seen in Figure 6.3, when the solution is agitated, and Figure 6.4 when the solutions were left to settle to show the colour of the liquid portion. By the end of the experiment period, all flasks were the clear red/orange solution with both orange and yellow powder settled out amongst the packing material (not shown). The packing material was beginning to bind together and to the bottom of the flask due to the bacterial activity, showing that visually there was bacterial growth, especially compared with the non-inoculated samples.

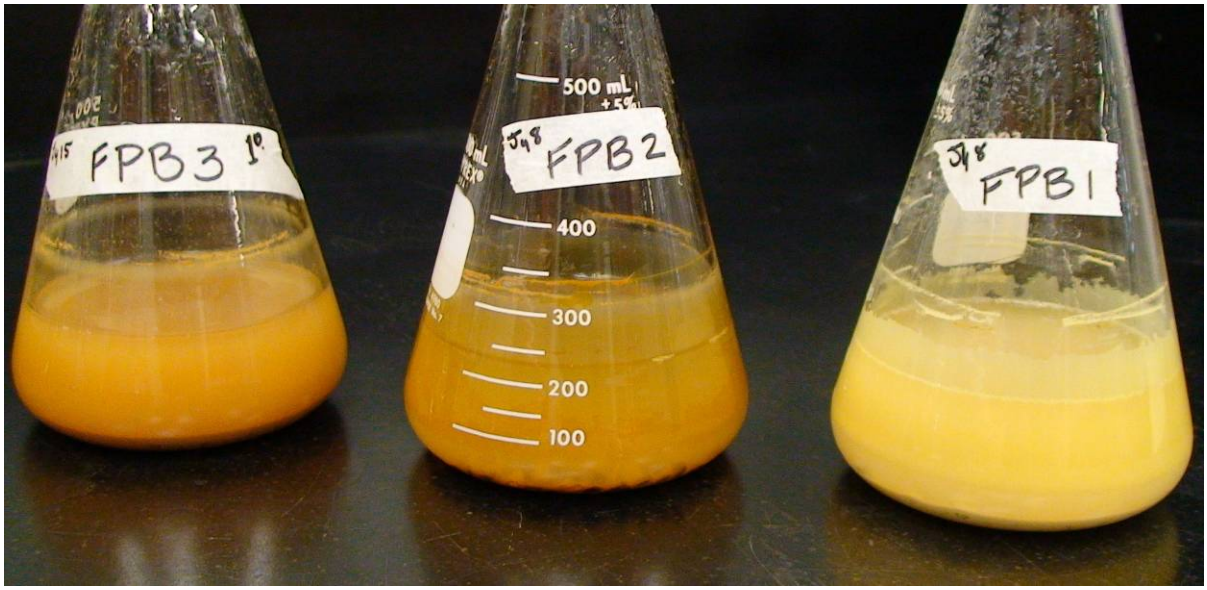

Figure 6.2 FPB samples at media change, day 13 (150rpm, 25°C)

Figure 6.3 Packing test solutions at media change - Agitated, day 20 (grown at 150rpm, 25°C)

Figure 6.4 Packing test solutions at media change – Settled, day 20 (grown at 150rpm, 25°C)

6.2.2 Packing test: pH evolution

Figure 6.5 displays the pH of each packing test flask (n=2, except n=3 for FPB) over the length of the experiment. The dashed vertical line at day 6, 13, 21, 26, and 34 indicate media changes. It can be seen that until approximately day 30 the FP samples had consistently higher pH values than all the others, caused by a buffering effect of the packing material. Towards the end of the experiment, contamination was seen of the FP flasks by a drop in the pH. It was decided to identify and exclude contaminated data sets, as discussed below.

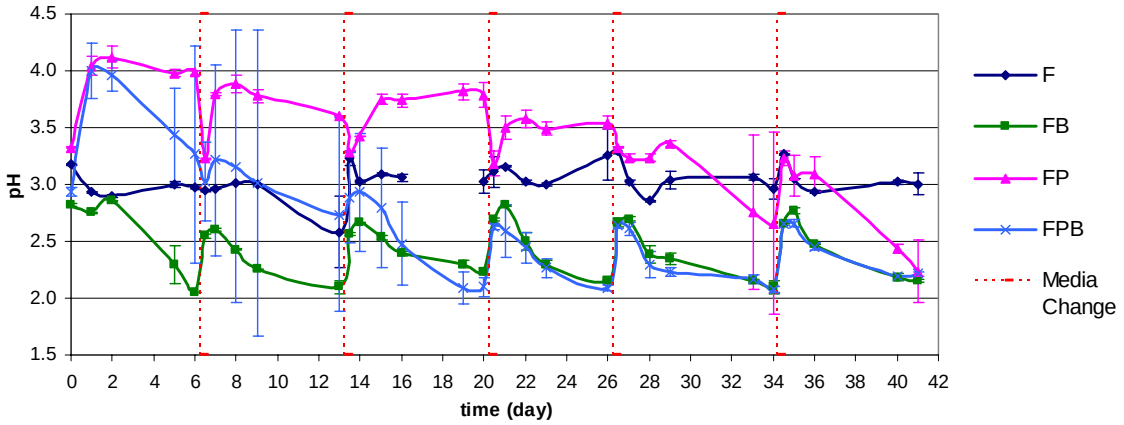

Figure 6.5 pH of packing tests, n=2, (150rpm, 25°C) Error bar represents standard deviation

Contamination in the uninoculated flasks (F and FP samples) occurred when these flasks displayed properties such as colour and pH similar to those with known bacterial growth (FB samples). Identification of contamination of these blank samples included pH variation, colour and transparency of the solution. Presented in Figure 6.6 is an example of contamination from day 6 to 16 for the F samples with presumed contamination of the F2 sample on day 13, before a media change.

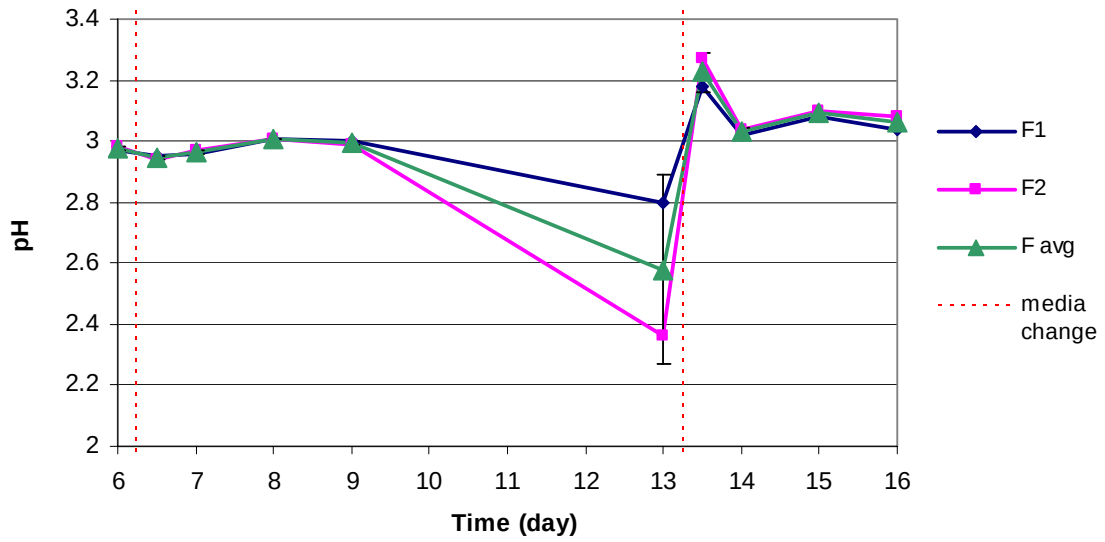

Figure 6.6 pH of packing tests: Contamination in F sample, n=2, (150rpm, 25°C) Error bar represents standard deviation

As seen in Figure 6.5, the pH of the F solutions was considered constant over most of the experiment at 3.04±0.14. In the case of the F2 sample during the period of day 6-13, it can be seen in Figure 6.6 that the pH of F2 drops below 2.4 on day 13. A colour change was observed at this time also as the normally clear slightly yellow liquid became a dark red or orange cloudy solution, closely resembling that of the FB samples. With both the pH and visual observations, this was considered as a contamination.

Contamination was also visible in the FP samples towards the end of the experimental period. The FP samples were generally a clear orange/red liquid with an orange/red precipitate, if any. When thought to be contaminated, the liquid of these samples changed to a yellow opaque colour with a yellow

precipitate at the bottom of the flask mixed in with the gravel. This closely resembled the FPB samples in the first weeks of growth when they appeared to be producing elemental sulphur that would precipitate out. The pH of the FP sample displaying this colour change is displayed as FP2 in Figure 6.7 below. The contamination values can be seen at day 34 before the media change where the FP2 readings are much lower than FP1 and the trend from day 22 to 29. Contamination is apparent in both FP samples at the last media change with both visual changes and a significant drop in the pH from 3.2 to 2.4.

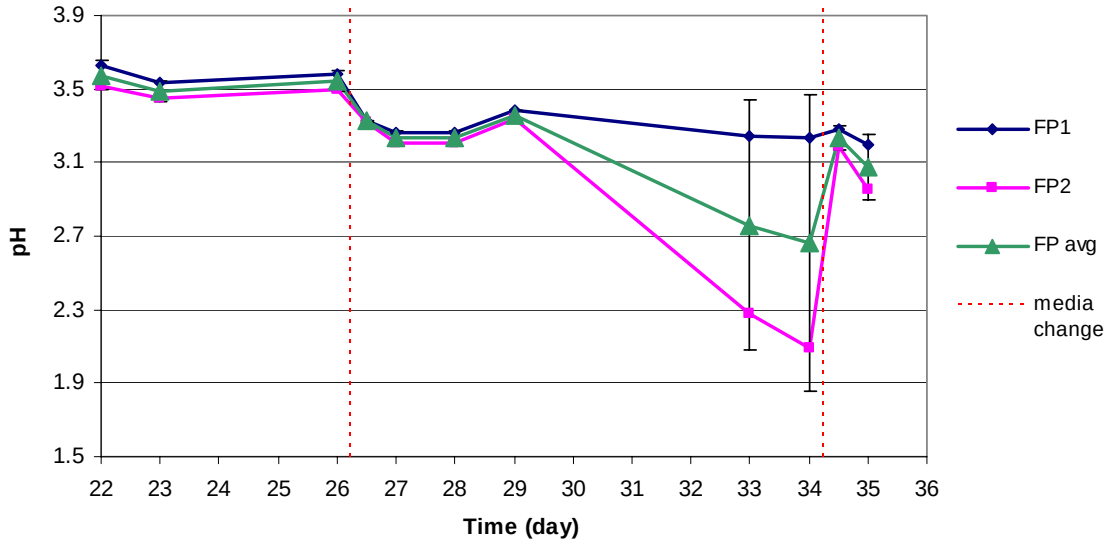

Figure 6.7 pH of packing tests: Contamination in FP sample, n=2 (150rpm, 25°C) Error bar represents standard deviation

Although it was possible to remove contamination from the F samples by cleaning, this was not possible with the FP samples as the contamination was in the packing material present. Beginning again with new packing material would have been as if restarting the experiment. The points that were decided to be contaminated were omitted from both pH and [Fe] trends and calculations.

Figure 6.8 below displays the pH of each condition group throughout the 40 day experiment, with the exclusion of contaminated points, discussed above. The F flasks are relatively constant at pH 3 over

time, while the FP samples remain at a higher pH due to a buffering effect of the packing material. This is seen especially after each media change when the pH immediately returns to the higher value, suggesting a chemical reaction. It was assumed that the packing material reacted with the high concentration of 25g/L $FeSO_4$ in the non-inoculated solution, forming precipitate. The exact mechanism of this, as well as the effect of the low pH of the solution was not investigated. The FB solutions followed consistently the same trend, decreasing in pH from 3 (or 2.5 after the second media change) to 2.1 after each media change. The FPB solutions also followed this trend after the second media change suggesting the packing material only impacted the pH of the FPB solutions for the first 14 days. There was higher variability in the FPB samples for the first 17 days as the transformations of each of the FPB flasks happened at a different rate. It was noted that an initial production of sulphur (forming yellow precipitate) in the FPB reactors at the beginning showed a drop in pH at the same time.

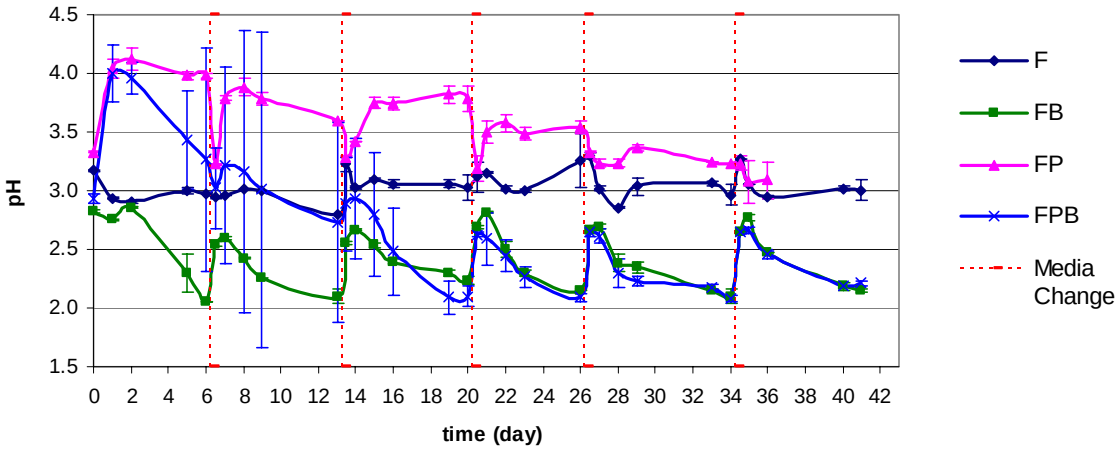

Figure 6.8 pH of packing tests, excluding contaminated points, n=2, (150rpm, 25°C) Error bar represents standard deviation

Overall, it was shown that there was an adjustment period for the inoculum to produce a lower pH solution in the presence of the packing material. This adjustment period took an average of 14 days depending on the conditions. After this period, those flasks with media packing and inoculum resembled closely those without packing.

6.2.3 Packing test: Fe^{2+}/Fe^{3+} results

The content of Fe_T, Fe^{2+} and Fe^{3+} were assessed over time for each of the packing test conditions. Figure 6.9, Figure 6.10, and Figure 6.11 show the Fe total, Fe^{2+}, and Fe^{3+}, respectively, for each solution at each media change. Each media change is represented by a point and not in a trend since each reading was thought separate as they represent points 1 week apart or more. These samples were stored in the refrigerator at 4°C and done in bulk at the end of the experimental period, on day 44. It was realized in later analysis that the content of Fe^{2+} and Fe^{3+} would change over time, even when stored in the refrigerator. This was verified testing a sample in duplicate 3 times in the span of 3 weeks. The effect of storage on the Fe^{2+} and Fe^{3+} values could not be accurately quantified, but it was concluded that this effect was significant. As the results reported here originate from samples that were stored in the refrigerator from 2 to 6 weeks, it must be concluded that the factor of storage may have had an effect on the results. As such, the results of the Fe^{2+} and Fe^{3+} testing are reported below, but no definite conclusions can be drawn at this time.

The concentration of Fe_T was 5000ppm in the nutrient media solution, and when tested, each flask had a total Fe content of approximately 5000ppm at day 0, with the addition to any Fe transferred from the old solution after a media change (30mL transferred of old solution). In Figure 6.9, displaying the total dissolved iron (Fe_T), the F samples containing only nutrient solution remained relatively constant between 4800 and 5000ppm the entire testing period. The total Fe of the FB samples also remained relatively constant throughout the experiment, indicating there were no major changes in the growth of the bacterial colony. This was also confirmed by the relatively constant pH seen in Figure 6.5 of the FB samples throughout the course of each period. The total iron of the FP samples increased throughout the experiment. The amount of precipitate formed decreased after each media change until there was very little precipitate being produced. The precipitate was a result of Fe compounds precipitating out of solution, thus lowering the total dissolved Fe. This accounts for the increase in Fe total over time with the FP samples, as less precipitate was formed in the FP samples towards the end of the experiment. The total Fe values of the FPB samples varied throughout the experiment, and were always lower than the other samples as the bacteria present transformed the dissolved iron present in solution into a precipitated iron compound. This compound either resembled an orange/red powder or a yellow powder, signifying sulphur and iron compounds.

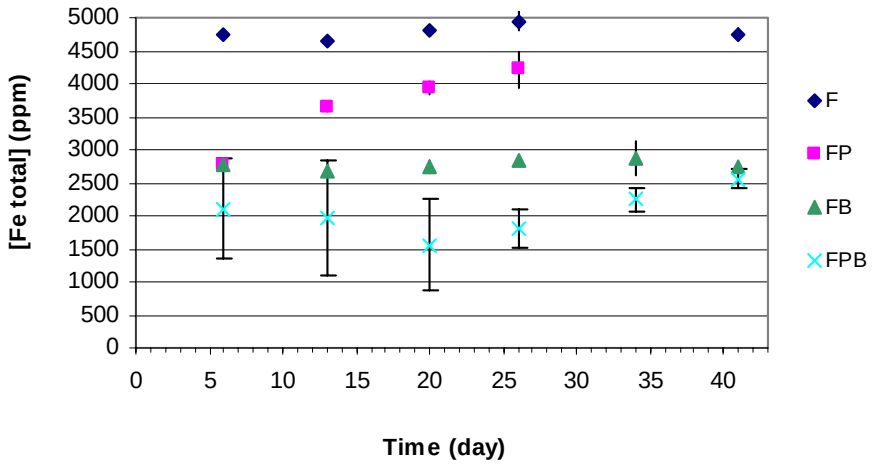

Figure 6.9 Packing test: total dissolved iron at each media change, n=2 (150rpm, 25°C) Error bar represents standard deviation

The changes in Fe^{2+} over the experimental period for each testing solution are seen in Figure 6.10. The concentration of Fe^{2+} is relatively constant for both the F samples containing only the nutrient media and for the FB samples. FP samples displayed an increase in Fe^{2+} over time, indicating interactions of Fe^{2+} with the packing material. After 20 days, the Fe^{2+} content in the FPB samples decreased to resemble that of the FB samples. This is similar to the FPB pH profile in Figure 6.8 which began to resemble the pH of FB samples around day 20 also. This indicates again that there was a period of adjustment, after which the bacteria were able to use the packing material as a growth support. The decrease in Fe^{2+} over time can be represented by Equation (6.1) (Jensen and Webb 1995), as the bacteria present became more efficient at oxidizing the Fe^{2+} present.

$$4Fe^{2+} + O_2 + 4H^+ \xrightarrow{A.\ ferrooxidans} 4Fe^{3+} + 2H_2O \qquad (6.1)$$

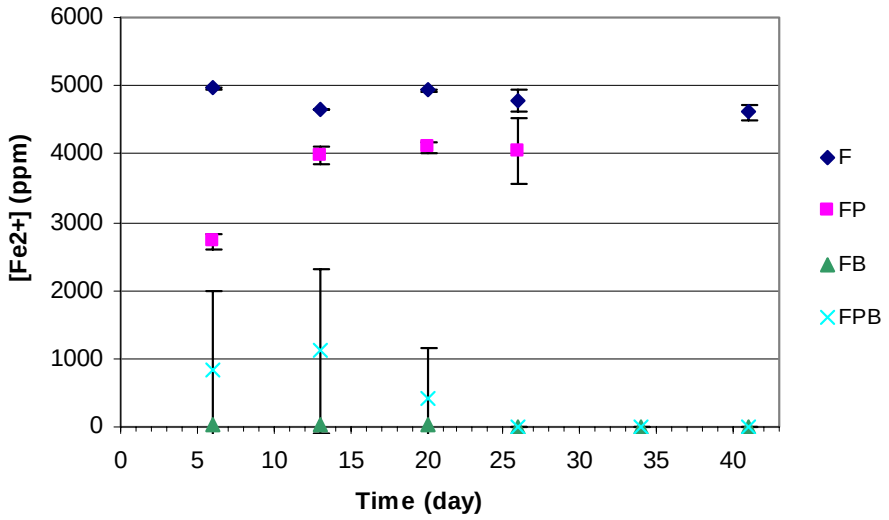

Figure 6.10 Packing test: Fe^{2+} concentration at each media change, n=2 (150rpm, 25°C) Error bar represents standard deviation

Figure 6.11 displays the Fe^{3+} concentrations at each media change. Both F and FP samples were constantly low in [Fe^{3+}]. This is because there was no inoculum present to convert the Fe^{2+} in solution to Fe^{3+}. The Fe^{3+} for the FB is also constant, with high Fe^{3+} as there was a constant amount of conversion from Fe^{2+} to Fe^{3+} by the bacteria as in Equation (6.1). The [Fe^{3+}] FPB increases over time with more Fe^{3+} production during each media change cycle.

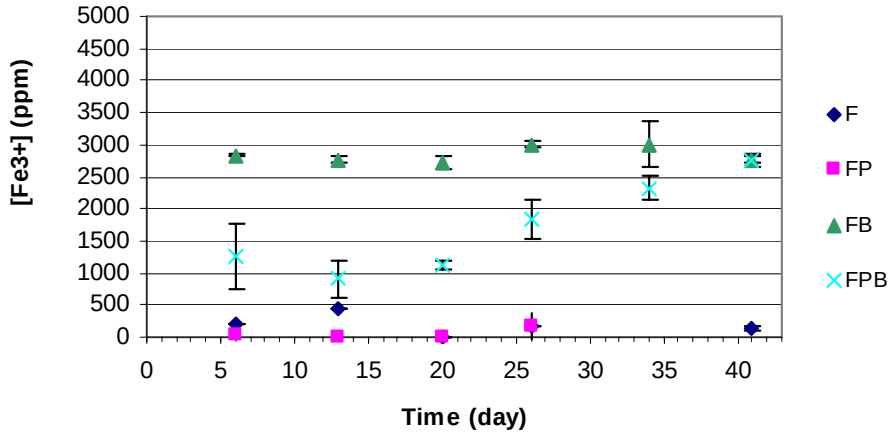

Figure 6.11 Packing test: Fe^{3+} concentration at each media change, n=2 (150rpm, 25°C) Error bar represents standard deviation

The ferric iron (Fe^{3+}) formed is then hydrolysed in solution by the following equations, producing acid (Jensen and Webb 1995)

$$Fe^{3+} + H_2O \leftrightarrow FeOH^{2+} + H^+ \quad (6.2)$$

$$Fe^{3+} + 2H_2O \leftrightarrow Fe(OH)_2^+ + 2H^+ \quad (6.3)$$

$$Fe^{3+} + 3H_2O \leftrightarrow Fe(OH)_3 + 3H^+ \quad (6.4)$$

Overall, the Fe testing showed that the F solutions were constant, and predominately Fe^{2+}, while the FB samples were predominantly Fe^{3+}, as it was oxidized to from Fe^{2+} to Fe^{3+} with biological activity. The FP samples saw an increase in Fe^{2+} over time, as less Fe^{2+} was converted to Fe^{3+} or lost to precipitation. The FPB samples had relatively constant total iron, with an increase in Fe^{3+} over the time of experimentation.

6.3 H_2S Removal in Non-Inoculated Biofilter: Supplementary

Initial and preliminary baseline testing was done with the expected biofilter operating conditions of 4%O_2 present in the inlet gas stream, gravel packing material and 25g/L of $FeSO_4$ in the nutrient solution. This was done to evaluate the chemical H_2S removal in the non-inoculated biofilter. It was found that there was significant H_2S removal, of approximately 60%. In order to evaluate the reason for this high H_2S removal in the non-inoculated biofilter, and to possibly minimize it in order to maximize the biological H_2S removal, an experimental factorial study was done to test the effect of the type of packing material, the $FeSO_4$ content in the nutrient solution and the air content in the inlet mixed gas stream. The summarized results for H_2S removal in a non-inoculated biofilter are presented in Section 4.4.1.

The extended effects of adsorption and absorption of H_2S over time were further investigated through a 48 hour experiment. The running conditions were air 25mL/min (25°C, 1atm), biogas 100mL/min (25°C, 1atm), gravel packed bed, and with no $FeSO_4$ content in the liquid wetting the filter.

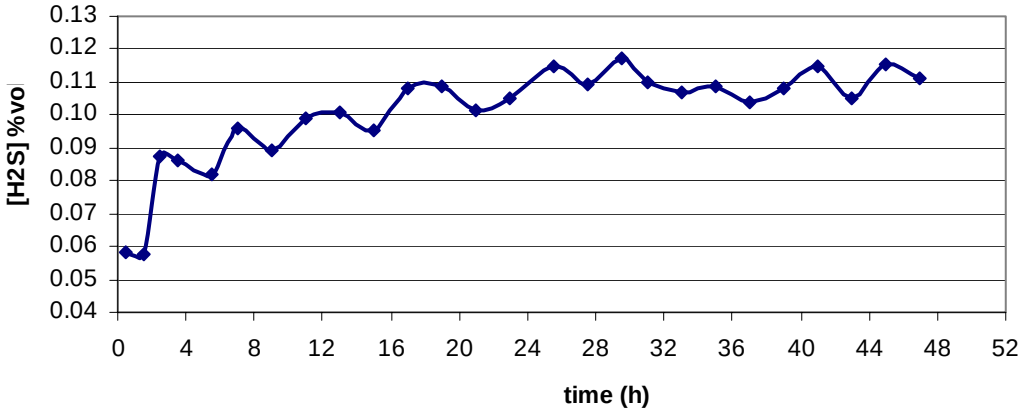

Figure 6.12 48 hour test on non-inoculated filter: Outlet [H_2S] (inlet 0.15%$_{vol}$ H_2S, 1psig, 25°C)

During this extended test, the initial inlet H_2S concentration was 0.15%. The outlet [H_2S] for the extended test is displayed in Figure 6.12. The outlet [H_2S] was considered to have reached equilibrium after two hours of operation, and the average H_2S outlet concentration after equilibrating

was 0.1%±0.01 std deviation over 33 hours. It was found that the initial period of 2 to 15 hours had H_2S removal of 38.5%±4.5 std deviation over 13 hours, and from 15 hours onward had H_2S removal of 27.5±3.7 std deviation over 33 hours. As discussed in Section 4.4.1, this increase in outlet [H_2S] is suspected to be due to the saturation of H_2S in the liquid phase and loss of moisture in the filter bed over time, resulting in less sulphide present in the aqueous phase to react with the oxygen added in the air stream. Although not performed, analysis for pH, elemental sulphur or sulphate produced would have given an indication as to the mechanisms present in the H_2S removal occurring in the non-inoculated biofilter.

The overall H_2S removal was 30.7%±6.3 std deviation over the entire period of 48 hours. Although this study does not indicate exact levels of H_2S chemically removed in the non-inoculated biofilter, it does indicate that H_2S removal in the biofilter is not entirely biologically based.

6.4 Start up and Acclimatization: Supplementary

Startup and acclimatization of the biofilter was done over 4 phases. The outline of each stage from Table 4.3 is re-presented in Table 6.1 below. The 1st stage (day 0 to 5) with only an air flow of 7.5l/h; the 2nd stage (day 5 to 19) with a total flow of 7.5L/h of and equal mix of air and biogas, and the 3rd stage (day 19 to 22) with total gas flow of 5L/h at 19% air, 81% biogas. The final stage (day 22-41) had the same inlet gas make up as the 3rd stage, but a change in [$FeSO_4$] in the nutrient solution from 25g/L to 8g/L, of which Fe^{2+} and Fe^{3+} results are displayed and discussed later in Section 6.4.2, Figure 6.18. To begin the startup, the previously inoculated packing material was placed into the column until the height measured 20cm on the side of the column with a packing weight of 690.8g.

Table 6.1 Biofilter startup and acclimatization: Operation conditions

Factor	**Unit**				
Day	*day*	0 - 5	5 – 19	19 – 22	22 - 41
Total Gas flow	*L/h*	7.5	7.5	5	5
Air flow	*L/h*	7.5	3.75	0.95	0.95
Biogas flow	*L/h*	--	3.75	4.05	4.05
Air (O_2)	$\%_{vol}$	100 (21)	50 (10.5)	19 (4)	19 (4)
$FeSO_4$ content in nutrient	*g/L*	25	25	25	8
H_2S loading rate	$gH_2S/m^3h\ bed$	0	28	30	30
[H_2S]	ppm_v	--	1015	1645	1645

As presented in Section 4.4.2, the initial H_2S removal from the inlet biogas stream during the startup and acclimatization period is summarized in Figure 6.13 below.

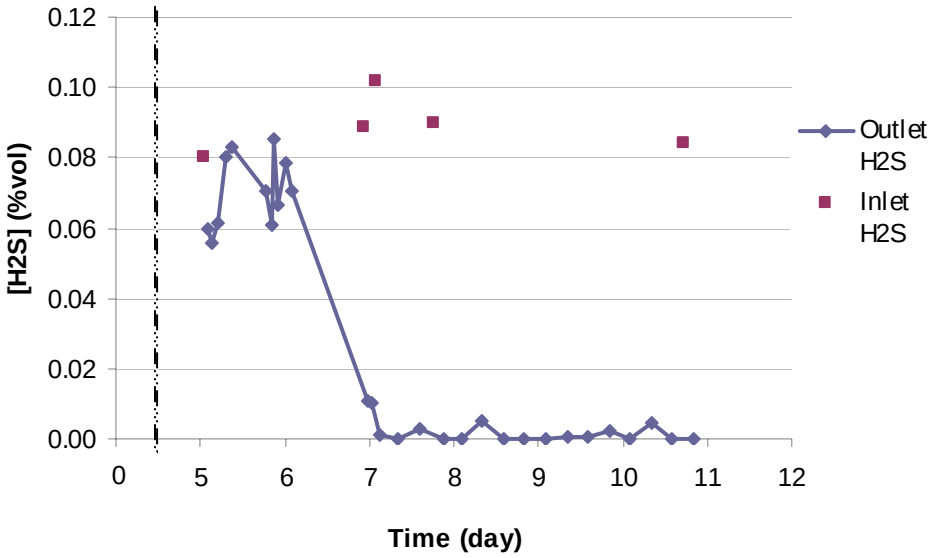

Figure 6.13 Biofilter start up phase: Inlet and outlet [H_2S], biogas inlet added day 5 (1pisg, 25°C)

The inlet and outlet gas compositions for CH_4, O_2, and N_2 are displayed in Figure 6.14, Figure 6.15, and Figure 6.16. The inlet and outlet gas concentrations do not vary significantly, based on the concentration present. Constant methane content in the inlet and outlet biogas of the biofilter is important as it is the energy component of the biogas.

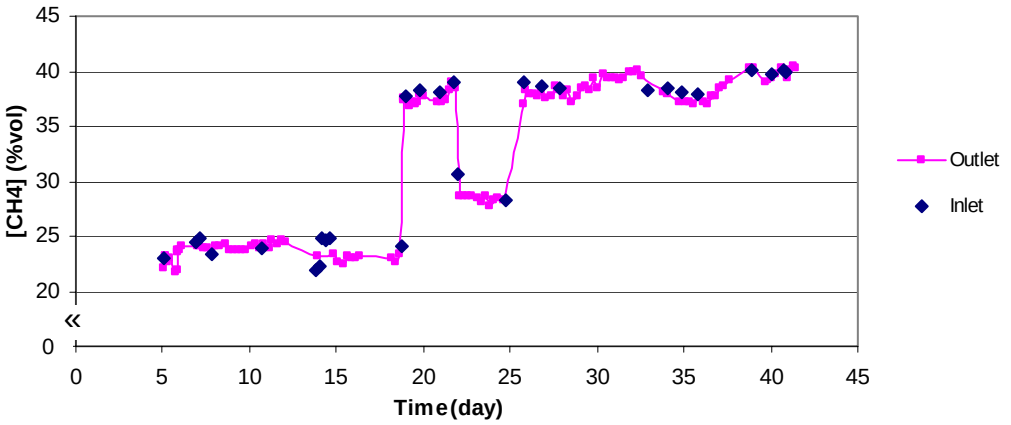

Figure 6.14 Biofilter startup phase: Inlet and Outlet $[CH_4]\%_{vol}$, (1atm, 25°C)

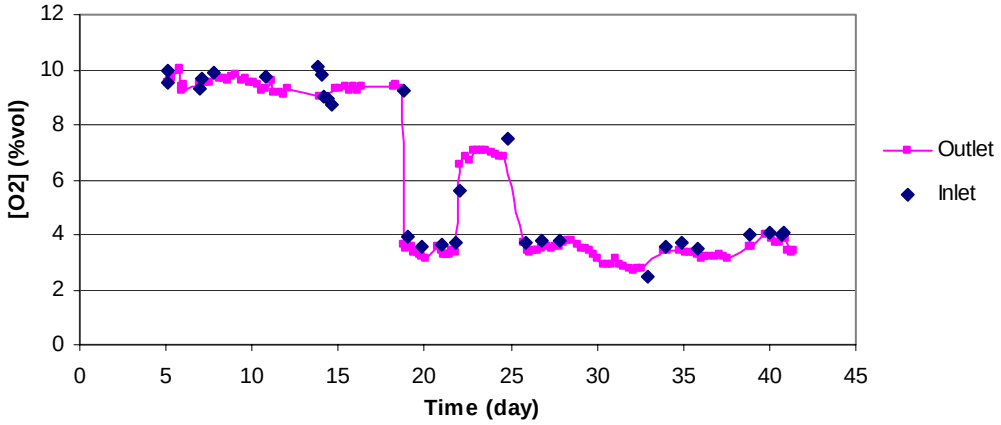

Figure 6.15 Biofilter startup phase: Inlet and Outlet $[O_2]\%_{vol}$, (1atm, 25°C)

The inlet and outlet $[N_2]$ is quite similar, with 0.55% difference between the inlet and outlet values during day 19-22. The inlet and outlet $[O_2]$ differs however, with an average difference of 9.6% over the same time period. This may indicate the use of O_2 by the bacteria present in the oxidation of H_2S.

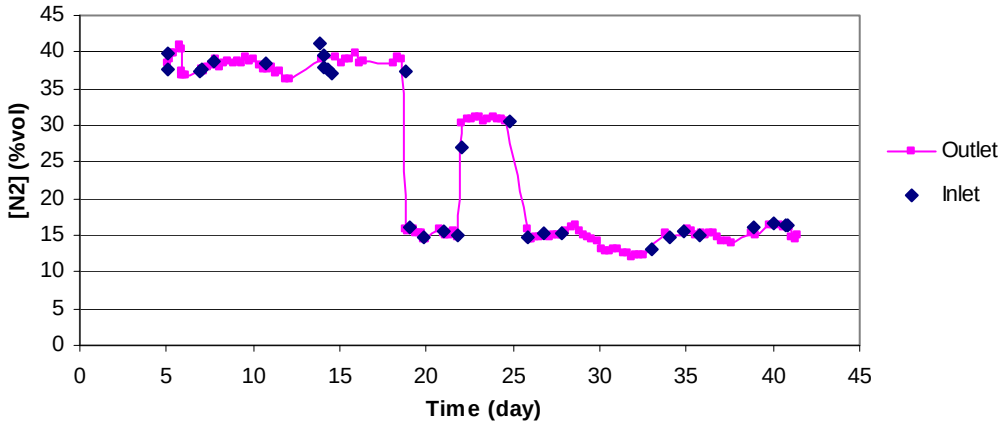

Figure 6.16 Biofilter startup phase: Inlet and Outlet $[N_2]\%_{vol}$ (1atm, 25°C)

6.4.1 Biofilter startup and acclimatization: Outlet pH

The liquid outlet was measured during the startup period. As can be seen in Figure 6.17, a drop from pH 2.8 to pH 2.2 was seen over the start up period of 41 days. In the oxidation of H_2S, SO_4^{2-} can result as seen in Equation (6.5), creating an increased acidic environment in the solution (Devinny et al. 1999).

$$H_2S + 2O_2 \rightarrow SO_4^{2-} + 2H^+ \qquad (6.5)$$

As the outlet sample was taken from the outlet nutrient tank, it did not represent the pH of the outlet solution leaving the biofilter, but rather the pH of the accumulating solution. The difference in pH between the outlet tank and samples taken from the outlet nutrient line was investigated during H_2S loading tests, and is described in 6.5.3.

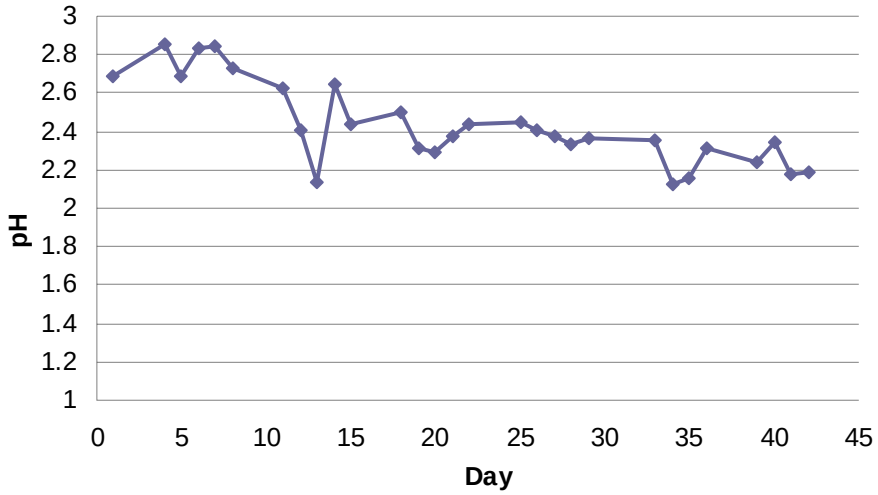

Figure 6.17 Biofilter start-up phase: pH of liquid outlet solution

6.4.2 Biofilter start-up and acclimatization: Outlet Fe^{2+} and Fe^{3+}

As discussed in Section 2.8.3, $FeSO_4$ may be a chemical aid in the oxidation of H_2S by *A. ferrooxidans*. Although it is not known specifically whether *A. ferrooxidans* is present in the biofilter, the growth media used to cultivate the sulphur oxidizing bacteria contained $FeSO_4$, and as such remained in the nutrient solution so as not to drastically change the growth environment of the bacteria present.

The Fe^{2+} and Fe^{3+} of the biofilter liquid outlet solution was measured from day 25 onwards as to assess the usage of Fe^{2+} in the $FeSO_4$ rich nutrient solution added. As 25g/L $FeSO_4$ was being added to the nutrient solution, it was hoped to decrease this to use less chemicals overall, while maintaining high H_2S removal efficiency. Figure 6.18 displays both the Fe^{2+} and Fe^{3+} content in the inlet and outlet nutrient solutions over the start-up and acclimatization period. The occurrence of Fe^{3+} in the inlet nutrient solution demonstrated that biological conversion of $FeSO_4$ had occurred with the oxidation of Fe^{2+} to Fe^{3+}. Initial testing on day 25 showed the inlet nutrient solution (25g/L $FeSO_4$) with 4756ppm Fe^{2+}, (5000ppm theoretically), and 121ppm Fe^{3+} present in inlet sample. The Fe^{3+} present in the inlet sample was the result of Fe^{2+} oxidation to Fe^{3+} by bacteria present, the mechanism shown in Equation (6.1).

The outlet samples of day 25 showed 3339ppmFe^{2+} and 1596ppmFe^{3+}, implying that not all the Fe^{2+} from the inlet solution was converted Fe^{3+}. With the assumption that the bacteria present were converting 1/3 of the 5000ppm of Fe^{2+} present in the inlet solution, the nutrient solution was adjusted to contain only 1/3 of the $FeSO_4$ content. This resulted in a decrease from 25 to 8g/L $FeSO_4$ in the nutrient solution, becoming a nutrient solution resembling that used by (Konishi et al. 1990) with $FeSO_4$ content of 5g/L $FeSO_4$ used by for the growth of *T. ferrooxidans* in bioleaching applications.

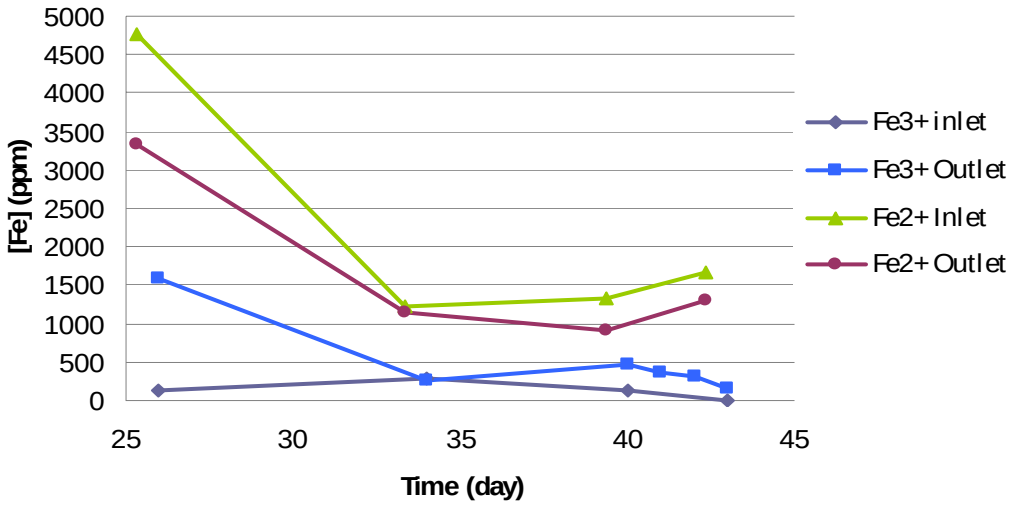

Figure 6.18 Biofilter start-up phase: Fe^{2+} and Fe^{3+} of inlet and outlet liquid nutrient solutions

The Fe^{2+} and Fe^{3+} content was then followed for the rest of the start up period, presented in Figure 6.18, with an inlet Fe^{2+} averaging 1405±221ppm. The outlet biofilter solution was 1117±194ppm Fe^{2+} and 311±121ppm Fe^{3+}. This indicates that the bacteria are more dynamic and do not simply convert Fe^{2+} to Fe^{3+}, and that independent of the [Fe^{2+}] added in solution, both Fe^{2+} and Fe^{3+} are present in the outlet solution. As discussed in Sections 2.5.1 and 2.8.3, *A. ferrooxidans* use ferrous iron (Fe^{2+}) for an electron donor (Syed et al. 2006), and would oxidize ferrous iron to ferric oxide by the following reaction (Jensen and Webb 1995)

$$2FeSO_4 + H_2SO_4 + \frac{1}{2}O_2 \xrightarrow{A.\ ferooxidans} Fe_2(SO_4)_3 + H_2O \qquad (6.6)$$

Optimization was not done further to minimize the use of $FeSO_4$ in the nutrient solution, but it is assumed that the $FeSO_4$ content in the nutrient solution could be additionally decreased.

6.5 Biofilter H_2S Loading Tests: Supplementary

The main results of H_2S removal during the loading tests can be found in 4.4.3, while supplementary results are presented here.

As the inlet air and biogas flow were changed in relation to a constant 4%O_2 inlet, the inlet H_2S concentration remained constant at 0.174%vol±0.012. Figure 6.19 shows the outlet [H_2S] was low throughout the loading tests, with an overall average of 0.002%$_{vol}$±0.0036 std deviation over 39 days.

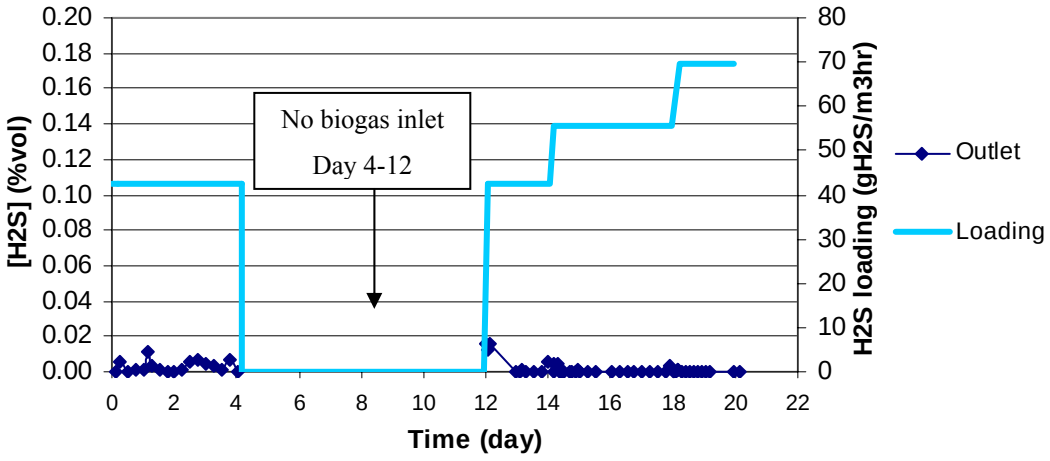

Figure 6.19 Loading test: H_2S loading and outlet [H_2S] %$_{vol}$ (Inlet 0.17%$_{vol}$ H_2S, 1psig, 25°C)

6.5.1 Biofilter H_2S loading test: filter bed blockage

During H_2S loading stage 4, the inlet flow was not stable and would decrease over time. It was concluded to be caused by blockage in the biofilter, although faulty pressure measurements were not able to confirm a pressure drop across the bed. Evidence of this blockage is presented in Figure 6.20, where the concentration of CH_4 becomes unstable after day 18, when the inlet volumetric flow of

biogas is increased. As the flow of biogas would fluctuate, the outlet concentration of CH_4 would change also. This was the result of the higher biogas flow being diminished more rapidly in relation to the lower air flow, causing a decrease in the concentration of each biogas component over time. It is more apparent in CO_2 and CH_4 than H_2S due to the higher concentrations.

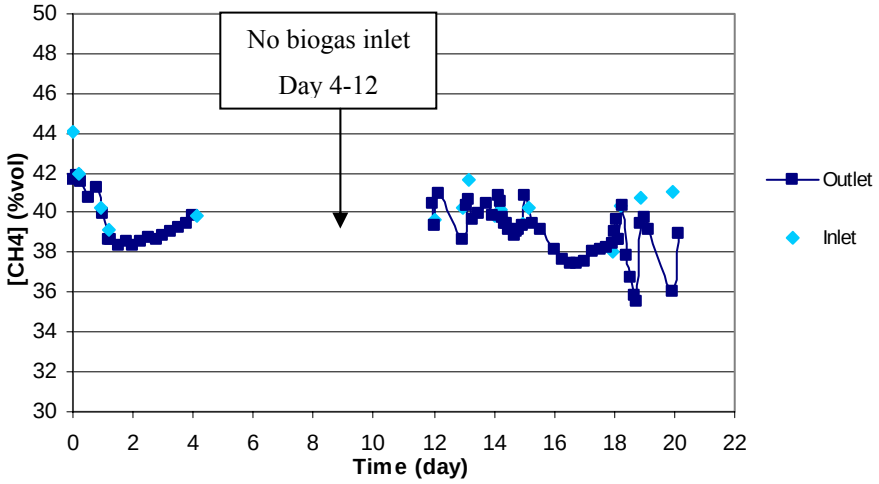

Figure 6.20 Loading test: Inlet and Outlet [CH_4] $\%_{vol}$, (1atm, 25°C)

In order to remedy this biofilter blockage, backwashing was performed with a minimum inlet air flow of 260mL/min (1psig, 25°C) and 170mL/min of water inlet for 30 minutes. This resulted in no change in the blockage. Instead the packing material was removed, washed and half was replaced with uninoculated packing. The effectiveness of the media change was never tested however as the Micro GC ceased to operate almost immediately after. The used packing material taken from the column was fused together due to microbial activity and deposits formed, creating a highly compacted solid piece that was difficult to break up. The filter bed blockage could be remedied using mechanical or chemical techniques, further discussed in Section 8.1.

6.5.2 Biofilter H_2S loading test: Inlet and outlet O_2 content

The use of oxygen by the bacteria present appeared not to change with the changes in H_2S loading rates. Due to differing pressures between the air and biogas inlet, it was difficult to regulate an air flow for 4% O_2 based on theoretical calculations. As such, the inlet [O_2] was often around 3%, as can

be seen in Figure 6.21. As was indicated by Schomaker et al. (2000), an O_2 level of 4% ensures high H_2S removal and conversion primarily to elemental sulphur. With less O_2 present, more sulphur would be produced in place of H_2SO_4. Although the O_2 level was lower than desired, the H_2S removal was high, indicating that the amount of O_2 present in the inlet gas can be further optimized.

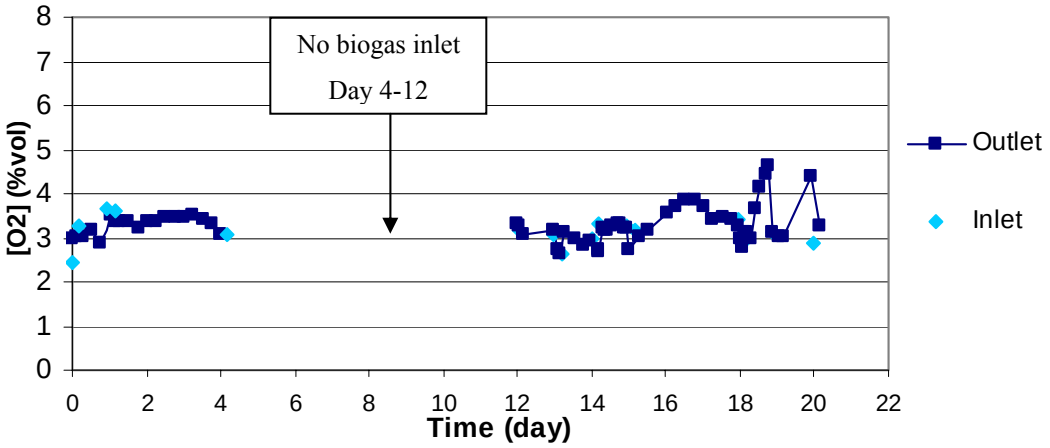

Figure 6.21 Loading test: Inlet and Outlet [O_2] $\%_{vol}$, (1atm, 25°C)

As discussed in Section 5.3.6, a theoretical material balance with respect to Equation (6.7) represents an environment with low [O_2] where elemental sulphur is the major H_2S degradation product.

$$H_2S + 1/2\ O_2 \rightarrow S + H_2O \qquad (6.7)$$

Based on this equation with respect to H_2S, only half of the moles of O_2 are required for the oxidation of H_2S by the bacteria. This amount can be represented for a situation with n_{total} (total moles) 100, and [H_2S] = $0.2\%_{vol}$

$$n_{O2} = \frac{1}{2}\left(\frac{n_{H2S}}{n_{total}}\right) = \frac{1}{2}\left(\frac{0.2}{100}\right) = 0.001 molsO2 \qquad (6.8)$$

Therefore, 0.001 mols O_2 are required. This is equivalent to $0.001\%_{vol}$ O_2 in the inlet when [H_2S] is $0.2\%_{vol}$. Although additional oxygen is required by the bacteria for respiration, it can be seen that the current level of O_2 in the inlet was largely in excess.

6.5.3 Biofilter H_2S loading test: Outlet pH

The pH of the inlet nutrient solution and the biofilter liquid outlet solution were monitored throughout the loading test. To evaluate if the outlet tank solution characteristics were different from a sample taken directly from the outlet line, samples from both the outlet line and outlet tank were analysed in parrallel. It was expected that the outlet tank pH would be lower than the outlet line pH if the bacteria present in solution would continue to oxidize the $FeSO_4$ creating an acidic environment. To investigate this potential difference, the pH of both the outlet tank and line sample were monitored over the course of the loading test. As can be seen in Figure 6.22, these two pH values were similar. The difference in outlet tank and line pH on day 21 was due to an attempted cleaning of the biofilter bed with deionised water on day 20 that resulted in a decrease in the outlet line pH on day 21. Other than this exception, both the outlet tank and line pH had similar values.

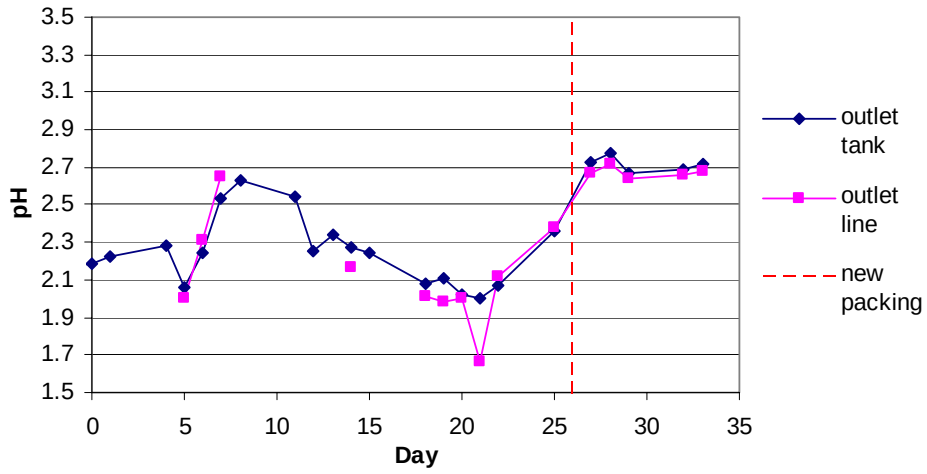

Figure 6.22 Loading test: pH of outlet tank and line solutions

Throughout the loading tests, the inlet nutrient solution pH was generally at pH 3, while the pH of the tank outlet solution was lowered due to biological activity to below pH 2.7, as seen in Figure 6.23. The monitoring was carried out throughout the loading test, in both the presence and absence of biogas in the inlet gas stream. It can be seen in Figure 6.23 that the pH tended to increase when no biogas was present in the system. The pH was lower at 2.0 to 2.3 when biogas was present compared

to 2.4 to 2.7 when no biogas was present. When biogas is present in the inlet gas the bacteria oxidize the H_2S to form SO_4^{2-} as well as elemental sulphur, as seen in Equations (6.5) and (6.7). This corresponds also to a less acidic environment when no biogas is added, as seen in Figure 6.23, during days 5-12 and days 22 – 34.

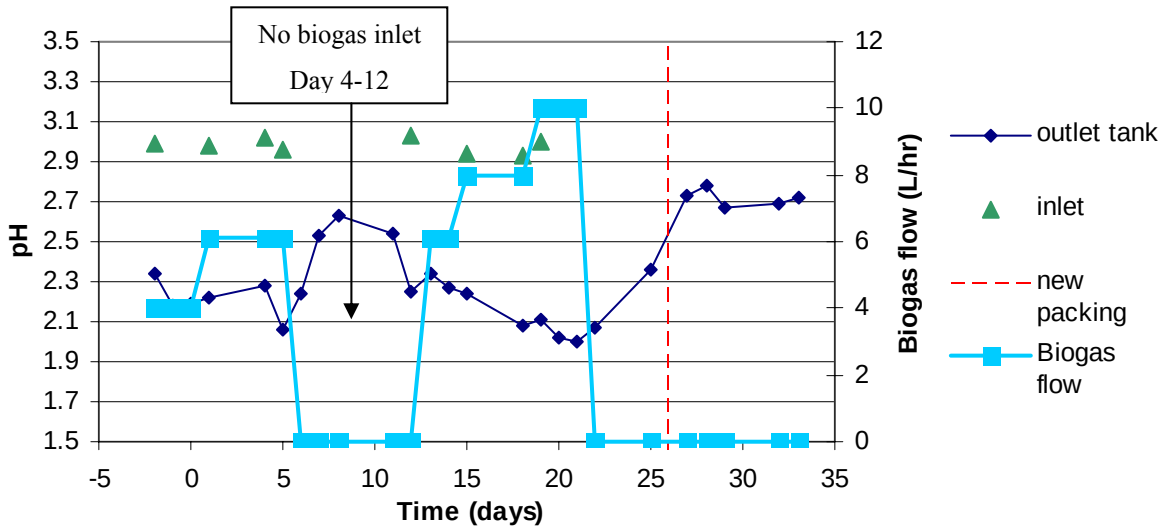

Figure 6.23 Loading test: Inlet and outlet pH with biogas flow (1atm, 25°C)

6.5.4 Biofilter loading tests: Outlet Fe^{3+}

The Fe^{3+} during biofilter H_2S loading tests are displayed in Figure 6.24 with the $[Fe^{3+}]$ of the outlet tank and line as well as the corresponding biogas flow. There was a decrease in outlet $[Fe^{3+}]$ with the increase of inlet biogas flow. This is presumed to be due to the presence of biogas as the bacteria also oxidize the H_2S present, resulting in less Fe^{2+} being oxidized. Refer to Equation (6.6).

As with the sampling of pH, it was decided that there could be a difference between the outlet tank and line sample. Figure 6.24 displays a difference between the $[Fe^{3+}]$ for both the outlet tank and line. It was seen that unlike the pH, the $[Fe^{3+}]$ continued to change in the lag time before sampling from the outlet tank. The outlet tank Fe^{3+} content was higher than that of the outlet line, indicating that the bacteria present in the outlet tank continued to oxidize Fe^{2+} to Fe^{3+} outside of the biofilter. This is seen especially on day 12 and day 25 when the outlet tank had been collecting outlet nutrient flow for 3 days in place of the usual 1day period. In general, the outlet tank Fe^{3+} followed the same trend of

the outlet line, except with higher concentration. On day 26 the packing media was replaced with half new, non inoculated packing material, resulting in a drop in the production of [Fe^{3+}]. Within 2 days however the Fe^{3+} production was similar to as it had been before in the absence of biogas.

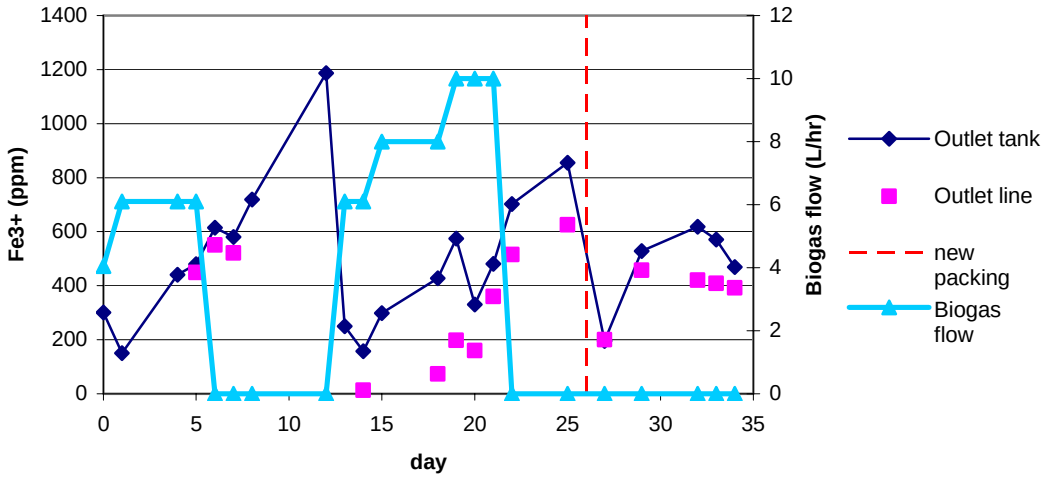

Figure 6.24 Loading test: biogas flow and [Fe^{3+}] of outlet liquid solution (Inlet 0ppm Fe^{3+})

6.6 Biofilter operation: Qualitative results

6.6.1 Filter bed

The biofilter displayed a colour gradient between the top of the biofilter and the bottom. It was noted that the packing at the top of the biofilter had an orange colouring and appeared to be drier, while the bottom of the packed bed showed faint yellow deposits (sulphur) amongst the packing material. More iron compounds would be produced at the top of the column where the $FeSO_4$ rich nutrient solution was added, while sulphur compound production would prevail in the bottom of the column where the biogas entered. This can be seen in Figure 6.25 on the left representing the filter bed on day 7 of biofilter operation, and Figure 6.26 on the right showing the filter bed on day 21 of biofilter operation. By the time the packing was changed, the entire bed displayed more of the orange/red colouring.

Figure 6.25 Biofilter packed bed: Startup and acclimatization, day 7

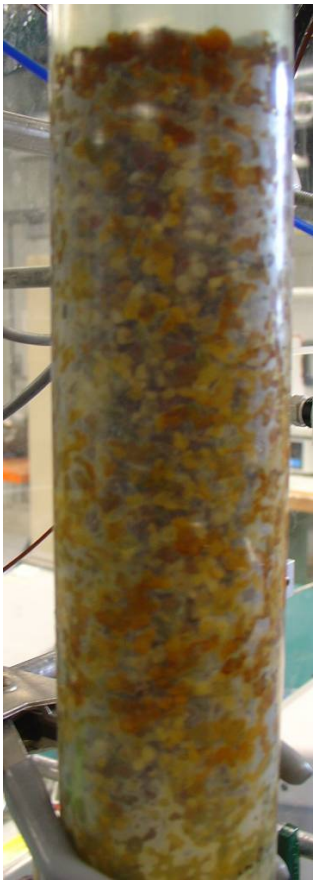

Figure 6.26 Biofilter packed bed: Startup and acclimatization, day 21

6.6.2 Outlet nutrient solution during loading test

When biogas was present in the inlet, the outlet liquid solution became clear with only a faint yellow color. When there was no biogas however, the outlet liquid solution was opaque and orange/red colour. This difference in coloration in the biofilter outlet liquid is seen in Figure 6.27. Solutions on the left with orange colouring represent samples taken from day 6 to 15, where there was no biogas inlet during day 6-12. The three clear sample solutions on the right were taken on days 18-20 during biogas loading stage 2 and 3. As would be expected, there was a phase between a biogas load restarted on day13, and the disappearance of orange colouring on day 15. Overall however, it can be seen that when biogas was present, the liquid outlet pH dropped as well as less colouring was present (iron compounds) in the outlet.

Figure 6.27 Loading test: Biofilter outlet solution, orange left: day 6-15, clear right: day 18-20

Chapter 7
Conclusions

The biofiltration system designed in this study, including packing material, inoculum and system setup, proved effective in the removal of H_2S from biogas. The use of activated sludge as an inoculum source conditioned with an *A. ferrooxidans* nutrient media was effective for enriching sulphur oxidizing bacteria.

A packing compatibility test concluded that the gravel packing material was effective for use as an inoculum support growth. This test resulted in solutions with media, bacteria and packing displaying the same visual and pH properties within 13 days.

Initial baseline H_2S removal testing with the non-inoculated biofilter resulted in 31-56%H_2S removal from 2-48 hours. A full factorial experimental plan with 3 factors was performed to determine the cause of the H_2S removal in the non-inoculated biofilter. Air was the only significant factor while packing material type and nutrient solution had no significant effect.

A theoretical material balance was performed attempting to anticipate behaviour and account for any loss in components present in the system. This was then compared with an experimental material balance of the gas components using experimental data obtained during the loading tests. The difference between the theoretical and experimental material balance for gas components present ranged between 6.8-14.6% for the inlet stream and 0.6-43.6% for the outlet gas stream, depending on the component. H_2S showed the greatest difference as it was present in low concentrations. Overall both theoretically and experimentally, it was found that there was minimal loss of all species except H_2S in the biofiltration process.

The biofilter with pre-inoculated packing material of 0.4L filter bed volume was operated for a total of 61 days, including a period of start-up and acclimatization of 41 days and H_2S loading tests for 20 days. The initial start-up and acclimatization stage with biogas showed complete H_2S removal after 2 days, with overall H_2S removal of 98.1%±2.9 std deviation over 34 days for H_2S loading rate of 30gH_2S/m^3h filter bed and a biogas flow of 3.75-4L/h (25^{o}C,1psig). Biofilter H_2S loading tests were performed with an inlet O_2 and H_2S concentrations of 4%$_{vol}$ and 1600ppm$_v$, respectively, and an H_2S loading rate ranging from 27.8-69.5 gH_2S/m^3h filter bed. Throughout the H_2S loading tests an average H_2S removal of 98.9%±2.1 std deviation over 20 days was observed. Although this loading test was

not completed and an H_2S breakthrough level was not identified due to complications with analysis instruments, the effective H_2S removal rate seen for the H_2S loading rates tested shows promising results for the use of this biofiltration system in the removal of H_2S from biogas.

Chapter 8
Recommendations

8.1 Experimental Setup

Certain aspects of the experimental setup could be enhanced for more precise operation and analysis. Mass flow meters could replace the flow meters currently used in the setup. This would increase the accuracy of the inlet gas and allow for more precise estimation of set points and mixing of the air and biogas. As a result, the material balance of the system would be more accurate.

As the gas chromatograph used in experimentation was not precise enough to accurately measure H_2S concentrations less than 100ppm, another gas analysis technique could be used. This would increase the accuracy of H_2S both entering and exiting the biofilter, and give more reliability especially to the outlet H_2S measurements. Previous studies analysing lower concentrations of H_2S have used and IR gas detector (Kim et al. 2008), gas detection tubes (Truong and Abatzoglou 2005), Tutweiler's apparatus (Rao et al. 2006), or Drager gas sensors (Jin et al. 2005a; Elias et al. 2002). Costs and usability of these instruments for our purposes is not known, and as such would be something to investigate.

8.2 Further Analysis

Continuation of the loading tests should be done in order to assess the maximum removal capacity of this biofiltration system. This would enable an approximation of the H_2S removal capability of such a setup, and give a basis from which to test process improvements. In addition, the relationship between the loading rate and elimination capacity of the system could be calculated with the H_2S removal efficiency decreasing with the increasing load. This would give further indication of the removal rate and the maximum elimination capacity of such a system. Another way to test this relationship would be to build a shorter column in order to test the system at lower removal efficiencies.

A study of the amount of oxygen required by the bacteria present for the degradation of H_2S should be done. The addition of air in the gas inlet adds another gas component which is not used in energy generation, and may decrease the effectiveness of the biogas. Thus limiting the amount of air added for biological oxidation of H_2S would be ideal. This may involve decreasing the oxygen (or air) level in the inlet gas until a change in the H_2S removal efficiency is seen. Although this would stress the

microorganisms present, it is important to know the minimum amount of oxygen required to complete H_2S oxidation biologically.

A study should also be performed to evaluate the minimum nutrient requirements of the biofilter. This includes both the content of the nutrient solution as well as the amount and frequency of the solution added. In this preliminary study, the nutrient solution was partially adjusted, and it is known that the chemical usage could be diminished substantially. A reduction in the $FeSO_4$ content in solution may influence the removal of H_2S from the biogas. If a reduction in H_2S removal is seen, this may demonstrate that the mechanism present incorporates the oxidation of H_2S chemically by ferric iron, followed by the biological reoxidation of the ferrous iron to ferric oxidation by *A. ferrooxidans* present.

The mechanisms present in this H_2S removal system should be further investigated. This includes both the abiotic and biotic mechanisms. An in depth theoretical study could be performed outlining in further detail the possible mechanisms present. This could be paired with experimental investigation of sulphur speciation including sulphur, sulphate and sulfite analysis of both the exiting liquid stream and of the accumulation in the biofilter. This could be done in parallel with pH and Fe^{2+}/Fe^{3+} analysis. This increased understanding of the mechanisms present in the biofilter as well as the fate of the sulphur could be used for further optimization of this H_2S removal system.

Pig manure could be investigated as an alternate inoculum source to activated sludge. Having an inoculum source that is readily available on a farm would be beneficial. Like activated sludge, pig manure is probably rich in a wide range of microorganisms, where sulphur oxidizing bacteria may be present.

8.3 Scale up Considerations

A scale up project could be performed to assess the usability of this biofiltration design. This would include the use of a real biogas source to assess the capability of a similar biofiltration system to respond to varying feed composition and gas flow rates, and to assess the overall robustness of such a system. Certain aspects would be important to consider or test, and these include:

Blockage in the biofilter due to build-up of biomass deposits became apparent after 2 months of use. Channelling, pressure drop and blockage of the biofiltration bed are major impacts in the biofiltration process, and should be further investigated if this system is to operate in a larger scale. A mixer or washing of the packed bed could be investigated to alleviate this problem.

If used on a farm, the operating temperatures of the biofilter may vary throughout the year. Either an assessment of the temperature ranges for which the microorganisms are capable to oxidize the H_2S efficiently would need to be performed, or designing an experimental setup that can keep the biofilter bed at a constant temperature. If the gas entering the system is at a constant temperature from the anaerobic digester, temperature changes may be less of an issue.

Appendix A

List of Equipment

Piece	Ref. from system Figure	Size and specifications	Company	Product number	Material	Details	Price
Gas							
Biogas (big bottle)	Premixed gas	3.7m3	Linde	24088126	NA	%vol CH_4, 49.8 % vol CO_2 and 2000ppm H_2S	750
Biogas (small bottle)	Premixed gas	0.7m3	Linde	24084261	NA	%vol CH_4, 49.8 % vol CO_2 and 2000ppm H_2S	720
Air	Air	0,1 grade, large bottle	BOC	24064467	NA	air, 0.1 grade	unknown
Gas flow							
Flow meter, air inlet	flowmeter#1 with valve	0-264mL/min, 150mm correlated	Coleparmer	03217-10	SS float	no modifications	162
Flow meter, air inlet (low flow)	not shown	0-60 mL/min, 150mm correlated	Coleparmer	03219-03	SS float	no modifications	297
Flow meter, biogas inlet	flowmeter#4 with valve	0-264mL/min, 150mm correlated	Coleparmer	PMR1-010331	SS float	modified: O-ring PTFE kit, Kalrez seal kit	276
Flow meter, mixed gas inlet	flowmeter#2 w/o valve	0-264mL/min, 150mm correlated	Coleparmer	03269-16	SS float	modified: O-ring PTFE kit, Kalrez seal kit	301
Flow meter, mixed gas outlet	flowmeter#3 with valve	0-264mL/min, 150mm correlated	Coleparmer	03219-11	SS float	modified: O-ring PTFE kit, Kalrez seal kit	276
Piping	lines	1/4" OD 1/8" ID tubing	in lab, unknown	unknown	stainless steel	NA	unknown
Valves							
check valve	Check valve 1/3 psi	0.3psi, 1/4" tube fitting	Swagelok	SS-4C-1/3	SS, o rings neoprene	changed to Neoprene o-rings, Swagelok	53
system isolation valves	V-1 to V-14	1/4" tube fitting	Swagelok	SS4P4T	stainless steel	o rings PTFE coated FKM	65
Liquid flow							
Nutrient tanks (inlet and outlet)	Fresh and Old nutrient tank	5L each	Fisher Scientific	02-923-11	polypropylene	heavy duty vacuum	128 each
Nutrient tank lids	Fresh and Old nutrient tank	three ports, air tight	Fisher Scientific	02-923-24	polypropylene	quick filling/ venting closures	315
Peristaltic pump	peristaltic pump	masterflex easy load II (tubing L/S 13,14,16,25)	Masterflex	77202-60	NA	digital standard drive	unknown
Liquid lines	nutrient cycling	1/4" L/S 16 tygon tubing	Cole parmer	06409-16	Tygon	package 50ft	65
Pressure							
Pressure regulator, air	Pressure reg.	output 0-100 psi	Harris	425-125	brass	NA	unknown
Pressure regulator, biogas	Pressure reg.	output 0-350psi	Linde	C200/2S 150A330C4	Stainless steel	double side, HiQ redline series	unknown
Pressure gauge	P-air, P-gas	0 to 15 psi	Matheson	63-5615M	Stainless steel	NA	500 each
Pressure transmitters	P-1, P-2	0 to 25psi	Coleparmer	68075-14	Stainless steel	4-20 mA	193 each
Temperature							
temperature transmitters	T-1, T-2, T-3	Type K, 0-1250 C	in lab, unknown	Type K	Stainless steel	NA	NA
Gas Sampling							
Sample valves	Gas inlet and outlet sample	3 way sample valve	Swagelok	SS-1VS4-X	stainless steel	NA	109
Gas sample lines	gas inlet sample, biofilter sample	1/16" ID	Coleparmer	96130-22	PTFE	NA	17.8
Biofilter and humidification							
packing material	visual	3-6mm diameter	Hagen, (Geosystems)	Na	small gravel, untreated	NA	$32/ 10 kg bag
column	visual	5cm ID, 50cm ht (25cm for humidification)	in lab, unknown	NA	unknown	made in lab	unknown
spray nozzle	visual	0,053" orifice, <1L/min	Cole parmer	EW-83251-00	PVDF	NA	$13,43 each
Gas disperser	bottom of column	3/4" ID dispenser, 1/4"ID tubing	Cole Parmer	06614-25	polyethylene	70 im porosity disk	48.46$ for 4
H2S safety							
coalescing filter	coalescing filter	1/4" tube fittings	Advanced Instruments Inc	30TR	plexi-glass housing	ordered with H2S scrubber	250
H2S scrubbing filter	H2S filter	1.5" x24" , plexi-glass	Advanced Instruments Inc	A-2839	aluminum oxide	change of colour life indicator	400
H2S portable detectors	Not shown	10 and 15ppm H2S	Honeywell (BW technologies)	GA24XT-H	NA	NA	290
respiration mask	Not shown	full face mask, 2 cartridges	North Safety	RT21P100 (cartridge)	NA	NA	250 (+44/cart)
CH4 and H2S in-lab detectors	Not shown	detection limits 10ppmH2S, 40% CH4	Armstrong	360 series	NA	NA	unknown
Electric valve for biogas	Not shown	normally closed valve	KIP Inc	A149111-0141	unknown	exterior brass, interior material unknown	unknown

Piece	Ref. from system Figure	Size and specifications	Company	Product number	Material	Details	Price
Data acquisition							
data logger	data acquisition	switch unit, 16 channels	Agilent	34970A	NA	NA	unknown
computer program	data acquisition	Agilent benchlink data logger	Agilent	Benchlink data logger	NA	NA	NA
Gas analysis							
micro Gas Chromatograph	Micro GC	NA	Agilent (Inficon for Micro GC)	3000A	N/A	NA	unknown
gas/liquid separator	gas/liquid separator	stainless steel, and internal membrane	Agilent (Genie)	170-505	stainless steel	added to outside inlet of GC	1012
Inlet filter assembly	Not shown	1/8"ID adapter and filter piece	Agilent	G2801-60900	stainless steel	NA	unknown
Inlet filter disk, 10um	Not shown	10um filter disk	Agilent	5183-4652	unknown	NA	unknown
dual end inlet ferrule	Not shown	for 1/16" ID connector	Agilent	FRL-1269	unknown	NA	unknown
outlet gas tube adapter	Not shown	male luer lock 1/8" ID	Coleparmer	45503-11	polypropylene	NA	unknown
Helium carrier gas	Not shown	helium, grade 5.0	BOC	24001333	NA	NA	unknown
carrier gas purifier	Not shown	oxygen and water filter	Agilent	G3440-60003	varies	NA	unknown
Fe 2+/Fe3+ analysis							
Spectrophotometer	Not shown	200-900 nm wavelength	Pharmacia Biotech	Ultrospec 1000E	N/A	UV/visible spectrophotometer	unknown
4.6 buffer solution	Not shown	1L	Fisher Scientific	SB100-1	N/A	NA	38.2
1,10 phenanthroline	Not shown	99+ %	Acros	157530250	N/A	NA	70
0.1MHCl	Not shown	0,1M	Fisher Scientific	SA54B-4	N/A	NA	N/A
Fe(II) std solution	Not shown	1000ug/mL in 2% H2SO4	Absolute Stds	54141	N/A	NA	25
Fe(III) std solution	Not shown	1000ug/mL in 2% HCl	Spex Certiprep	PLFE1-2X	N/A	NA	N/A
Calibration Gases							
Air level 1	Not shown	141L	Linde	24086117	N/A	0.1% O_2, 0.5% N_2, 99.4% He	350
Air level 2	Not shown	141L	Linde	24086118	N/A	10% O_2, 40% N_2, 50% He	350
Air level 3	Not shown	170L	Linde	24085224	N/A	20% O_2, 80% N_2	350
Biogas level 1	Not shown	170L	Linde	24084264	N/A	0.1% H_2S, 12.5% CO_2, 12.5% CH_4, 74.9% He	744
Biogas level 2	Not shown	170L	Linde	24084263	N/A	0.2% H_2S, 25% CO_2, 25% CH_4, 49.8% He	497
Biogas level 3	Not shown	170L	Linde	24084262	N/A	0.3% H_2S, 49.7% CO_2, 50% CH_4, 0% He	491
Chemicals							
$(NH_4)_2SO_4$	Not shown	1kg	Sigma	A5132	N/A	NA	56.6
KCl	Not shown	250g	Sigma	P5405	N/A	NA	24.8
K_2HPO_4	Not shown	500g	Sigma	PX1570	N/A	NA	35
$MgSO_4 7H_2O$	Not shown	500g	Sigma	M1880	N/A	NA	35.4
$Ca(NO_3)_2$	Not shown	500g	Sigma	C1396	N/A	NA	62.9
$FeSO_4 7H_2O$	Not shown	1kg	VWR	CA99501-856	N/A	NA	40
special H2S compatible pieces							
PTFE O-ring seal kit for flow meters	Not shown	specifically for flow meters in system	Aalborg	OR-KT-1	PTFE	NA	8.8
Kalrez seal kit, for flow meters	Not shown	specifically for flow meters in system	Aalborg	PK-P2K	Kalrez	NA	43.5

Bibliography

Aroca, G., Urrutia, H., Nunez, D., Oyarzun, P., Arancibia, A., Guerrero, K. (2007). "Comparison on the Removal of Hydrogen Sulphide in Biotrickling Filters Inoculated with Thiobacillus Thioparus and Acidithiobacillus Thiooxidans." *EJB,* 10(4), 514-520.

Arsenault, I. (2009). "Properties of Cultivation of *A. Ferrooxidans* in *A. Ferrooxidans* Media." *Universite De Sherbrooke,* Cultivation of A. ferrooxidans in A. ferrooxidans media.

Barona, A., Elias, A., Amurrio, A., Cano, I., Arias, R. (2005). "Hydrogen Sulphide Adsorption on a Waste Material used in Bioreactors." *Biochem. Eng. J.,* 24(1), 79-86.

Chou, T. C., Lin, T. Y., Hwang, B. J., Wang, C. C. (1986). "Selective Removal of H2s from Biogas by a Packed Silica-Gel Adsorber Tower." *Biotechnol. Prog.,* 2(4), 203-209.

Chung, Y. C., Huang, C. P., Tseng, C. P., Pan, J. R. (2000). "Biotreatment of H2S- and NH3-Containing Waste Gases by Co-Immobilized Cells Biofilter." *Chemosphere,* 41(3), 329-336.

Chung, Y. C., Huang, C. P., Tseng, C. P. (1996). "Microbial Oxidation of Hydrogen Sulphide with Biofilter." *J. Environ. Sci. Health Part A-Environ. Sci. Eng. Toxic Hazard. Subst. Control,* 31(6), 1263-1278.

CRC Handbook of Chemistry and Physics, (1982). Boca Raton, Fla. : CRC Press, Boca Raton, Fla.

Degorce-Dumas, J. R., Kowal, S., Le Cloirec, P. (1997). "Microbiological Oxidation of Hydrogen Sulphide in a Biofilter." *Can. J. Microbiol. /Rev. can. Microbiol.,* 43(3), 264-271.

Delhomenie, M. C., and Heitz, M. (2005). "Biofiltration of Air: A Review." *Crit. Rev. Biotechnol.,* 25(1-2), 53-72.

Devinny, J. S., Deshusses, M. A., Webster, T. S. (1999). *Biofiltration for Air Pollution Control,* Lewis Publishers, Boca Raton, Fla.

Duan, H. Q., Yan, R., Koe, L. C. C. (2005). "Investigation on the Mechanism of H2S Removal by Biological Activated Carbon in a Horizontal Biotrickling Filter." *Appl. Microbiol. Biotechnol.,* 69(3), 350-357.

Elias, A., Barona, A., Arreguy, A., Rios, J., Aranguiz, I., Penas, J. (2002). "Evaluation of a Packing Material for the Biodegradation of H2S and Product Analysis." *Process Biochem.,* 37(8), 813-820.

Energy Information Administration, US department of Energy. (1997). *Renewable Energy Annual, 1996, Chapter 10,* DOE/EIA-0603(96) Ed., Energy Information Administration, US Department of Energy, Washington, DC.

Harrison, A. P. (1984). "The Acidophilic Thiobacilli and Other Acidophilic Bacteria that Share their Habitat." *Annu. Rev. Microbiol.,* 38, 265-292.

Hirai, M., Kamamoto, M., Yani, M., Shoda, M. (2001). "Comparison of the Biological H2S Removal Characteristics among Four Inorganic Packing Materials." *Journal of Bioscience and Bioengineering,* 91(4), 396-402.

Hobson, P. N., and Wheatley, A. (1993). *Anaerobic Digestion : Modern Theory and Practice,* Elsevier Applied Science, London ; New York.

Hua, G. X., Zhang, Q. Z., McManus, D., Slawin, A. M. Z., Woollins, J. D. (2006). "Novel Non-Aqueous Fe(III)." *Dalton Trans.,* (9), 1147-1156.

Jensen, A. B., and Webb, C. (1995). "Ferrous Sulfate Oxidation using Thiobacillus-Ferrooxidans - a Review." *Process Biochem.,* 30(3), 225-236.

Jin, Y. M., Veiga, M. C., Kennes, C. (2005a). "Effects of pH, CO2, and Flow Pattern on the Autotrophic Degradation of Hydrogen Sulphide in a Biotrickling Filter." *Biotechnol. Bioeng.,* 92(4), 462-471.

Jin, Y. M., Veiga, M. C., Kennes, C. (2005b). "Autotrophic Deodorization of Hydrogen Sulphide in a Biotrickling Filter." *J. Chem. Technol. Biotechnol.,* 80(9), 998-1004.

Kim, J. H., Rene, E. R., Park, H. S. (2008). "Biological Oxidation of Hydrogen Sulphide Under Steady and Transient State Conditions in an Immobilized Cell Biofilter." *Bioresour. Technol.,* 99(3), 583-588.

Kohl, A. L., and Riesenfeld, F. C. (1979). *Gas Purification,* 3d ed. - Ed., Gulf Pub. Co., Book Division, Houston.

Konishi, Y., Asai, S., Katoh, H. (1990). "Bacterial Dissolution of Pyrite by Thiobacillus-Ferrooxidans." *Bioprocess Eng.,* 5(5), 231-237.

Lastella, G., Testa, C., Cornacchia, G., Notornicola, M., Voltasio, F., Sharma, V. K. (2002). "Anaerobic Digestion of Semi-Solid Organic Waste: Biogas Production and its Purification." *Energy Conversion and Management,* 43(1), 63-75.

Lee, E. Y., Lee, N. Y., Cho, K. S., Ryu, H. W. (2006). "Removal of Hydrogen Sulphide by Sulfate-Resistant Acidithiobacillus Thiooxidans AZ11." *J. Biosci. Bioeng.,* 101(4), 309-314.

McNevin, D., Barford, J., Hage, J. (1999). "Adsorption and Biological Degradation of Ammonium and Sulphide on Peat." *Water Res.,* 33(6), 1449-1459.

Perry's Chemical Engineers' Handbook, (1984). New York ; Toronto : McGraw-Hill, New York ; Toronto.

Rao, A. G., Ravichandra, P., Jetty, A. (2006). "Operation of Biofilter with Mixed Agricultural Residue as Filter Material: Effects of Humidification and Inlet Hydrogen Sulphide Volume Fraction on the Performance." *Chem. Biochem. Eng. Q.,* 20(2), 189-196.

Rasi, S., Veijanen, A., Rintala, J. (2007). "Trace Compounds of Blogas from Different Blogas Production Plants." *Energy,* 32(8), 1375-1380.

Robertson, L. A., and Kuenen, J. G. (2006). "The Genus *Thiobacillus*." Springer, New York, 812.

Schomaker, A. H. H. M., Boerboom, A. A. M., Visser, A., Pfeifer, A. E. (2000). *Anaerobic Digestion of Agro-Industrial Wastes: Information Networks. Technical Summary of Gas Treatment,* DG12-SSMI Ed., AD-NETT report, Netherlands.

Soreanu, G., Al-Jamal, M., Beland, M. (2005). "Biogas treatment using an anaerobic biosystem." *Proc., Proceedings of the 3rd Canadian Organic Residuals Recycling Conference,* Calgary, AB.

Strevett, K. A., Vieth, R. F., Grasso, D. (1995). "Chemo-Autotrophic Biogas Purification for Methane Enrichment - Mechanism and Kinetics." *Chem. Eng. J. Biochem. Eng. J.,* 58(1), 71-79.

Syed, M., Soreanu, G., Falletta, P., Beland, M. (2006). "Removal of Hydrogen Sulphide from Gas Streams using Biological Processes - A Review." *Canadian Biosystems Engineering / Le Genie Des Biosystems Au Canada,* 48, 2-1.

ter Maat, H., Hogendoorn, J. A., Versteeg, G. F. (2005). "The Removal of Hydrogen Sulphide from Gas Streams using an Aqueous Metal Sulfate Absorbent - Part I. the Absorption of Hydrogen Sulphide in Metal Sulfate Solutions." *Sep. Purif. Technol.,* 43(3), 183-197.

Truong, L. V. A., and Abatzoglou, N. (2005). "A H2S Reactive Adsorption Process for the Purification of Biogas Prior to its use as a Bioenergy Vector." *Biomass Bioenerg.,* 29(2), 142-151.

van der Zee, F. P., Villaverde, S., Garcia, P. A., Fdz-Polanco, F. (2007). "Sulphide Removal by Moderate Oxygenation of Anaerobic Sludge Environments." *Bioresour. Technol.,* 98(3), 518-524.

Vishniac, W., and Santer, M. (1957). "Thiobacilli." *Bacteriol. Rev.,* 21(3), 195-213.

Wellinger, A., and Lindberg, A. (2001). *Biogas Upgrading and Utilisation,* IEA Bioenergy, Task 24: Energy from biological conversion of organic waste, Sweden.

Willey, J. M., Sherwood, L., Woolverton, C., J., Prescott, L. M. M. (2008). *Prescott, Harley, and Klein's Microbiology,* 7th ed Ed., McGraw-Hill Higher Education, New York.

Yadvika, Santosh, Sreekrishnan, T. R., Kohli, S., Rana, V. (2004). "Enhancement of Biogas Production from Solid Substrates using Different Techniques - a Review." *Bioresour. Technol.,* 95(1), 1-10.

Yuan, W. X., and Bandosz, T. J. (2007). "Removal of Hydrogen Sulphide from Biogas on Sludge-Derived Adsorbents." *Fuel,* 86(17-18), 2736-2746.